

**UCSF**

**UC San Francisco Electronic Theses and Dissertations**

**Title**

Enhanced Skeletal Anabolism by Concurrently Targeting the Parathyroid Hormone 1 Receptor (PTH1R) and Extracellular Calcium-Sensing Receptor (CaSR)

**Permalink**

<https://escholarship.org/uc/item/8n900213>

**Author**

Santa Maria, Christian Norman Davey Yuzon

**Publication Date**

2020

Peer reviewed|Thesis/dissertation

Enhanced Skeletal Anabolism by Concurrently Targeting the Parathyroid Hormone 1 Receptor (PTH1R) and Extracellular Calcium-Sensing Receptor (CaSR)

by  
Christian Santa Maria

DISSERTATION

Submitted in partial satisfaction of the requirements for degree of  
DOCTOR OF PHILOSOPHY

in

Oral and Craniofacial Sciences

in the

GRADUATE DIVISION

of the

UNIVERSITY OF CALIFORNIA, SAN FRANCISCO

Approved:

DocuSigned by:

*Pamela Den Besten*

Pamela Den Besten

0E9309D50C9D432...

Chair

DocuSigned by:

*Wenhan Chang, PhD*

Wenhan Chang

DocuSigned by:

*Ralph Marcucio*

Ralph Marcucio

DocuSigned by:

*Dolores Shoback*

Dolores Shoback

C7A2BC61A5D94EC...

Committee Members



# Dedication

It is with genuine gratefulness and warmest regard that I dedicate this work to the following individuals.

To my wife, Janelle, for your unconditional love and unwavering support from beginning to end of this academic journey I set on.

To my son, Christian Azrael, to always pursue your most ambitious goals, for if you put your mind to it, you can accomplish anything.

To my father and mother, Davey and Glenda, in gratitude for the tremendous sacrifices you made for me to get where I am now.

To my younger sisters, Christine and Amanda, for whom I tried to be a role model for as an older brother.

Lastly, this dissertation is in memoriam Hanren Chang, the youngest daughter of Wenhan and Chia-Ling. The completion of my doctorates and this scientific work are in commemoration of your life.

*On the mountains I will bow my life to The One who set me there.*

*In the valley, I will lift my eyes to The One who sees me there.*

*When I'm standing on the mountain aft, didn't get there on my own.*

*When I'm walking through the valley end, no I am not alone.*

## Acknowledgments

I will forever cherish my time as a DDS/PhD trainee at UCSF. The program provided me with an environment of professionalism, close-knit relationships, and involved mentorship. I depart from this phase of my training extremely proud of what I have learned and accomplished, grateful for the unique experiences afforded to me and for friendships that I have made, and excited for what comes next for me in my career. The decision to pursue this rigorous academic excursion in 2012 was largely influenced by support from my family and close friends. Reflecting on this journey, I recognize the individuals listed below to whom I am forever indebted.

Thank you to my PhD thesis advisor and scientific mentor, Wenhan Chang, PhD, who has been a father figure to me for over a decade. In 2009, you saw my potential and, with confidence, took a chance on me as a young man fresh out of college. My time as the manager of the VA Bone Core Imaging Facility (2009-2012) was an enriching experience that further inspired me to advance my education by pursuing a dual doctorate degree. You will always have my utmost gratitude for your constant support, unwavering advocacy, and demand for me to strive for the highest achievement.

Thank you to my qualifying exam and dissertation committee members; Pamela Den Besten, MS, DDS; Ralph Marcucio, PhD; and Dolores Shoback, MD for your expertise, assistance in refining my research questions, and demanding the highest caliber of science from me.

Thank you to past and present members of the Chang lab and UCSF Endocrine Research Unit as a whole for your thoughtful insights, intellectual contributions, and efforts: Zhiqiang Cheng, MD; Alfred Li, DDS; Chia-Ling Tu, PhD; Jenna Hwong; Amanda Herberger, PhD; Nathan Liang; Fuqing Song; Katie Lee, MD; Katherine Popovich; and Nicholas Szeto.

Thank you to my clinical mentors at the UCSF School of Dentistry, Antonio Ragadio, DDS; Lori Doran-Garcia, DDS; Jeffory Eaton, DDS; Mark Dellinges, DDS, FACP; Maungmaung Thaw, DDS; Diane Nguyen, DDS; Wilson Hsin, DMD; and Guo-Hao Lin, MS, DDS; for your guidance, critique, suggestions, and encouragement during my dual degree training.

Thank you to Ralph Marcucio, PhD; Pamela Den Besten, DDS, MS; and Deans John Featherstone, PhD and Michael Reddy, DMD, DMSc; for your strong commitment to ensuring the existence and maintained excellence of the integrated DDS/PhD training program at UCSF. Thank you to the Dean's office, especially Kathryn Gabriel for handling my training grant and financial questions. Lastly, I give a special thank you to my good friend, Roger Mraz, who mentored me as far back as 2011 since before I even thought about applying to the program.

Thank you to my dental school coaching group and friends from the Class of 2016, 2019, and 2020: Eric Brown, DDS; Randy Rosales, DDS; Ngan Tran, DDS; Chris Berguia, DDS; Maritess Aristorenas, DDS; Annie Hsu, DDS; Anoush Akopyan, DDS;

Brad Shemluck, DDS; Brian Lin, DDS; Brittany Zhang, DDS; Danny Ta, DDS; Derrell Washington, DDS; Ella Saeed, DDS; Emily Yang, DDS; Jason Yip, DDS; Jennifer Hofmann, DDS; Jessica Lam, DDS; Jimmy Tran, DDS; Jonathan Lee, DDS; José Carrasco, DDS; Joti Kaler, DDS; K-Lynn Hogh, DDS; Khanh Nguyen, DDS; Kyle Nguyen, DDS; Lais “Mo” Lodin, DDS; Matt Bonzell, DDS; Matthew Hurd, DDS; Noel De Leon, DDS; Rebecca Tom, DDS; Rhett, DDS; Sam Su, DDS; Taran Cheema, DDS; Todd Alpert, DDS; Eric Hsu, DDS; Michael Nguyen, DDS; Trung Nguyen, DDS; Victoria Nguyen, DDS; for your comedic interludes, timely encouragement, and emotional support during the completion of my doctorates.

Thank you to my mentors during my time as an undergraduate at UC Davis (2005-2009): Connie Champagne, PhD, director of the Biology Undergraduate Scholars Program at UC Davis; Kenneth Burtis, PhD, former dean of the College of Biological Sciences and current Provost; Simon Chan, PhD, my project advisor who passed away in 2012; Aaron Straight, PhD and Kristina Godek, PhD who were my mentors during my summer research project at Stanford University in 2008; Mr. Rolf Unterleitner, my undergraduate mentor and general/organic chemistry tutor who passed away in 2016. My time as a BUSP and AMGEN Scholar was formative in cementing my desire to pursue this challenging yet fulfilling academic route.

Without any of the aforementioned individuals, this scientific work and the successful attainment of my doctorate degrees would not have been possible.

...I'M BATMAN!

## Contributions

The text of Chapter 1 of this dissertation is an updated reprint of the manuscript as it appears in *Seminars in Cell and Developmental Biology*. It has been adapted to fit the format and content guidelines of this dissertation. The co-authors listed (Drs. Cheng, Shoback, Tu, and Chang) directed and/or supervised the research that forms the basis for the thesis.

**Santa Maria C**, Cheng Z, Shoback D, Tu CL, Chang W. Interplay between CaSR and PTH1R signaling in skeletal development and osteoanabolism. *Seminars in Cell and Developmental Biology*. 49:11-23, (2016).



# Abstract

Enhanced Skeletal Anabolism by Concurrently Targeting The Parathyroid Hormone 1

Receptor (PTH1R) and Extracellular Calcium-Sensing Receptor (CaSR)

by

Christian Norman Davey Yuzon Santa Maria

Maintaining normal  $\text{Ca}^{2+}$  homeostasis is essential for all biological functions. Parathyroid glands (PTGs) were developed in land vertebrates to defend against hypocalcemic challenges by tightly regulated secretion of parathyroid hormone (PTH), which activates the PTH1R in target tissues to increase  $\text{Ca}^{2+}$  recycling in kidneys,  $\text{Ca}^{2+}$  absorption from the small intestine via indirect renal production of 1,25-dihydroxyvitamin D3 (1,25-D), and  $\text{Ca}^{2+}$  release from bone matrices. These PTH-mediated calciotropic activities are subsided by elevated concentrations of serum  $\text{Ca}^{2+}$  through actions of its putative receptor, the extracellular  $\text{Ca}^{2+}$ -sensing receptor (CaSR), in PTGs to suppress PTH secretion, in kidneys to enhance Ca secretion, and in bone to remineralize matrices and suppress bone resorbing activity, together with PTH/ PTH1R, constituting a “yin/yang” feedback mechanism to maintain  $\text{Ca}^{2+}$  homeostasis at a steady state. Interestingly, intermittent PTH (iPTH), administered by once-daily injections, can produce skeletal anabolism in the presence of  $\text{Ca}^{2+}$  sufficiency. However, more effective dosages could not be achieved for clinical use, mainly due to its intolerable hypercalcemic side-effects. This dissertation explores interplays between the actions of PTH1R and CaSR and exploits these interactions to harness hypercalcemic effects of PTH while enhancing its skeletal anabolism to prevent bone loss and enhance bone

fracture repair. Our strategy leverages the ability of co-injecting an allosteric agonist of CaSR (or calcimimetic) to normalize PTH induced hypercalcemia and synergize anabolic actions of CaSR and PTH1R in bone cells. The study employed state-of-the-art technologies, including high-resolution microCT imaging, automated comprehensive serological assays, Nanostring nCounter gene expression profiling, steady and dynamic histomorphometry, biomechanics testing, and novel genetically manipulated murine models. Our findings reveal novel synergistic actions of PTH and CaSR in bone and their underlying mechanisms, which hold powerful clinical implications for future strategies needed to treat osteoporotic disease and skeletal fractures.

# Table of Contents

<b>Chapter 1: Introduction</b> .....	1
1.1 Background.....	2
1.2 Endochondral bone formation.....	6
1.3 PTHrP and PTH1R in endochondral bone formation.....	8
1.4 Signaling transduction of the CaSR.....	11
1.5 CaSR in chondrocyte differentiation and cartilage development.....	13
1.6 Interplay between Ca <sup>2+</sup> /CaSR and PTHrP/PTH1R signaling in chondrocytes.....	18
1.7 Bone modeling and remodeling.....	20
1.8 Actions of PTH and PTH1R in bone.....	21
1.9 Actions of Ca <sup>2+</sup> and CaSR in bone – Osteoblastogenesis and Osteoclastogenesis...24	
1.10 Interplay between Ca <sup>2+</sup> /CaSR and PTHrP/PTH1R signaling in bone.....	28
1.11 Skeletal anabolism by targeting the PTH1R and CaSR in bone.....	30
1.12 Conclusion.....	33
1.13 References.....	34
<b>Chapter 2: Enhanced Skeletal Anabolism by Targeting the PTH1R and CaSR.....</b>	<b>64</b>
2.1 Introduction.....	65
2.2 Results.....	70
2.3 Discussion.....	114
2.4 Materials and Methods.....	118
2.5 Conclusion and Future Directions.....	125
2.6 References.....	126

# List of Figures

Figure 1.1. Schema for the actions of PTH/PTH1R and Ca<sup>2+</sup>/CaSR signaling.....61

Figure 1.2. Schema for growth plate chondrocyte differentiation and its regulation.....62

Figure 1.3. Direct actions of Ca<sup>2+</sup> and CaSR on chondrocyte differentiation.....63

Figure 2.1. Co-injections of the calcimimetic NPS-R568 offset the hypercalcemic side-effects of PTH(1-34) in 3-month-old male mice.....84

Figure 2.2. Co-injections of the calcimimetic NPS-R568 offset the hypercalcemic side-effects of PTH(1-34) 12-month-old female mice.....86

Figure 2.3. Co-injections of the calcimimetic NPS-R568 produce additive osteoanabolic effects in trabecular and cortical bone of 3-month-old male mice.....88

Figure 2.4. Mice treated with combined PTH(1-34) and NPS-R568 exhibit increased compressive strength at the mid-femur.....90

Figure 2.5. Mice treated with combined PTH(1-34) and NPS-R568 exhibit increased fluorescent labeling.....91

Figure 2.6. Co-injections of the calcimimetic NPS-R568 produce additive osteoanabolic effects in trabecular and cortical bone of 12-month-old female mice.....92

Figure 2.7. Co-injections of the calcimimetic NPS-R568 offset the hypercalcemic side-effects of analogs PTH(1-34) and LA-PTH in 3-month-old male mice.....94

Figure 2.8. LA-PTH produces more robust osteoanabolic effects than PTH(1-34) with and without co-injection with calcimimetic NPS-R568.....96

Figure 2.9. Co-injections of the calcimimetic NPS-R568 offset the hypercalcemic side-effects of LA-PTH in 12-month-old female and male mice.....98

Figure 2.10. LA-PTH produces more robust osteoanabolic effects, which is generally annulled with calcimimetics in aged female mice.....99

Figure 2.11. LA-PTH produces more robust osteoanabolic effects, which is generally annulled with calcimimetics in aged female mice..... 101

Figure 2.12. The osteoanabolic effects of intermittent PTH and NPS-R568 treatment were abrogated in osteoblast-specific CaSR knockout mice..... 103

Figure 2.13. Nanostring confirms gene expression shift towards bone anabolism.....104

Figure 2.14. 3-pt-bending creates closed-unfixed tibial midshaft fractures in mice.....110

Figure 2.15. Co-injections of the calcimimetic NPS-R568 produce additive osteoanabolism in bony calluses.....111

## List of Tables

Table 2.1. Primer sets used for Genotyping Assays.....	113
--	-----

## List of Abbreviations

<b>1,25D</b>	1,25-dihydroxyvitamin D
<b>Agg</b>	aggrecan
<b>ALP</b>	alkaline phosphatase
<b>BRU</b>	bone remodeling unit
<b>BUN</b>	blood urea nitrogen
<b>CaSR</b>	extracellular calcium-sensing receptor
<b>[Ca]<sub>e</sub></b>	extracellular calcium concentration
<b>Col(I)</b>	type I collagen
<b>Col(I) α<sub>1</sub>(I)</b>	alpha 1 subunit of the type I collagen
<b>Col(II)</b>	type II collagen
<b>Col(II) α<sub>1</sub>(II)</b>	alpha 1 subunit of the type II collagen
<b>Creat</b>	creatinine
<b>Ctsk</b>	cathepsin K
<b>DMP1</b>	dentin matrix protien-1
<b>Floxed-CaSR</b>	control mice carrying loxP sequences flanking the exon 7 of the <i>Casr</i> gene
<b>Exon<sup>5</sup>CaSR<sup>-/-</sup></b>	mice with insertion a neomycin gene cassette into the exon 5 of the <i>Casr</i> gene
<b>Cart<sup>Cre</sup>CaSR<sup>Δflox/Δflox</sup></b>	mice with constitutive ablation of the exon 7 of the <i>Casr</i> gene targeted specifically to chondrocytes

Tam- <b>Cart<sup>+</sup>CaSR<sup>Δflox/Δflox</sup></b>	mice with tamoxifen-induced ablation of the exon 7 of the <i>Casr</i> gene targeted specifically to chondrocytes
<b>OB<sup>+</sup>CaSR<sup>Δflox/Δflox</sup></b>	mice with constitutive osteoclast-specific ablation of the exon 7 of the <i>Casr</i> gene
<b>Gcm2</b>	glial cells missing homolog 2
<b>Gcm2<sup>-/-</sup></b>	mice with global deletion of <i>Gcm2</i>
<b>GP</b>	growth plate
<b>GPC</b>	growth plate chondrocyte
<b>HPT</b>	hyperparathyroidism
<b>IGF1</b>	insulin-like growth factor
<b>Ihh</b>	Indian hedgehog
<b>iPTH</b>	daily injection (or intermittent) PTH treatment
<b>KO</b>	gene knockout
<b>LA-PTH</b>	long-acting PTH analog
<b>M-CSF</b>	macrophage colony-stimulating factor
<b>MMP</b>	matrix metalloproteinase
<b>μCT</b>	micro-computed tomography
<b>OB</b>	osteoblast
<b>OCL</b>	osteoclast
<b>OCN</b>	osteocalcin
<b>ON</b>	osteonectin



<b>OPG</b>	osteoprotegerin
<b>OPN</b>	osteopontin
<b>PG</b>	proteoglycan
<b>PTC</b>	parathyroid cell
<b>PTG</b>	parathyroid gland
<b>PTH</b>	parathyroid hormone
<b>PTH<sup>-/-</sup></b>	mice with global deletion of <i>Pth</i> gene
<b>PTH1R</b>	parathyroid hormone 1 receptor
<b>PTHrP</b>	parathyroid hormone-related protein
<b>RANK</b>	receptor activator of nuclear factor kappa- B
<b>RANKL</b>	RANK ligand

# **Chapter 1:**

## **Introduction**

## 1.1 Background

The parathyroid hormone (PTH)-related peptide (PTHrP) controls the pace of pre- and post-natal growth plate development by activating the PTH1R in chondrocytes, while PTH maintains mineral and skeletal homeostasis by modulating calciotropic activities in kidneys, gut, and bone. The extracellular calcium-sensing receptor (CaSR) is a member of family C G-protein-coupled receptor, which regulates mineral and skeletal homeostasis by controlling PTH secretion in parathyroid glands and  $\text{Ca}^{2+}$  excretion in kidneys. Recent studies showed the expression of CaSR in chondrocytes, osteoblasts, and osteoclasts and confirmed its non-redundant roles in modulating the recruitment, proliferation, survival, and differentiation of the cells. This review emphasizes the actions of CaSR and PTH1R signaling responses in cartilage and bone and discusses how these two signaling cascades interact to control growth plate development and maintain skeletal metabolism in physiological and pathological conditions. Lastly, novel therapeutic regimens that exploit interrelationship between the CaSR and PTH1R are proposed to produce more robust osteoanabolism.

Maintaining normal  $\text{Ca}^{2+}$  homeostasis is essential for all cellular functions in our body. Land vertebrates develop large bony skeleton to store excess  $\text{Ca}^{2+}$  in the form of hydroxyapatite [ $\text{Ca}_{10}(\text{PO}_4)_6(\text{OH})_2$ ] and releases it to meet systemic demands at the time of  $\text{Ca}^{2+}$  deficiency. The parathyroid gland (PTG) also evolves to coordinate the calciotropic activities in the skeleton with those in the gut and kidney, by secreting the parathyroid hormone (PTH). The current working model for the regulation of serum  $\text{Ca}^{2+}$  concentration (s $\text{Ca}^{2+}$ ) emphasizes: (i) the ability of parathyroid cell (PTC) to

respond to subtle changes in  $sCa^{2+}$  that promptly alter PTH secretion (**Figure 1.1 A**, ①); (ii) the ability of PTH to activate its receptor, PTH1R (②), in the kidney to promote  $Ca^{2+}$  reabsorption (③) and stimulate 1,25dihydroxyvitamin D (1,25D) production to increase intestinal  $Ca^{2+}$  absorption (④); (iii) the ability of PTH to enhance bone turnover (⑤-⑨, see detailed descriptions in Section 8 Actions of PTH and PTH1R in bone) to release  $Ca^{2+}$  into the circulation (⑩); and (iv) the negative feedback of increasing  $sCa^{2+}$  and serum 1,25D (s1,25D) to suppress PTH secretion by activating the extracellular  $Ca^{2+}$ -sensing receptor (CaSR) and vitamin D receptor (VDR) (⑪) to close this regulatory loop [1-3]. Defects at any point in this pathway disturb mineral balance and produce endocrine and skeletal dysfunction.

Skeletal development begins in the embryo and continues throughout adolescence until a peak bone mass is attained in early adulthood. The mature skeleton is then maintained by continuous bone turnover (or remodeling) through balanced bone-forming activities of osteoblasts (OBs) and bone-resorbing activities of osteoclasts (OCLs) (**Figure 1.1 A**, ⑥-⑨) in the bone-remodeling units (BRUs). Excessive bone resorption due to aging, post-menopause, use of glucocorticoids, and metabolic diseases, like hyperparathyroidism (HPT), produces osteoporotic skeleton with increased risk of fracture [4-13].

$Ca^{2+}$  availability critically impacts skeletal development and bone turnover [14].  $Ca^{2+}$  deficiency produces rickets and osteomalacia, characterized by inadequate cartilage or bone matrix mineralization, in patients [15-18]. Supplementation of the diet with  $Ca^{2+}$

and vitamin D, and in some cases with  $\text{Ca}^{2+}$  alone, completely heals those cartilage and bone defects [14, 15, 19-21]. Similarly, rachitic changes in bone and cartilage in VDR knockout (KO) mice are prevented by a high  $\text{Ca}^{2+}$  diet [22-24]. The above observations underscore the importance of adequate  $\text{Ca}^{2+}$  supply to normal cartilage and bone development. Although  $\text{Ca}^{2+}$  could contribute passively to bone mineralization as an essential substrate, recent discoveries of CaSR in chondrocytes, OBs, and OCLs have prompted investigations for direct  $\text{Ca}^{2+}$  actions on those cells as a critical “growth factor”.

Inactivating mutations in the *CASR* gene reduce the responsiveness of PTC to changes in  $\text{sCa}^{2+}$  and produce familial hypocalciuric hypercalcemia (FHH) and neonatal severe HPT (NSHPT) in patients, who show elevated serum PTH (sPTH),  $\text{s1,25D}$ , and  $\text{sCa}^{2+}$  levels and in the severest forms a growth-retarded and under-mineralized skeleton [25-28]. Skeletal defects in NSHPT patients are likely caused by aberrant PTH secretion and the associated mineral and hormonal disturbances. Direct effects of mutant CaSR in chondrocyte and bone cell, however, cannot be ruled out [29-38].

Prolonged elevation of sPTH produces catabolic effects on bone [39-42], but once-daily (or intermittent) injections of supra-physiological doses of PTH1-34 or PTH1-84 increase trabecular bone mass in normal and osteoporotic animal models and in osteoporosis patients [43-47]. The anabolic effect of intermittent PTH (iPTH) appears to rely on its ability to promote bone-forming activities of OBs to a greater extent than the bone-resorbing activities of OCLs at the beginning of the treatment -- creating a so-

called “anabolic window”, but its underlying cellular and molecular mechanisms remain unclear.

In the past decades, investigations using genetically manipulated mouse models and cell cultures have confirmed essential roles for the CaSR and PTH1R signaling in controlling pre- and post-natal skeletal development and maintenance of adult skeleton. However, perspectives on how these two signaling pathways interact in cartilage and bone are lacking. In light of two recent review articles that provide comprehensive updates on general systemic and local actions of the CaSR and PTH on bone and mineral metabolism [30, 48], this review emphasizes the interplay between the CaSR and PTH1R signaling in chondrocytes, OBs, and OCLs and proposes novel regimens exploiting this receptor interaction to enhance osteoanabolism for treatment of skeletal disease.

## 1.2 Endochondral bone formation

In vertebrates, all weight-bearing axial and appendicular skeletons are formed by endochondral bone formation that begins in early embryos. This process starts with the condensation of mesenchymal progenitors and their commitment to the chondrocytic lineage to form cartilaginous anlagen that later becomes a growth plate (GP). In the GP, chondrocytes proliferate, mature, and hypertrophy sequentially within single cell columns and then begin to deposit  $\text{Ca}^{2+}$ /phosphate-containing minerals into the surrounding matrix after they reach terminal differentiation (**Figure 1.2 A**). Within this mineralized matrix, the terminally differentiated chondrocytes produce matrix metalloproteinases to remodel surrounding matrix [49-51] and release growth factors to induce vascular invasion and promote OB differentiation at the chondro-osseous junction. It was originally proposed, mainly based on histological observations, that terminally differentiated hypertrophic chondrocytes in the GP undergo cell death and OBs arise from the osteoprogenitors delivered by the invading vasculature to replace the dying chondrocytes and produce new bone. This classic scheme of chondro-to-osteo transition has just undergone a significant paradigm shift [52-54]. By using protein-based fluorescent probes to label chondrocytes in vivo and by following the fate of the labeled cells in the bone using time-lapse cell/tissue imaging, it has been clearly shown that the majority of hypertrophic chondrocytes can trans-differentiate directly into OBs in the GP during endochondral bone formation or in the healing callus of fractured bone [53, 55-57]. GPs exist throughout adolescence to support longitudinal bone growth by repeating the above cell differentiation programs until the chondroprogenitor pool is

exhausted at the time of GP closure in early adulthood. Aberrant acceleration or delay in chondrocyte differentiation produces disorganized GPs and impede bone growth [58].



### 1.3 PTHrP and PTH1R in endochondral bone formation

Many transcription [58-69] and autocrine/paracrine factors [56, 70-83] were found to induce the commitment of progenitors to the chondrocytic lineage and to pace their differentiation [49, 56, 76, 84, 85]. Among them, the parathyroid hormone–related protein/Indian hedgehog (PTHrP/Ihh) feedback loop is the best-established pathway that prevents aberrant acceleration of chondrocyte differentiation and early closure of the GP [58, 86, 87]. According to the current model, PTHrP produced by perichondral cells in embryonic skeleton or by maturing/prehypertrophic chondrocytes in postnatal GPs diffuses into the proliferation zone where it activates the PTH1R and downstream signaling cascades to sustain the proliferative activities of the cells and delay their further differentiation [88] (**Figure 1.2 A**). When chondrocytes eventually mature, they increase the production of Ihh to simulate its receptor Patched in the neighboring cells and increase PTHrP production via mechanisms that remain to be determined, thus constituting a feedback loop to slow down cell differentiation [87, 89] (**Figure 1.2 A**). *Pth1r*, *Pthrp*, and *Ihh* gene KOs in mice all led to accelerated chondrocyte differentiation, early GP closure, and dwarfism [87]. Transgenic mice overexpressing PTHrP specifically in chondrocytes also presented short-limbed dwarfism, but their growth plates were composed exclusively of proliferating cells and lacked endochondral ossification [90], confirming the role of PTHrP/PTH1R signaling in preventing an early entry of proliferating chondrocyte into terminal differentiation.

Several elegant investigations explored signaling events underlying the actions of PTHrP on cartilage development with emphases on its ability to activate different

heterotrimeric GTP-binding proteins (G-proteins) and multiple down-stream effectors in chondrocytes [86]. In fibroblastic COS-7 cells expressing exogenous PTH1Rs, binding of PTHrP to the receptor stimulated Gs-mediated cAMP synthesis as well as Gq-mediated intracellular  $Ca^{2+}$  releases, indicating the multifaceted actions of PTHrP/PTH1R signaling [91]. To determine the impact of Gs-mediated signaling responses on GP development, chimeric mice with GPs comprising mixed populations of normal and  $Gs\alpha$ -deficient chondrocytes were studied [92]. In the chimeric GPs,  $Gs\alpha$ -deficient chondrocytes appeared to stop proliferating and become hypertrophic prematurely [91] -- phenotypes similar to those of chondrocyte-specific PTH1R KO mice [93, 94]. It was, therefore, concluded that PTHrP activates Gs-mediated signaling responses to sustain chondrocyte proliferation [87].

In cultured chondrocytes, pharmacological stimulation of Gq-coupled protein kinase C (PKC) and mitogen-activated protein kinase kinase (MEK) pathway suppressed proliferation, enhanced cell hypertrophy, and increased expression of type X collagen [95, 96], supporting a role for Gq-mediated signaling in promoting chondrocyte terminal differentiation. But there has been no report on the study of mice with targeted ablation of  $Gaq$  specifically in chondrocytes to clearly define its impact on GP development *in vivo*. Instead, studies of mice with a knock-in of an engineered *Pth1r* mutant gene, which encodes a mutant PTH1R that retains the ability to activate Gs, but not Gq, signaling pathway, showed delayed GP ossification and increased chondrocyte proliferation [97]. Though, the effects were modest, likely due to the relatively restricted expression of PTH1R in the proliferation zone. Nevertheless, the investigators of the

study concluded that the PTH1R-mediated Gs and Gq signaling cascades constitute a “Yin-Yang” relationship to control the pace of cell differentiation [86, 87]. However, the fact that chondrocyte-specific PTH1R KO mice presented profoundly accelerated chondrocyte differentiation and early GP closure indicates the existence of other, perhaps Gq-coupled, mediators that can promote the terminal differentiation of chondrocyte and engage in a “tug-of-war” relationship with the PTHrP/PTH1R/Ihh feedback loop to control the pace of GP development. Recent studies suggest that  $\text{Ca}^{2+}$  and its receptor, CaSR, constitute a critical signaling pathway that instigates such “pro-differentiation” activities in chondrocytes.

## 1.4 Signaling transduction of the CaSR

The CaSR is a member of family C G-protein coupled receptor (GPCR), which consists of a large extracellular domain (ECD;  $\approx$ 450–600 amino acids) for ligand binding, a seven-transmembrane domain (7-TMD) for G protein coupling, and a long intracellular C-terminal tail ( $\approx$ 250 amino acids) for recruitment of signaling molecules and for receptor binding to cytoskeletons [98, 99]. Members of family C GPCRs function exclusively in the form of multimeric complex [100, 101]. The CaSR can form homodimers [100, 101] or heterodimerize with other members of family C GPCRs, including metabotropic glutamate receptors [102] and type B gamma-aminobutyric acid receptors (GABA<sub>B</sub>R1 and GABA<sub>B</sub>R2) [103, 104]. Like other GPCRs, the CaSR activates multiple downstream signaling cascades by coupling to 3 major groups of G proteins, Gq/11, Gi/o and G12/13 [99]. Through coupling to the Gq/11, the CaSR activated different subtypes ( $\beta$ ,  $\gamma$ ,  $\delta$ ,  $\epsilon$ ,  $\zeta$ ,  $\eta$ ) of phospholipase C (PLC) to cleave the phospholipid phosphatidylinositol 4,5-bisphosphate (PIP<sub>2</sub>) into diacyl glycerol (DAG), which activates protein kinase C, and inositol 1,4,5-trisphosphate (IP<sub>3</sub>), which releases Ca<sup>2+</sup> from intracellular stores by binding to IP<sub>3</sub> receptors in the stores [99]. This signaling cascade has been demonstrated in most of the cell systems tested, including parathyroid cells [105, 106], keratinocytes [107], chondrocytes, osteoblasts [29], and transformed cells expressing the CaSR exogenously [108], to regulate diverse cell functions ranging from PTH secretion [109], osteoblast migration [35], and cell growth, survival, and differentiation [33]. By coupling to the pertussis toxin-sensitive Gi/o, the CaSR suppressed adenylyl cyclase activities and cAMP production in PTCs [110] and OBs [29]. Activation of Gi/o also activated the extracellular-signal-regulated kinases

(ERK1/2) in PTCs [111, 112], OBs [113, 114], and HEK-293 cells expressing exogenous CaSRs [115-117]. Through the activation of G12/13, the CaSR enhanced Wnt3a- $\beta$ catenin signaling to promote osteoblast differentiation [118], but inhibited osteoclastogenesis by suppressing the expression of the receptor activator of nuclear factor kappa-B ligand (RANKL) and increasing osteoprotegerin (OPG) expression [119]. The CaSR could also activate phospholipase D through coupling to G12/13 in Madin-Darby canine kidney cells [120].

## 1.5 CaSR in chondrocyte differentiation and cartilage development

Ca<sup>2+</sup> deficiency produced rickets in childhood [18] and in VDR and Cyp27b1 KO mice [24, 121] by delaying chondrocyte differentiation and blocking matrix mineralization in their GPs. The ability of dietary Ca<sup>2+</sup> supplements to reverse the GP defects [21] signifies the importance of Ca<sup>2+</sup> availability to GP development. The expression of CaSR first appears in maturing chondrocytes in the GP and increases in hypertrophic chondrocytes (**Figure 1.2 B**) [29] including those being released from the cartilage matrix at the chondro-osseous junction (**Figure 1.2 C**, red arrowheads) and adjacent OBs [29]. This expression pattern supports a role for the CaSR in mediating the terminal differentiation of hypertrophic chondrocytes and their transformation into osteoblastic lineage, according to the newly established paradigm [52-54].

Direct actions of Ca<sup>2+</sup> and CaSR on chondrocyte differentiation have been confirmed by studies of primary cells cultured from cartilage of different species, chondrogenic cell lines, and metatarsal bone rudiments explants. Chondrocytes in a high-density culture exhibited spontaneous differentiation that recapitulates key steps of chondrogenesis as seen in vivo (**Figure 1.3 A**) [29, 103, 122-124]. For example, mouse GP chondrocytes proliferated robustly and produced a proteoglycans (PG)-rich matrix immediately after plating (**Figure 1.3 A**). Mineral deposition appeared to start in the matrix surrounding the hypertrophic chondrocytes (**Figure 1.3 A**, 7-day post-confluence, insert). As mineral deposition increased in the cultures, PG accumulation declined and the cells lost their chondrocytic morphology (**Figure 1.3 A**, 21-day post-

confluence, insert). Along with those morphological changes, RNA levels for early differentiation markers -- aggrecan (Agg) and type II collagen  $\alpha_1$  subunit [ $\alpha_1$ (II)] -- were highest in early cultures and decreased in later cultures (by >90%), while the expression of late differentiation markers -- alkaline phosphatase (ALP) and type X collagen  $\alpha_1$  subunit [ $\alpha_1$ (X)], and putative OB markers -- osteopontin (OPN), osteocalcin (OCN) and osteonectin (ON) increased with time of culture (**Figure 1.3 B**). The above changes in cell morphology, gene expression, and matrix protein synthesis recapitulate steps of chondrogenesis and indicate time-dependent transformation of the cultured chondrocytes into the osteoblastic lineage.

Changes in  $[\text{Ca}^{2+}]_e$  profoundly impacted the differentiation of cultured chondrocytes. In tibio-tarsal chondrocytes cultured from chicken embryos, high  $[\text{Ca}^{2+}]_e$  increased the expression of  $\alpha_1$ (X) [125]. In mouse GP chondrocyte cultures, raising  $[\text{Ca}^{2+}]_e$  dose-dependently suppressed PG accumulation, increased mineral accumulation (**Figure 1.3 C and 3D** -PTHrP), reduced expression of chondrocyte markers [Agg,  $\alpha_1$ (II), and  $\alpha_1$ (X)], and increased expression of OPN (**Figure 1.3 E**, Control) [29, 103, 122, 123]. Similar effects of high  $[\text{Ca}^{2+}]_e$  were seen in cultures of non-transformed chondrogenic RCJ3.1C5.18 (or C5.18) cells, cloned from fetal rat calvarias [29, 124, 126]. The ability of high  $[\text{Ca}^{2+}]_e$  to increase intracellular  $\text{Ca}^{2+}$  mobilization and promote terminal differentiation in C5.18 cells could be blocked by overexpression of a dominant-negative CaSR or anti-sense RNA in the cells [29, 124, 126]. In cultures of fetal rat metatarsal bone explants, administration of CaSR agonist (or calcimimetics) increased their longitudinal growth by enhancing chondrocyte differentiation in the GP [127]. The above

studies confirm the actions of  $\text{Ca}^{2+}$  and CaSR in promoting chondrocyte differentiation and mineralizing functions, and perhaps to speed up their transformation to acquire osteogenic phenotypes.

A global CaSR KO ( $\text{Exon}^5\text{CaSR-/-}$ ) mouse model was generated by inserting a neomycin gene cassette into the exon 5 of the gene, which encodes 77 amino acids in the ECD of the receptor. The  $\text{Exon}^5\text{CaSR-/-}$  mice manifested severe phenotypes of human disorder NSHPT -- HPT, hypercalcemia, hypocalciuria, hypophosphatemia, parathyroid hyperplasia, and failure to thrive and the mice died before 3-4 weeks of age. Analyses of their bones revealed severe rickets with delayed formation of secondary ossification center, expanded and disorganized growth plate, and impaired bone formation [36, 128]. Interestingly, the growth and skeletal defects and early death of the  $\text{Exon}^5\text{CaSR -/-}$  mice could be rescued by preventing the development of HPT after breeding the mice with PTH $^{-/-}$  mice lacking PTH gene or Gcm2 $^{-/-}$  mice lacking the development of PTG [129, 130]. The reversal of skeletal defects in the  $\text{Exon}^5\text{CaSR -/-};\text{PTH-/-}$  and  $\text{Exon}^5\text{CaSR -/-};\text{Gcm2-/-}$  double KO mice led to the conclusion that the CaSR is not essential for skeletal development [129, 130] and prompted searches for other  $\text{Ca}^{2+}$ -sensing mechanism(s) [131, 132]. However, it was not realized at the time that the exon 5 gene-targeting strategy allowed an in-frame gene-splicing event to exclude the exon 5 along with the inserted neomycin cassette from the full-length transcript, producing a truncated CaSR lacking 77 amino acids in its ECD. This truncated receptor was expressed in the skin, growth plate, and bone of the  $\text{Exon}^5\text{CaSR -/-}$  mice [122, 133] and is sufficient to render  $\text{Ca}^{2+}$ -responsiveness in GPCs cultured from the mice [122].



To clearly define the role of CaSR in skeletal development, a floxed-CaSR mouse model was generated by flanking the exon 7 of the *Casr* gene with two loxP sites. The exon 7 encodes the entire 7-TM domain and the C-terminal tail, which are absolutely required for the coupling of the receptor to downstream signaling cascades [33]. The utility of this floxed-CaSR model was validated by the generation of PTC-specific CaSR KO mice ( $^{PTC}CaSR^{\Delta flox/\Delta flox}$ ) through breeding the floxed-CaSR mice with PTH-Cre mice expressing Cre-recombinase under the control of PTH promoter [33]. Analyses of genomic DNA, RNA, and protein extracted from different tissues of the  $^{PTC}CaSR^{\Delta flox/\Delta flox}$  mice showed completely deletion of the exon 7 of the gene in PTGs, but not in other vital organs [33].  $^{PTC}CaSR^{\Delta flox/\Delta flox}$  mice presented severe HPT, hypercalcemia, skeletal and growth phenotypes, and early death as seen in the  $^{Exon5}CaSR^{-/-}$  mice, except that the  $^{PTC}CaSR^{\Delta flox/\Delta flox}$  mice developed hypercalciuria, but not hypocalciuria, due to the preservation of normal renal CaSR functions, which enhances  $Ca^{2+}$  excretion in response to hypercalcemia [33].

To determine the role of CaSR in GP development, the floxed-CaSR mice were bred with Col(II)-Cre mice, which express Cre recombinase under the control of  $\alpha_1(II)$  gene promoter [134]. Unexpectedly, the resulting  $^{Cart}CaSR^{\Delta flox/\Delta flox}$  embryos died before embryonic day 13 (E13), with severely under-mineralized skeleton [33]. The cause for the early death of  $^{Cart}CaSR^{\Delta flox/\Delta flox}$  embryos remains unclear [33]. As chondrogenesis also takes place during the development of heart valve [135-138], defective cardiac functions could have caused the death of  $^{Cart}CaSR^{\Delta flox/\Delta flox}$  embryos. These

observations also support the ability of exon5-less CaSR to sustain the development of <sup>Exon5</sup>CaSR <sup>-/-</sup> embryos. An additional mouse model was made to study the impact of CaSR function at later stages of GP development by breeding floxed-CaSR mice with Tam-Col(II)-Cre mice, which express tamoxifen-inducible Cre recombinase under the control of  $\alpha_1(\text{II})$  gene promoter [139] to achieve time-dependent chondrocyte-specific CaSR gene ablation. The resulting <sup>Tam-Cart</sup>CaSR<sup>flox/flox</sup> mice developed normally until adulthood in the absence of tamoxifen. Induction of CaSR KO in E18-19 embryos by a single maternal injection of tamoxifen profoundly ablated CaSR expression in the GPs of the newborn <sup>Tam-Cart</sup>CaSR <sup>$\Delta$ flox/ $\Delta$ flox</sup> mice, which presented short stature with expanded and under-mineralized GPs and delayed chondrocyte terminal differentiation as seen in rickets [33]. These in vivo studies confirm a non-redundant role for the CaSR in mediating chondrocyte differentiation and GP development.

## 1.6 Interplay between $\text{Ca}^{2+}$ /CaSR and PTHrP/PTH1R signaling in chondrocytes

Studies of cultured GP chondrocytes revealed a close interaction between PTHrP/PTH1R and  $\text{Ca}^{2+}$ /CaSR signaling pathways in controlling the pace of chondrocyte differentiation. Raising  $[\text{Ca}^{2+}]_e$  profoundly inhibited PTH1R and PTHrP expression in cultures of mouse GP chondrocytes (**Figure 1.3 E**, Control and unpublished observations) [123]. Conversely, treating those cultures with PTHrP(1-34) significantly blunted the ability of high  $[\text{Ca}^{2+}]_e$  to suppress PG accumulation and promote mineral deposition (**Figure 1.3 D**; -PTHrP vs +PTHrP). In cells maintained at 0.5 mM  $\text{Ca}^{2+}$ , treatment with PTHrP significantly increased Agg expression and markedly reduced the expression of  $\alpha_1(\text{X})$  and ALP -- markers of maturing and hypertrophic chondrocytes (**Figure 1.3 E**). Incubation with PTHrP also blocked the ability of high  $[\text{Ca}^{2+}]_e$  to inhibit Agg and  $\alpha_1(\text{II})$  expression and to increase OPN RNA levels (**Figure 1.3 E**), suggesting that increased PTHrP/PTH1R signaling can counteract the effects of high  $[\text{Ca}^{2+}]_e$  on cell differentiation.

In the GPs of  $\text{Tam-Cart}^{\text{CaSR}}\Delta^{\text{flox}}/\Delta^{\text{flox}}$  mice, the expression of IGF1 and IGF1R was profoundly reduced [33], suggesting that  $\text{Ca}^{2+}$ /CaSR could promote chondrocyte differentiation at least in part by enhancing IGF1 signaling (**Figure 1.2 A**). This scenario is supported by the ability of *lgf1r* gene knockdown to suppress the ability of high  $[\text{Ca}^{2+}]_e$  to promote terminal differentiation and matrix mineralization in cultured chondrocytes [33]. Furthermore, ablating the *lgf1r* gene specifically in GP chondrocytes in mice increased their expression of PTHrP, but not PTH1R [140], indicating a negative

regulation of PTHrP expression by IGF1R signaling. These observations support a paradigm in which  $\text{Ca}^{2+}$ /CaSR signaling counteracts PTHrP/PTH1R signaling by suppressing PTH1R expression independently of IGF1/IGF1R signaling and by inhibiting PTHrP expression via the IGF1R-dependent pathway to support normal progression of chondrocyte differentiation and growth plate development (**Figure 1.2 A**).

## 1.7 Bone modeling and remodeling

At the end of chondrogenesis in the GP, vascular invasion recruits OCL precursors to the chondro-osseous junction where they differentiate and resorb mineralized cartilage matrix to facilitate the release of GP-derived OB precursors [53, 55-57]. The vasculature may also provide a migratory pathway for osterix-expressing osteoprogenitors from the periosteum to future bone sites [141, 142]. The relative contributions of various sources of OB precursors to overall bone development remain unclear.

In the primary spongiosa beneath the GP, osteoprogenitors progress through the stages of pre-OBs, committed OBs, mature OBs, and osteocytes, which are characterized by the expression of specific marker proteins, osterix (Osx), type I collagen [Col(I)], OCN, and dentin matrix protein 1 (DMP1), respectively. The immature OBs produce a large quantity of Col(I), which constitutes the majority of protein matrix (or osteoid), while mature OBs exert mineralizing functions to deposit  $\text{Ca}^{2+}$  and phosphate into the protein matrix to increase its mechanical strength. At the end of bone-forming activity, OBs, which are embedded in the mineralized matrix, become osteocytes, while others turn into inactive flattened bone-lining OBs. Upon stimulation by calcemic factors, like PTH, bone-lining OBs are reactivated and OCLs are recruited to the BRUs, which serve to liberate matrix  $\text{Ca}^{2+}$  to meet systemic demands of  $\text{Ca}^{2+}$  and repair micro damages of the bone.

## 1.8 Actions of PTH and PTH1R in bone

Comparison of the skeletal phenotypes in PTH<sup>-/-</sup> mice and PTH<sup>-/-</sup>;PTHrP<sup>-/-</sup> double KO mice indicated PTH-dependent bone-forming activities in the primary spongiosa of long bone [143]. Bone cell-specific PTH1R KO mouse models are, however, required to further define cell-autonomous actions of the receptor. Thus far, there is no report on study of mice with PTH1R KO at early stages of osteoblast differentiation. Mice with osteocyte-specific PTH1R KO showed increases in bone mineral density and trabecular and cortical bone volume and thickness, along with a low bone turnover state due to suppressed OB and OCL activities [144]. Interestingly, mice with osteocyte-specific overexpression of a constitutively active PTH1R also showed increased trabecular and cortical bone mass, but in the state of high bone turnover [145, 146]. These studies support a role for the osteocytic PTH1R in controlling bone turnover, but other factors are involved in balancing bone forming and resorbing activities and determining overall bone accrual.

Direct actions of PTH on OBs were deduced from in vitro studies using cultures of bone marrow-derived osteoprogenitors, osteoblasts/osteocytes released from bone fragments, and osteogenic cell lines, and in vivo studies of mice injected with PTH [44-47]. Those studies together support the scheme that PTH increases osteoblastic activities by recruiting osteoprogenitors and sustaining the proliferation and survival of the committed OBs (**Figure 1.1 A**, ©). Although, iPTH could increase bone accrual and more importantly bone mineralization in vivo [44-47], PTH actually inhibits terminal differentiation of primary OBs or OB-like cell lines and their mineralizing functions in

culture [147-151]. This paradox between in vivo and in vitro observations suggests that iPTH in vivo must produce other changes in bone microenvironment that are needed to promote terminal differentiation of the newly recruited OBs by iPTH. This effect is not recapitulated in OB cultures, likely due to the absence of OCL activity.

In vivo, PTH enhances osteoclastic activities by increasing osteoblastic expression of RANKL, macrophage colony stimulating factor (M-CSF), and other cytokines to recruit osteoclast precursors and promote their growth and differentiation through activation of RANK, c-fms (M-CSF receptor), and other signaling pathways in the cells (**Figure 1.1 A**, ©) [152-155]. The above PTH actions on OBs are mediated by cell-autonomous responses as well as by locally produced growth factors and cytokines, including IGF1 [155-157], fibroblast growth factor-2 (FGF-2) [158, 159], Wnt signaling-related agonists and antagonists [160-163], periostin [164], and sympathetic tone [165]. These sequential effects of PTH on OBs and then OCLs provide not only a cellular basis for iPTH to increase bone turnover rate, but also a time window to produce anabolic effects before its catabolic effects catch up [44-47].

The importance of OCL activity in producing osteoanabolism is shown by studies of antiresorptives, such as bisphosphonates and the humanized monoclonal antibody denosumab, which binds to and neutralizes the activity of RANKL and therefore suppresses osteoclastogenesis and bone resorption [166-170]. Antiresorptive agents not only block bone resorption, but also impede bone-forming activities in the BRUs. The exact mechanisms for coupling bone resorption to formation remain unclear. It is

proposed that OCLs interact with OBs directly through binding of their cell-surface receptors (e.g., the RANK/RANKL and Ephrin/Eph systems) [152-155] to promote mutual cell differentiation and functions. Alternatively, OCLs actively release growth factors (e.g., IGF1 and TGF $\beta$ ) [171, 172] and other constituents (e.g., Ca<sup>2+</sup>) from the matrix that may serve as anabolic signals to recruit osteoprogenitors and promote their differentiation. It has been shown that local [Ca<sup>2+</sup>] can rise to >40 mM at sites of active resorption [173] and that Ca<sup>2+</sup> can function as a strong anabolic signal for OB recruitment, growth, survival, and differentiation [29, 31, 33, 174-178]. Based on this coupling mechanism, inhibition of bone resorption by antiresorptives is expected to limit local Ca<sup>2+</sup> availability and thereby slow down OB differentiation and bone formation. On the other hand, increasing bone turnover by iPTH is anticipated to increase local [Ca<sup>2+</sup>] bathing the OBs and promoting their differentiation (**Figure 1.1 A**, ⑧).



## 1.9 Actions of $\text{Ca}^{2+}$ and CaSR in bone – osteoblast and osteoclast

### Osteoblastogenesis

Studies of primary OBs and osteocytes and osteoblastic cell lines in culture demonstrated the ability of extracellular  $\text{Ca}^{2+}$  to stimulate acute signaling responses and enhance the migration, proliferation, survival, expression of terminal differentiation markers, and mineralizing functions of the cells by activating the CaSR [29, 32, 33, 35, 37, 174, 178-181]. In bone, the CaSR was found in active OBs, inactive bone-lining cells, and osteocytes ([29] and **Figure 1.2 B, 1.2 E**). As seen in cultured chondrocytes, CaSR activation with specific agonists stimulated Gq-mediated PLC activity, increased production of  $\text{IP}_3$ , elevated  $[\text{Ca}^{2+}]_i$ , and opened  $\text{Ca}^{2+}$ -dependent  $\text{K}^+$  channels to promote chemotaxis and cell proliferation in cultures of osteoblastic MC3T3-E1 [35, 182]. In calvarial OBs, CaSR activation (i) stimulated ERK 1/2 and downstream Akt and glycogen synthase kinase 3 $\beta$  (GSK3 $\beta$ ) signaling cascades to promote cell growth, survival, and matrix mineralization [178, 180] and (ii) activated PLC and store-operated  $\text{Ca}^{2+}$  entry to increase  $[\text{Ca}^{2+}]_i$  to support cell proliferation [183]. The above observations are just few of many studies demonstrating the multifaceted actions of the CaSR in mediating OB proliferation, survival, and terminal differentiation.

While the above in vitro studies support a role for the CaSR in OB differentiation, its role in vivo had been controversial. This was due to the ability of concurrent *Pth* or *Gcm2* gene KO to rescue the skeletal defects in the global <sup>Exon5</sup>CaSR<sup>-/-</sup> mice [184]. It was concluded at the time that the development of HPT due to defective CaSRs in PTCs

was the main cause for skeletal defects observed in the <sup>Exon5</sup>CaSR<sup>-/-</sup> mice [129, 130]. Again, follow-up studies revealed the expression of the truncated exon 5-less CaSR in the cartilage and bone of the <sup>Exon5</sup>CaSR<sup>-/-</sup> mice. This truncated CaSR appeared to be sufficient to support overall skeletal development. The latter notion was further supported by studies of mice with OB-specific ablation of the exon 7 of the *Casr* gene KO [185].

Deletion of the exon 7 of *Casr* at the early stage of OB differentiation in vivo by crossing the floxed-CaSR mice with mice expressing Cre under the control of two different versions (2.3 and 3.6 kb) of the Col(I)-a1 gene promoter produced the <sup>OB</sup>CaSR<sup>Δflox/Δflox</sup> mice [185], which died before 3-4 weeks of age with severely blunted growth. μCT images revealed their severely under-mineralized skeletons with multiple unhealed bone fractures [33, 175]. Histomorphometric analyses of the CaSR-deficient bones showed reduced bone formation rates and bone volume and large quantities of unmineralized osteoid deposited in both trabecular and cortical bone. Gene expression profiling showed profoundly reduced expression of OB differentiation markers, but increased expression of IL-10 gene -- an inducer of cell apoptosis. The up-regulation of the latter gene was consistent with an increased number of apoptotic OBs and osteocytes in the bones of the KO mice [33, 175]. The above skeletal defects were presented in the presence of lower serum PTH levels, further supporting cell-autonomous effects of the gene KO. These data together confirm an essential role for the CaSR in mediating OB proliferation, survival, and mineralizing functions.

Mice with transgenic overexpression of a constitutively active CaSR mutant cDNA under the control of a 3.5-kb OCN gene promoter were also made to examine the impact of the CaSR in mature OBs [176, 177]. The transgenic mice displayed mild osteopenia due to increased number and activity of osteoclast as a result of increased RANKL expression, supporting a role for the CaSR in mediating the coupling between osteoblastic and osteoclastic activities.

### **Osteoclastogenesis**

OCLs responded to changes in  $[Ca^{2+}]_e$  in culture [186-189]. CaSR expression has been detected in monocytes and macrophages freshly isolated from human bone marrow [190], and in osteoclasts cultured from bone marrow and spleen [37, 38]. In situ hybridization and immunohistochemistry (**Figure 1.2 C**, green arrowheads) confirmed the expression of CaSR mRNA and protein, respectively, in bone marrow cells and osteoclasts in resorbing pits [29]. High  $[Ca^{2+}]_e$  and/or CaSR agonists stimulated PLC, elevated  $[Ca^{2+}]_i$  [187-189, 191], and enhanced the translocation of nuclear factor NF- $\kappa$ B [189] in cultured OCLs. Some of those signaling responses were blunted in OCLs cultured from <sup>Exon5</sup>CaSR<sup>-/-</sup> mice [189]. High  $[Ca^{2+}]_e$  also inhibited the differentiation [37], secretion of acid phosphatase [188], and bone-resorbing functions in cultured OCLs [38] and increased apoptosis of mature OCLs [189]. The above in vitro data support the scheme that CaSR activation inhibits bone-resorbing activities by suppressing differentiation and secretory function of OCL and promoting cell apoptosis. Interestingly, allosteric activator of the CaSR (e.g., cinacalcet HCl) at the concentration, which suppresses PTH secretion in PTCs, had no effect on resorbing functions of human OCLs

in culture [192]. Similarly, the inhibitory effect of the allosteric inhibitor of the CaSR, NPS 2143, on resorbing functions of cultured human OCLs could be seen only at concentrations that are 250 fold higher than those required to block the CaSR in PTCs [193]. These data indicate different pharmacological profiles of the CaSR in OCLs vs PTCs. As decreasing pH renders the CaSR a right-shifted  $\text{Ca}^{2+}$  set-point [194], so the CaSR in OCLs are predicted to be less responsive to its ligand (i.e.,  $\text{Ca}^{2+}$ ) and perhaps its modulators (calcimimetics and calcilytics) in actively resorbing pits. By using a combination  $\text{H}^+$  and  $\text{Ca}^{2+}$  double-barreled electrode, Silver et al. showed that the pH reached a lower limit of 4.7 and the  $[\text{Ca}^{2+}]_e$  rose to a maximum of 40 mM in the erosion sites of the bone. It is plausible that the OCL CaSRs could be operational under such high  $[\text{Ca}^{2+}]_e$  environments despite the low pH. Future in vitro studies of OCL cultures with better controls of  $[\text{Ca}^{2+}]_e$  and pH that mimic in vivo conditions and in vivo studies of OCL-specific CaSR KO mice are required to clearly define the CaSR actions in OCLs.

## 1.10 Interplay between $\text{Ca}^{2+}/\text{CaSR}$ and PTHrP/PTH1R signaling in bone

Based on the studies reviewed above, we propose the following models for the regulation of mineral and bone metabolism by the interactions between  $\text{Ca}^{2+}/\text{CaSR}$  and PTHrP/PTH1R signaling. Under a physiological state (**Figure 1.1 A**), a normal  $\text{sCa}^{2+}$  level (①) maintains a steady supply of PTH from PTCs (②) to support basal  $\text{Ca}^{2+}$  reabsorption in the kidney (③) and  $\text{Ca}^{2+}$  absorption in the gut (via stimulation of renal 1,25D production) (④), together maintaining  $\text{Ca}^{2+}$  homeostasis at the level that meets the systemic demand. This level of PTH also supports steady bone forming activities by recruiting OB progenitors, activating bone-lining OBs, and sustaining their survival to maintain an adequate number of bone-forming cells (**Figure 1.1 A**, ⑤) [44, 157, 158, 195-200]. Through production of growth factors and/or direct physical interactions, the OBs aid in the recruitment of osteoclast precursors and their survival and differentiation (⑥) in the BRUs. The resulting bone resorbing activities liberate matrix  $\text{Ca}^{2+}$  into fluid bathing OBs and OCLs (⑦). Under conditions of  $\text{Ca}^{2+}$  sufficiency, low systemic demand of  $\text{Ca}^{2+}$  (⑩) allows retention of the liberated  $\text{Ca}^{2+}$  to increase local  $[\text{Ca}^{2+}]$  that stimulates OB maturation and their mineralizing functions to redeposit the  $\text{Ca}^{2+}$  into newly formed matrices (⑧). The increasing  $[\text{Ca}^{2+}]_e$  also feeds back to OCLs to prevent their further expansion and aberrant bone resorption (⑨). These balanced bone-forming and bone-resorbing activities sustain a steady bone turnover rate to continuously remodel the skeleton without bone loss.

In conditions of chronic  $\text{Ca}^{2+}$  deficiency (**Figure 1.1 B**), e.g., insufficient  $\text{Ca}^{2+}$  and/or vitamin D intakes, reduced  $\text{sCa}^{2+}$  levels increase PTH secretion (①) in PTGs to enhance (②) renal  $\text{Ca}^{2+}$  reabsorption (③) and 1,25D production to increase intestinal  $\text{Ca}^{2+}$  absorption in an attempt to restore  $\text{sCa}^{2+}$  levels to normal. But inadequate intestinal  $\text{Ca}^{2+}$  intakes (④) prevent such normalization and lead to chronic hypocalcemia and sustained elevation of sPTH, which drastically increases bone turnover rates (⑤-⑦). As a result, excessive bone resorption releases a large amount of  $\text{Ca}^{2+}$  (⑧), which is shunted into the circulation (⑩) to further meet the systemic demands of  $\text{Ca}^{2+}$ . Consequently, the decreasing  $[\text{Ca}^{2+}]_e$  in the BRUs retards the maturation and differentiation of the OBs as well as their mineralizing functions (⑨), leading to accumulation of unmineralized osteoid and osteomalacia. Inability of low  $[\text{Ca}^{2+}]_e$  to check on the osteoclastogenesis (⑨) further increases bone resorption and exacerbates the catabolic effects of chronic HPT.

## 1.11 Skeletal anabolism by targeting the PTH1R and CaSR in bone

Osteoporosis is a growing epidemic that afflicts aging men and women across the world [201]. iPTH is the only FDA-approved therapy that produces skeletal anabolism [43-47], but its dosing is limited to the lowest level that produces anabolic effects with an acceptable rate of hypercalcemia as an adverse effect[43, 45]. A better understanding of the mechanism underlying the anabolic effects of iPTH is needed to improve the therapy. Based on the current data, we propose that daily injections of supra-physiological doses of PTH1-34 (**Figure 1.1 C**, ②) in addition to the endogenous PTH1-84 transiently enhance calcemic activities in the kidney (③) and the gut (④) to a degree that can cause hypercalcemia and perhaps shunting of  $\text{Ca}^{2+}$  into the bone (⑩). As a result, local  $[\text{Ca}^{2+}]_e$  is elevated in the BRUs and promotes the differentiation and mineralizing functions (⑧) of the OBs recruited by the injected PTH (⑤). Although the increased OB activity is also anticipated to promote osteoclastogenesis (⑥) in the BRUs, this effect could be transient due to a short half-life of PTH (in minutes) and a negative feedback of the increasing  $[\text{Ca}^{2+}]$  (⑨) at least before the  $\text{Ca}^{2+}$  is redeposit into the matrix. The above events together give an anabolic window for a bone gain. We hypothesize that continuous infusion of PTH eventually allows osteoclastic activities to surpass the osteoblastic activities due to the enhancement of RANKL/RANK signaling, therefore producing catabolic effects on bone. According to this scheme, the efficacy of iPTH treatment will highly depend on the availability of  $\text{Ca}^{2+}$  and calcemic functions in the kidney and the intestine. This may explain for the considerably variable efficacies of the treatment in patients. This regulatory scheme also critically relies on a functional

CaSR in OBs. Indeed, a blunted anabolic effect of iPTH was recently observed in the  $^{OB}CaSR^{\Delta flox/\Delta flox}$  mice [202]. The latter study also raises the possibility of targeting the CaSRs in OBs and OCLs to enhance skeletal anabolism.

We have proposed to co-inject calcimimetics to enhance the anabolic effects of iPTH. Calcimimetics are non-ionic allosteric CaSR agonists that are being used clinically to treat HPT and hypercalcemia by potentiating extracellular  $Ca^{2+}$ -induced inhibition of PTH secretion and thereby suppressing the calciotropic actions in the kidney, intestine, and bone [203-206]. We theorize that transient activation of CaSR in PTCs with calcimimetics will dampen the secretion of endogenous PTH1-84, and therefore reduce its calciotropic activities in the kidney (③) and gut (④), therefore alleviating some of the adverse hypercalcemic effects in patients also receiving iPTH (**Figure 1.1 D**). According to our working model, the injected PTH will continue to promote OB (⑤) and then OCL activities (⑥) in the BRUs. Although a smaller increase in  $sCa^{2+}$  level is anticipated to give a less increase in local  $[Ca^{2+}]_e$  in the BRUs (⑩), when compared to iPTH treatment alone, the injected calcimimetic is anticipated to enhance the  $Ca^{2+}$ -responsiveness of OB by shifting the  $Ca^{2+}$  set-point of the CaSR to the left and therefore promote the differentiation and functions of OBs (⑧). The inhibitory actions of calcimimetics on OCL activities are anticipated to slow down bone resorption by inhibiting OCL recruitment, differentiation and survival (⑨), therefore expanding the anabolic window. The actions of both agents together are expected to produce more robust anabolism with less or no hypercalcemia. Preliminary studies indeed showed that daily co-injections of a calcimimetic, (NPS-R568, 20 nmole/kg) with PTH1-34 (40-80  $\mu$ g/kg) for 4-6 weeks in



both adult (3 months old) male and aging (12 months old) female mice (i) completely prevented the development of hypercalcemia, (ii) produced anabolic effects on trabecular bone that was 2-3 fold more robust than that with iPTH treatment alone, and (iii) produced significant anabolic effects and increased bone strength at cortical sites, which were absent with iPTH treatment alone [207]. The ability of this combined PTH/calcimimetic treatment to address the issue of hypercalcemia may allow use of higher doses of PTH to build more bone mass perhaps over a shorter time-course to minimize possible risks of osteosarcoma and make treatment more effective and cost less. Cinacalcet, an orally active calcimimetic, is approved to treat hypercalcemia in patients with primary and secondary HPT and has been in clinical use for several years. Translation of this novel combination drug strategy to human disease therapy could be facilitated.

## 1.12 Conclusion

In cartilage and bone, close complementary interactions between CaSR and PTH1R signaling are required for smooth progression of chondrocyte, OB, and OCL differentiation. Regimens with combined pharmaceuticals concurrently targeting these two receptors have the propensity of producing more robust anabolic bone effects than treatments with individual compound. However, the dosing of the compounds and timing (concurrent vs sequential) for the drug deliveries remain to be optimized. Based on their cDNA sequences, the CaSRs expressed in OBs and chondrocytes are identical to that cloned from the PTGs [29, 122]. Immunoblotting analyses, however, showed distinct glycosylation patterns of the receptor in chondrocytes and OBs compared to that in PTGs and in HEK-293 cells expressing CaSR cDNA [29]. This difference in post-translational modification could produce different pharmacological profiles of the receptor at different anatomical sites (e.g., OCLs in the resorbing pits), but this concept has not been formally addressed. In addition, the CaSR forms heteromeric complexes with type B  $\gamma$ -aminobutyric acid receptor (GABA<sub>B</sub>R1 and R2) in OBs and chondrocytes [[103], and unpublished data]. In GABA<sub>B</sub>R1-deficient chondrocytes, the ability of Ca<sup>2+</sup> to stimulate acute signaling responses was reduced significantly [103]. Since GABA<sub>B</sub>R1 and R2 are co-localized with the CaSR in many tissues at various levels [103, 104], it is plausible that different stoichiometric interactions among these receptors and perhaps with other members of family C GPCRs could produce receptor complexes with distinct pharmacological files in a cell-specific manner. These differences in receptor processing and complex formation provide opportunities for designs of tissue-specific compounds to enhance skeletal anabolism.

## 1.13 References

- [1] Civitelli R, Ziambaras K. Calcium and phosphate homeostasis: concerted interplay of new regulators. *J Endocrinol Invest* 2011;34:3-7.
- [2] Shoback D. Clinical practice. Hypoparathyroidism. *N Engl J Med* 2008;359:391-403.
- [3] Peacock M. Calcium metabolism in health and disease. *Clin J Am Soc Nephrol* 2010;5 Suppl 1:S23-30.
- [4] Makras P, Delaroudis S, Anastasilakis AD. Novel therapies for osteoporosis. *Metabolism* 2015;64:1199-214.
- [5] Reid IR. Short-term and long-term effects of osteoporosis therapies. *Nat Rev Endocrinol* 2015;11:418-28.
- [6] Hendrickx G, Boudin E, Van Hul W. A look behind the scenes: the risk and pathogenesis of primary osteoporosis. *Nat Rev Rheumatol* 2015;11:462-74.
- [7] Andreopoulou P, Bockman RS. Management of postmenopausal osteoporosis. *Annu Rev Med* 2014;66:329-42.
- [8] Chen JF, Yang KH, Zhang ZL, Chang HC, Chen Y, Sowa H, et al. A systematic review on the use of daily subcutaneous administration of teriparatide for treatment of patients with osteoporosis at high risk for fracture in Asia. *Osteoporos Int* 2014;26:11-28.
- [9] Khan TS, Fraser LA. Type 1 diabetes and osteoporosis: from molecular pathways to bone phenotype. *J Osteoporos* 2015;2015:174186.
- [10] Bandeira F, Griz LH, Bandeira C, Pinho J, Lucena CS, Alencar C, et al. Prevalence of cortical osteoporosis in mild and severe primary

hyperparathyroidism and its relationship with bone markers and vitamin D status.  
J Clin Densitom 2009;12:195-9.

- [11] Yendt ER, Kovacs KA, Jones G. Secondary hyperparathyroidism in primary osteoporosis and osteopenia: optimizing calcium and vitamin D intakes to levels recommended by expert panels may not be sufficient for correction. Clin Endocrinol (Oxf) 2008;69:855-63.
- [12] Monchik JM, Gorgun E. Normocalcemic hyperparathyroidism in patients with osteoporosis. Surgery 2004;136:1242-6.
- [13] Mazzuoli GF, D'Erasmus E, Pisani D. Primary hyperparathyroidism and osteoporosis. Aging (Milano) 1998;10:225-31.
- [14] Ray D, Goswami R, Gupta N, Tomar N, Singh N, Sreenivas V. Predisposition to vitamin D deficiency osteomalacia and rickets in females is linked to their 25(OH)D and calcium intake rather than vitamin D receptor gene polymorphism. Clin Endocrinol (Oxf) 2009;71:334-40.
- [15] Bergstrom WH. When you see rickets, consider calcium deficiency. J Pediatr 1998;133:722-4.
- [16] Wharton B, Bishop N. Rickets. Lancet 2003;362:1389-400.
- [17] Pettifor JM. Nutritional rickets: deficiency of vitamin D, calcium, or both? Am J Clin Nutr 2004;80:1725S-9S.
- [18] Holick MF. Resurrection of vitamin D deficiency and rickets. J Clin Invest 2006;116:2062-72.

- [19] Thacher T, Glew RH, Isichei C, Lawson JO, Scariano JK, Hollis BW, et al. Rickets in Nigerian children: response to calcium supplementation. *J Trop Pediatr* 1999;45:202-7.
- [20] Clark SA, Boass A, Toverud SU. Effects of high dietary contents of calcium and phosphorus on mineral metabolism and growth of vitamin D-deficient suckling and weaned rats. *Bone Miner* 1987;2:257-70.
- [21] Thacher TD. Calcium-deficiency rickets. *Endocr Dev* 2003;6:105-25.
- [22] Li YC, Pirro AE, Amling M, Dellling G, Baron R, Bronson R, et al. Targeted ablation of the vitamin D receptor: an animal model of vitamin D-dependent rickets type II with alopecia. *Proc Natl Acad Sci U S A* 1997;94:9831-5.
- [23] Li YC, Amling M, Pirro AE, Priemel M, Meuse J, Baron R, et al. Normalization of mineral ion homeostasis by dietary means prevents hyperparathyroidism, rickets, and osteomalacia, but not alopecia in vitamin D receptor-ablated mice. *Endocrinology* 1998;139:4391-6.
- [24] Amling M, Priemel M, Holzmann T, Chapin K, Rueger JM, Baron R, et al. Rescue of the skeletal phenotype of vitamin D receptor-ablated mice in the setting of normal mineral ion homeostasis: formal histomorphometric and biomechanical analyses. *Endocrinology* 1999;140:4982-7.
- [25] Brown EM. Clinical utility of calcimimetics targeting the extracellular calcium-sensing receptor (CaSR). *Biochem Pharmacol* 2010;80:297-307.
- [26] Pollak MR, Seidman CE, Brown EM. Three inherited disorders of calcium sensing. *Medicine* 1996;75:115-23.

- [27] Hannan FM, Nesbit MA, Zhang C, Cranston T, Curley AJ, Harding B, et al. Identification of 70 calcium-sensing receptor mutations in hyper- and hypo-calcaemic patients: evidence for clustering of extracellular domain mutations at calcium-binding sites. *Hum Mol Genet* 2012;21:2768-78.
- [28] Marx SJ, Simonds WF, Agarwal SK, Burns AL, Weinstein LS, Cochran C, et al. Hyperparathyroidism in hereditary syndromes: special expressions and special managements. *J Bone Miner Res* 2002;17 Suppl 2:N37-43.
- [29] Chang W, Tu C, Chen TH, Komuves L, Oda Y, Pratt SA, et al. Expression and signal transduction of calcium-sensing receptors in cartilage and bone. *Endocrinology* 1999;140:5883-93.
- [30] Goltzman D, Hendy GN. The calcium-sensing receptor in bone--mechanistic and therapeutic insights. *Nat Rev Endocrinol* 2015;11:298-307.
- [31] Riccardi D, Brennan SC, Chang W. The extracellular calcium-sensing receptor, CaSR, in fetal development. *Best Pract Res Clin Endocrinol Metab* 2013;27:443-53.
- [32] Liang N, Chen TH, Cheng Z, Li A, Santa Maria C, Tu C, et al. Calcium-sensing receptors (CaSRs) in mature osteoblasts regulate bone formation and maintenance of bone mass: studies in osteocalcin (OCN) conditional knockout mice. *J Bone Miner Res* 2012;27:Available at <http://www.asbmr.org/Meetings/AnnualMeeting/AbstractDetail.aspx?aid=51d4e88b-f79d-47e2-a15b-134f0c57b52e> .

- [33] Chang W, Tu C, Chen TH, Bikle D, Shoback D. The extracellular calcium-sensing receptor (CaSR) is a critical modulator of skeletal development. *Science signaling* 2008;1:ra1.
- [34] Brown EM, Lian JB. New insights in bone biology: unmasking skeletal effects of the extracellular calcium-sensing receptor. *Science signaling* 2008;1:pe40.
- [35] Godwin SL, Soltoff SP. Calcium-sensing receptor-mediated activation of phospholipase C-gamma1 is downstream of phospholipase C-beta and protein kinase C in MC3T3-E1 osteoblasts. *Bone* 2002;30:559-66.
- [36] Garner SC, Pi M, Tu Q, Quarles LD. Rickets in cation-sensing receptor-deficient mice: an unexpected skeletal phenotype. *Endocrinology* 2001;142:3996-4005.
- [37] Kanatani M, Sugimoto T, Kanzawa M, Yano S, Chihara K. High extracellular calcium inhibits osteoclast-like cell formation by directly acting on the calcium-sensing receptor existing in osteoclast precursor cells. *Biochem Biophys Res Commun* 1999;261:144-8.
- [38] Kameda T, Mano H, Yamada Y, Takai H, Amizuka N, Kobori M, et al. Calcium-sensing receptor in mature osteoclasts, which are bone resorbing cells. *Biochem Biophys Res Commun* 1998;245:419-22.
- [39] Onyia JE, Helvering LM, Gelbert L, Wei T, Huang S, Chen P, et al. Molecular profile of catabolic versus anabolic treatment regimens of parathyroid hormone (PTH) in rat bone: an analysis by DNA microarray. *J Cell Biochem* 2005;95:403-18.
- [40] Qin L, Raggatt LJ, Partridge NC. Parathyroid hormone: a double-edged sword for bone metabolism. *Trends Endocrinol Metab* 2004;15:60-5.

- [41] Frolik CA, Black EC, Cain RL, Satterwhite JH, Brown-Augsburger PL, Sato M, et al. Anabolic and catabolic bone effects of human parathyroid hormone (1-34) are predicted by duration of hormone exposure. *Bone* 2003;33:372-9.
- [42] Ma YL, Cain RL, Halladay DL, Yang X, Zeng Q, Miles RR, et al. Catabolic effects of continuous human PTH(1--38) in vivo is associated with sustained stimulation of RANKL and inhibition of osteoprotegerin and gene-associated bone formation. *Endocrinology* 2001;142:4047-54.
- [43] FDA. NDA#21-318: Statistical review and evaluation -- clinical studies. [http://wwwfdagov/ohrms/dockets/ac/01/briefing/3761b2\\_04\\_statisticshtm](http://wwwfdagov/ohrms/dockets/ac/01/briefing/3761b2_04_statisticshtm) 2000.
- [44] Jilka RL. Molecular and cellular mechanisms of the anabolic effect of intermittent PTH. *Bone* 2007;40:1434-46.
- [45] Neer RM, Arnaud CD, Zanchetta JR, Prince R, Gaich GA, Reginster JY, et al. Effect of parathyroid hormone (1-34) on fractures and bone mineral density in postmenopausal women with osteoporosis. *N Engl J Med* 2001;344:1434-41.
- [46] Cusano NE, Bilezikian JP. Combination anabolic and antiresorptive therapy for osteoporosis. *Endocrinol Metab Clin North Am* 2012;41:643-54.
- [47] Aslan D, Andersen MD, Gede LB, de Franca TK, Jorgensen SR, Schwarz P, et al. Mechanisms for the bone anabolic effect of parathyroid hormone treatment in humans. *Scandinavian journal of clinical and laboratory investigation* 2012;72:14-22.
- [48] Cianferotti L, Gomes AR, Fabbri S, Tanini A, Brandi ML. The calcium-sensing receptor in bone metabolism: from bench to bedside and back. *Osteoporos Int* 2015;26:2055-71.



- [49] Malesud CJ. Matrix metalloproteinases: role in skeletal development and growth plate disorders. *Front Biosci* 2006;11:1702-15.
- [50] Wu CW, Tchetina EV, Mwale F, Hasty K, Pidoux I, Reiner A, et al. Proteolysis involving matrix metalloproteinase 13 (collagenase-3) is required for chondrocyte differentiation that is associated with matrix mineralization. *J Bone Miner Res* 2002;17:639-51.
- [51] Holmbeck K, Bianco P, Caterina J, Yamada S, Kromer M, Kuznetsov SA, et al. MT1-MMP-deficient mice develop dwarfism, osteopenia, arthritis, and connective tissue disease due to inadequate collagen turnover. *Cell* 1999;99:81-92.
- [52] Tsang KY, Chan D, Cheah KS. Fate of growth plate hypertrophic chondrocytes: death or lineage extension? *Dev Growth Differ* 2015;57:179-92.
- [53] Yang L, Tsang KY, Tang HC, Chan D, Cheah KS. Hypertrophic chondrocytes can become osteoblasts and osteocytes in endochondral bone formation. *Proc Natl Acad Sci U S A* 2014;111:12097-102.
- [54] Yeung Tsang K, Wa Tsang S, Chan D, Cheah KS. The chondrocytic journey in endochondral bone growth and skeletal dysplasia. *Birth Defects Res C Embryo Today* 2014;102:52-73.
- [55] Bahney CS, Hu DP, Miclau T, 3rd, Marcucio RS. The multifaceted role of the vasculature in endochondral fracture repair. *Front Endocrinol (Lausanne)* 2015;6:4.
- [56] Xie Y, Zhou S, Chen H, Du X, Chen L. Recent research on the growth plate: Advances in fibroblast growth factor signaling in growth plate development and disorders. *J Mol Endocrinol* 2014;53:T11-34.

- [57] Jing Y, Zhou X, Han X, Jing J, von der Mark K, Wang J, et al. Chondrocytes Directly Transform into Bone Cells in Mandibular Condyle Growth. *J Dent Res* 2015.
- [58] Kronenberg HM. Developmental regulation of the growth plate. *Nature* 2003;423:332-6.
- [59] Kronenberg H, Kobayashi T. Transcriptional regulation in development of bone. *Endocrinology* 2004.
- [60] Gerstenfeld LC, Shapiro FD. Expression of bone-specific genes by hypertrophic chondrocytes: implication of the complex functions of the hypertrophic chondrocyte during endochondral bone development. *J Cell Biochem* 1996;62:1-9.
- [61] Goltzman D, Hendy GN, White JH. Vitamin D and its receptor during late development. *Biochim Biophys Acta* 2015;1849:171-80.
- [62] Huang W, Chung UI, Kronenberg HM, de Crombrughe B. The chondrogenic transcription factor Sox9 is a target of signaling by the parathyroid hormone-related peptide in the growth plate of endochondral bones. *Proc Natl Acad Sci U S A* 2001;98:160-5.
- [63] Huang W, Zhou X, Lefebvre V, de Crombrughe B. Phosphorylation of SOX9 by cyclic AMP-dependent protein kinase A enhances SOX9's ability to transactivate a Col2a1 chondrocyte-specific enhancer. *Mol Cell Biol* 2000;20:4149-58.
- [64] Iwasaki M, Le AX, Helms JA. Expression of indian hedgehog, bone morphogenetic protein 6 and gli during skeletal morphogenesis. *Mech Dev* 1997;69:197-202.

- [65] Long F, Schipani E, Asahara H, Kronenberg H, Montminy M. The CREB family of activators is required for endochondral bone development. *Development* 2001;128:541-50.
- [66] McEwen DG, Green RP, Naski MC, Towler DA, Ornitz DM. Fibroblast growth factor receptor 3 gene transcription is suppressed by cyclic adenosine 3',5'-monophosphate. Identification of a chondrocytic regulatory element. *J Biol Chem* 1999;274:30934-42.
- [67] O'Keefe RJ, Loveys LS, Hicks DG, Reynolds PR, Crabb ID, Puzas JE, et al. Differential regulation of type-II and type-X collagen synthesis by parathyroid hormone-related protein in chick growth-plate chondrocytes. *J Orthop Res* 1997;15:162-74.
- [68] Riemer S, Gebhard S, Beier F, Poschl E, von der Mark K. Role of c-fos in the regulation of type X collagen gene expression by PTH and PTHrP: localization of a PTH/PTHrP-responsive region in the human COL10A1 enhancer. *J Cell Biochem* 2002;86:688-99.
- [69] Xiao ZS, Hjelmeland AB, Quarles LD. Selective deficiency of the "bone-related" Runx2-II unexpectedly preserves osteoblast-mediated skeletogenesis. *J Biol Chem* 2004;279:20307-13.
- [70] Amizuka N, Davidson D, Liu H, Valverde-Franco G, Chai S, Maeda T, et al. Signalling by fibroblast growth factor receptor 3 and parathyroid hormone-related peptide coordinate cartilage and bone development. *Bone* 2004;34:13-25.
- [71] Barak-Shalom T, Schickler M, Knopov V, Shapira R, Hurwitz S, Pines M. Synthesis and phosphorylation of osteopontin by avian epiphyseal growth-plate

- chondrocytes as affected by differentiation. *Comp Biochem Physiol C Pharmacol Toxicol Endocrinol* 1995;111:49-59.
- [72] Chung R, Xian CJ. Recent research on the growth plate: Mechanisms for growth plate injury repair and potential cell-based therapies for regeneration. *J Mol Endocrinol* 2014;53:T45-61.
- [73] Farquharson C, Jefferies D. Chondrocytes and longitudinal bone growth: the development of tibial dyschondroplasia. *Poult Sci* 2000;79:994-1004.
- [74] Hill DJ, Logan A. Peptide growth factors and their interactions during chondrogenesis. *Prog Growth Factor Res* 1992;4:45-68.
- [75] Isgaard J, Moller C, Isaksson OG, Nilsson A, Mathews LS, Norstedt G. Regulation of insulin-like growth factor messenger ribonucleic acid in rat growth plate by growth hormone. *Endocrinology* 1988;122:1515-20.
- [76] Michigami T. Current understanding on the molecular basis of chondrogenesis. *Clin Pediatr Endocrinol* 2014;23:1-8.
- [77] Nilsson A, Isgaard J, Lindahl A, Dahlstrom A, Skottner A, Isaksson OG. Regulation by growth hormone of number of chondrocytes containing IGF-I in rat growth plate. *Science* 1986;233:571-4.
- [78] Pacifici M, Shimo T, Gentili C, Kirsch T, Freeman TA, Enomoto-Iwamoto M, et al. Syndecan-3: a cell-surface heparan sulfate proteoglycan important for chondrocyte proliferation and function during limb skeletogenesis. *J Bone Miner Metab* 2005;23:191-9.

- [79] Reddi AH, Ma SS, Cunningham NS. Induction and maintenance of new bone formation by growth and differentiation factors. *Ann Chir Gynaecol* 1988;77:189-92.
- [80] Smink JJ, Koster JG, Gresnigt MG, Rooman R, Koedam JA, Van Buul-Offers SC. IGF and IGF-binding protein expression in the growth plate of normal, dexamethasone-treated and human IGF-II transgenic mice. *J Endocrinol* 2002;175:143-53.
- [81] van der Eerden BC, Karperien M, Wit JM. Systemic and local regulation of the growth plate. *Endocr Rev* 2003;24:782-801.
- [82] Wu LN, Genge BR, Ishikawa Y, Wuthier RE. Modulation of cultured chicken growth plate chondrocytes by transforming growth factor-beta 1 and basic fibroblast growth factor. *J Cell Biochem* 1992;49:181-98.
- [83] Yoshida E, Noshiro M, Kawamoto T, Tsutsumi S, Kuruta Y, Kato Y. Direct inhibition of Indian hedgehog expression by parathyroid hormone (PTH)/PTH-related peptide and up-regulation by retinoic acid in growth plate chondrocyte cultures. *Exp Cell Res* 2001;265:64-72.
- [84] Schipani E, Mangiavini L, Merceron C. HIF-1alpha and growth plate development: what we really know. *Bonekey Rep* 2015;4:730.
- [85] Michigami T. Regulatory mechanisms for the development of growth plate cartilage. *Cell Mol Life Sci* 2013;70:4213-21.
- [86] Chagin AS, Kronenberg HM. Role of G-proteins in the differentiation of epiphyseal chondrocytes. *J Mol Endocrinol* 2014;53:R39-45.

- [87] Kronenberg HM. PTHrP and skeletal development. *Ann N Y Acad Sci* 2006;1068:1-13.
- [88] Chung UI, Lanske B, Lee K, Li E, Kronenberg H. The parathyroid hormone/parathyroid hormone-related peptide receptor coordinates endochondral bone development by directly controlling chondrocyte differentiation. *Proc Natl Acad Sci U S A* 1998;95:13030-5.
- [89] Karp SJ, Schipani E, St-Jacques B, Hunzelman J, Kronenberg H, McMahon AP. Indian hedgehog coordinates endochondral bone growth and morphogenesis via parathyroid hormone related-protein-dependent and -independent pathways. *Development* 2000;127:543-8.
- [90] Weir EC, Philbrick WM, Amling M, Neff LA, Baron R, Broadus AE. Targeted overexpression of parathyroid hormone-related peptide in chondrocytes causes chondrodysplasia and delayed endochondral bone formation. *Proc Natl Acad Sci U S A* 1996;93:10240-5.
- [91] Abou-Samra AB, Juppner H, Force T, Freeman MW, Kong XF, Schipani E, et al. Expression cloning of a common receptor for parathyroid hormone and parathyroid hormone-related peptide from rat osteoblast-like cells: a single receptor stimulates intracellular accumulation of both cAMP and inositol trisphosphates and increases intracellular free calcium. *Proc Natl Acad Sci U S A* 1992;89:2732-6.
- [92] Bastepe M, Weinstein LS, Ogata N, Kawaguchi H, Juppner H, Kronenberg HM, et al. Stimulatory G protein directly regulates hypertrophic differentiation of growth plate cartilage in vivo. *Proc Natl Acad Sci U S A* 2004;101:14794-9.

- [93] Lanske B, Karaplis AC, Lee K, Luz A, Vortkamp A, Pirro A, et al. PTH/PTHrP receptor in early development and Indian hedgehog-regulated bone growth. *Science* 1996;273:663-6.
- [94] Lanske B, Amling M, Neff L, Guiducci J, Baron R, Kronenberg HM. Ablation of the PTHrP gene or the PTH/PTHrP receptor gene leads to distinct abnormalities in bone development. *J Clin Invest* 1999;104:399-407.
- [95] Matta C, Mobasher A. Regulation of chondrogenesis by protein kinase C: Emerging new roles in calcium signalling. *Cell Signal* 2014;26:979-1000.
- [96] Nurminsky D, Magee C, Faverman L, Nurminskaya M. Regulation of chondrocyte differentiation by actin-severing protein adseverin. *Dev Biol* 2007;302:427-37.
- [97] Guo J, Chung UI, Kondo H, Bringhurst FR, Kronenberg HM. The PTH/PTHrP receptor can delay chondrocyte hypertrophy in vivo without activating phospholipase C. *Dev Cell* 2002;3:183-94.
- [98] Chang W, Shoback D. Extracellular Ca<sup>2+</sup>-sensing receptors--an overview. *Cell Calcium* 2004;35:183-96.
- [99] Conigrave AD, Ward DT. Calcium-sensing receptor (CaSR): pharmacological properties and signaling pathways. *Best Pract Res Clin Endocrinol Metab* 2013;27:315-31.
- [100] Bai M. Dimerization of G-protein-coupled receptors: roles in signal transduction. *Cell Signal* 2004;16:175-86.
- [101] Pin JP, Galvez T, Prezeau L. Evolution, structure, and activation mechanism of family 3/C G-protein-coupled receptors. *Pharmacol Ther* 2003;98:325-54.

- [102] Gama L, Wilt SG, Breitwieser GE. Heterodimerization of calcium sensing receptors with metabotropic glutamate receptors in neurons. *J Biol Chem* 2001;276:39053-9.
- [103] Cheng Z, Tu C, Rodriguez L, Chen TH, Dvorak MM, Margeta M, et al. Type B gamma-aminobutyric acid receptors modulate the function of the extracellular Ca<sup>2+</sup>-sensing receptor and cell differentiation in murine growth plate chondrocytes. *Endocrinology* 2007;148:4984-92.
- [104] Chang W, Tu C, Cheng Z, Rodriguez L, Chen TH, Gassmann M, et al. Complex formation with the Type B gamma-aminobutyric acid receptor affects the expression and signal transduction of the extracellular calcium-sensing receptor. Studies with HEK-293 cells and neurons. *J Biol Chem* 2007;282:25030-40.
- [105] Brown E, Enyedi P, LeBoff M, Rotberg J, Preston J, Chen C. High extracellular Ca<sup>2+</sup> and Mg<sup>2+</sup> stimulate accumulation of inositol phosphates in bovine parathyroid cells. *FEBS Lett* 1987;218:113-8.
- [106] Shoback D, Thatcher J, Leombruno R, Brown E. Effects of extracellular Ca<sup>++</sup> and Mg<sup>++</sup> on cytosolic Ca<sup>++</sup> and PTH release in dispersed bovine parathyroid cells. *Endocrinology* 1983;113:424-6.
- [107] Tu CL, Oda Y, Komuves L, Bikle DD. The role of the calcium-sensing receptor in epidermal differentiation. *Cell Calcium* 2004;35:265-73.
- [108] Chang W, Pratt S, Chen TH, Nemeth E, Huang Z, Shoback D. Coupling of calcium receptors to inositol phosphate and cyclic AMP generation in mammalian cells and *Xenopus laevis* oocytes and immunodetection of receptor protein by region-specific antipeptide antisera. *J Bone Miner Res* 1998;13:570-80.



- [109] Wettschureck N, Lee E, Libutti SK, Offermanns S, Robey PG, Spiegel AM. Parathyroid-specific double knockout of Gq and G11 alpha-subunits leads to a phenotype resembling germline knockout of the extracellular Ca<sup>2+</sup>-sensing receptor. *Mol Endocrinol* 2007;21:274-80.
- [110] Chen CJ, Barnett JV, Congo DA, Brown EM. Divalent cations suppress 3',5'-adenosine monophosphate accumulation by stimulating a pertussis toxin-sensitive guanine nucleotide-binding protein in cultured bovine parathyroid cells. *Endocrinology* 1989;124:233-9.
- [111] Avlani VA, Ma W, Mun HC, Leach K, Delbridge L, Christopoulos A, et al. Calcium-sensing receptor-dependent activation of CREB phosphorylation in HEK293 cells and human parathyroid cells. *Am J Physiol Endocrinol Metab*;304:E1097-104.
- [112] Kifor O, Diaz R, Butters R, Kifor I, Brown EM. The calcium-sensing receptor is localized in caveolin-rich plasma membrane domains of bovine parathyroid cells. *J Biol Chem* 1998;273:21708-13.
- [113] Pi M, Quarles LD. Osteoblast calcium-sensing receptor has characteristics of ANF/7TM receptors. *J Cell Biochem* 2005;95:1081-92.
- [114] Fromigue O, Hay E, Barbara A, Petrel C, Traiffort E, Ruat M, et al. Calcium sensing receptor-dependent and receptor-independent activation of osteoblast replication and survival by strontium ranelate. *J Cell Mol Med* 2009;13:2189-99.
- [115] Goolam MA, Ward JH, Avlani VA, Leach K, Christopoulos A, Conigrave AD. Roles of intraloops-2 and -3 and the proximal C-terminus in signalling pathway selection from the human calcium-sensing receptor. *FEBS Lett* 2014;588:3340-6.

- [116] Davey AE, Leach K, Valant C, Conigrave AD, Sexton PM, Christopoulos A. Positive and negative allosteric modulators promote biased signaling at the calcium-sensing receptor. *Endocrinology* 2012;153:1232-41.
- [117] Thomsen AR, Hvidtfeldt M, Brauner-Osborne H. Biased agonism of the calcium-sensing receptor. *Cell Calcium* 2011;51:107-16.
- [118] Rybchyn MS, Slater M, Conigrave AD, Mason RS. An Akt-dependent increase in canonical Wnt signaling and a decrease in sclerostin protein levels are involved in strontium ranelate-induced osteogenic effects in human osteoblasts. *J Biol Chem* 2011;286:23771-9.
- [119] Brennan TC, Rybchyn MS, Green W, Atwa S, Conigrave AD, Mason RS. Osteoblasts play key roles in the mechanisms of action of strontium ranelate. *Br J Pharmacol* 2009;157:1291-300.
- [120] Huang C, Hujer KM, Wu Z, Miller RT. The Ca<sup>2+</sup>-sensing receptor couples to G<sub>α12/13</sub> to activate phospholipase D in Madin-Darby canine kidney cells. *Am J Physiol Cell Physiol* 2004;286:C22-30.
- [121] Goltzman D, Miao D, Panda DK, Hendy GN. Effects of calcium and of the Vitamin D system on skeletal and calcium homeostasis: lessons from genetic models. *J Steroid Biochem Mol Biol* 2004;89-90:485-9.
- [122] Rodriguez L, Tu C, Cheng Z, Chen TH, Bikle D, Shoback D, et al. Expression and functional assessment of an alternatively spliced extracellular Ca<sup>2+</sup>-sensing receptor in growth plate chondrocytes. *Endocrinology* 2005;146:5294-303.

- [123] Rodriguez L, Cheng Z, Chen TH, Tu C, Chang W. Extracellular calcium and parathyroid hormone-related peptide signaling modulate the pace of growth plate chondrocyte differentiation. *Endocrinology* 2005;146:4597-608.
- [124] Chang W, Tu C, Bajra R, Komuves L, Miller S, Strewler G, et al. Calcium sensing in cultured chondrogenic RCJ3.1C5.18 cells. *Endocrinology* 1999;140:1911-9.
- [125] Bonen DK, Schmid TM. Elevated extracellular calcium concentrations induce type X collagen synthesis in chondrocyte cultures. *J Cell Biol* 1991;115:1171-8.
- [126] Chang W, Tu C, Pratt S, Chen TH, Shoback D. Extracellular Ca(2+)-sensing receptors modulate matrix production and mineralization in chondrogenic RCJ3.1C5.18 cells. *Endocrinology* 2002;143:1467-74.
- [127] Wu S, Palese T, Mishra OP, Delivoria-Papadopoulos M, De Luca F. Effects of Ca<sup>2+</sup> sensing receptor activation in the growth plate. *FASEB J* 2004;18:143-5.
- [128] Ho C, Conner DA, Pollak MR, Ladd DJ, Kifor O, Warren HB, et al. A mouse model of human familial hypocalciuric hypercalcemia and neonatal severe hyperparathyroidism. *Nat Genet* 1995;11:389-94.
- [129] Tu Q, Pi M, Karsenty G, Simpson L, Liu S, Quarles LD. Rescue of the skeletal phenotype in CasR-deficient mice by transfer onto the Gcm2 null background. *J Clin Invest* 2003;111:1029-37.
- [130] Kos CH, Karaplis AC, Peng JB, Hediger MA, Goltzman D, Mohammad KS, et al. The calcium-sensing receptor is required for normal calcium homeostasis independent of parathyroid hormone. *J Clin Invest* 2003;111:1021-8.
- [131] Pi M, Zhang L, Lei SF, Huang MZ, Zhu W, Zhang J, et al. Impaired osteoblast function in GPRC6A null mice. *J Bone Miner Res* 2010;25:1092-102.

- [132] Pi M, Quarles LD. A novel cation-sensing mechanism in osteoblasts is a molecular target for strontium. *J Bone Miner Res* 2004;19:862-9.
- [133] Oda Y, Tu CL, Pillai S, Bikle DD. The calcium sensing receptor and its alternatively spliced form in keratinocyte differentiation. *J Biol Chem* 1998;273:23344-52.
- [134] Ovchinnikov DA, Deng JM, Ogunrinu G, Behringer RR. Col2a1-directed expression of Cre recombinase in differentiating chondrocytes in transgenic mice. *Genesis* 2000;26:145-6.
- [135] Peacock JD, Levay AK, Gillaspie DB, Tao G, Lincoln J. Reduced sox9 function promotes heart valve calcification phenotypes in vivo. *Circ Res* 2010;106:712-9.
- [136] Lincoln J, Alfieri CM, Yutzey KE. Development of heart valve leaflets and supporting apparatus in chicken and mouse embryos. *Dev Dyn* 2004;230:239-50.
- [137] Lopez D, Duran AC, Sans-Coma V. Formation of cartilage in cardiac semilunar valves of chick and quail. *Ann Anat* 2000;182:349-59.
- [138] Swiderski RE, Daniels KJ, Jensen KL, Solursh M. Type II collagen is transiently expressed during avian cardiac valve morphogenesis. *Dev Dyn* 1994;200:294-304.
- [139] Nakamura E, Nguyen MT, Mackem S. Kinetics of tamoxifen-regulated Cre activity in mice using a cartilage-specific CreER(T) to assay temporal activity windows along the proximodistal limb skeleton. *Dev Dyn* 2006;235:2603-12.
- [140] Wang Y, Cheng Z, Elalieh HZ, Nakamura E, Nguyen MT, Mackem S, et al. IGF-1R signaling in chondrocytes modulates growth plate development by interacting with the PTHrP/Ihh pathway. *J Bone Miner Res* 2011;26:1437-46.

- [141] Mizoguchi T, Pinho S, Ahmed J, Kunisaki Y, Hanoun M, Mendelson A, et al. Osterix marks distinct waves of primitive and definitive stromal progenitors during bone marrow development. *Dev Cell* 2014;29:340-9.
- [142] Liu Y, Strecker S, Wang L, Kronenberg MS, Wang W, Rowe DW, et al. Osterix-cre labeled progenitor cells contribute to the formation and maintenance of the bone marrow stroma. *PLoS One* 2013;8:e71318.
- [143] Miao D, He B, Karaplis AC, Goltzman D. Parathyroid hormone is essential for normal fetal bone formation. *J Clin Invest* 2002;109:1173-82.
- [144] Saini V, Marengi DA, Barry KJ, Fulzele KS, Heiden E, Liu X, et al. Parathyroid hormone (PTH)/PTH-related peptide type 1 receptor (PPR) signaling in osteocytes regulates anabolic and catabolic skeletal responses to PTH. *J Biol Chem* 2013;288:20122-34.
- [145] Rhee Y, Allen MR, Condon K, Lezcano V, Ronda AC, Galli C, et al. PTH receptor signaling in osteocytes governs periosteal bone formation and intracortical remodeling. *J Bone Miner Res* 2011;26:1035-46.
- [146] O'Brien CA, Plotkin LI, Galli C, Goellner JJ, Gortazar AR, Allen MR, et al. Control of bone mass and remodeling by PTH receptor signaling in osteocytes. *PLoS One* 2008;3:e2942.
- [147] Ishizuya T, Yokose S, Hori M, Noda T, Suda T, Yoshiki S, et al. Parathyroid hormone exerts disparate effects on osteoblast differentiation depending on exposure time in rat osteoblastic cells. *J Clin Invest* 1997;99:2961-70.
- [148] Koh AJ, Beecher CA, Rosol TJ, McCauley LK. 3',5'-Cyclic adenosine monophosphate activation in osteoblastic cells: effects on parathyroid hormone-1

- receptors and osteoblastic differentiation in vitro. *Endocrinology* 1999;140:3154-62.
- [149] Zerega B, Cermelli S, Bianco P, Cancedda R, Cancedda FD. Parathyroid hormone [PTH(1-34)] and parathyroid hormone-related protein [PTHrP(1-34)] promote reversion of hypertrophic chondrocytes to a prehypertrophic proliferating phenotype and prevent terminal differentiation of osteoblast-like cells. *J Bone Miner Res* 1999;14:1281-9.
- [150] van der Horst G, Farih-Sips H, Lowik CW, Karperien M. Multiple mechanisms are involved in inhibition of osteoblast differentiation by PTHrP and PTH in KS483 Cells. *J Bone Miner Res* 2005;20:2233-44.
- [151] Choudhary S, Huang H, Raisz L, Pilbeam C. Anabolic effects of PTH in cyclooxygenase-2 knockout osteoblasts in vitro. *Biochem Biophys Res Commun* 2008;372:536-41.
- [152] Wang Y, Menendez A, Fong CT, Elalieh HZ, Chang W, Bikle DD. Ephrin B2/EphB4 mediates the actions of IGF-I signaling in regulating endochondral bone formation. *J Bone Miner Res* 2014;In Press.
- [153] Matsuo K, Otaki N. Bone cell interactions through Eph/ephrin: bone modeling, remodeling and associated diseases. *Cell adhesion & migration* 2012;6:148-56.
- [154] Greenfield EM. Anabolic effects of intermittent PTH on osteoblasts. *Current molecular pharmacology* 2012;5:127-34.
- [155] Bikle DD, Wang Y. Insulin like growth factor-I: a critical mediator of the skeletal response to parathyroid hormone. *Current molecular pharmacology* 2012;5:135-42.

- [156] Bikle DD. Growth hormone/insulin-like growth factor-1/PTH axis in bone. *J Bone Miner Res* 2008;23:581-3.
- [157] Yakar S, Bouxsein ML, Canalis E, Sun H, Glatt V, Gundberg C, et al. The ternary IGF complex influences postnatal bone acquisition and the skeletal response to intermittent parathyroid hormone. *J Endocrinol* 2006;189:289-99.
- [158] Fei Y, Xiao L, Hurley MM. The impaired bone anabolic effect of PTH in the absence of endogenous FGF2 is partially due to reduced ATF4 expression. *Biochem Biophys Res Commun* 2011;412:160-4.
- [159] Fei Y, Hurley MM. Role of fibroblast growth factor 2 and Wnt signaling in anabolic effects of parathyroid hormone on bone formation. *J Cell Physiol* 2012;227:3539-45.
- [160] Bergenstock MK, Partridge NC. Parathyroid hormone stimulation of noncanonical Wnt signaling in bone. *Ann N Y Acad Sci* 2007;1116:354-9.
- [161] Canalis E. Update in new anabolic therapies for osteoporosis. *J Clin Endocrinol Metab* 2010;95:1496-504.
- [162] Kramer I, Keller H, Leupin O, Kneissel M. Does osteocytic SOST suppression mediate PTH bone anabolism? *Trends Endocrinol Metab* 2010;21:237-44.
- [163] Lee M, Partridge NC. Parathyroid hormone signaling in bone and kidney. *Curr Opin Nephrol Hypertens* 2009;18:298-302.
- [164] Bonnet N, Conway SJ, Ferrari SL. Regulation of beta catenin signaling and parathyroid hormone anabolic effects in bone by the extracellular matrix protein periostin. *Proc Natl Acad Sci U S A* 2012;109:15048-53.

- [165] Hanyu R, Wehbi VL, Hayata T, Moriya S, Feinstein TN, Ezura Y, et al. Anabolic action of parathyroid hormone regulated by the beta2-adrenergic receptor. *Proc Natl Acad Sci U S A* 2012;109:7433-8.
- [166] Josse R, Khan A, Ngui D, Shapiro M. Denosumab, a new pharmacotherapy option for postmenopausal osteoporosis. *Curr Med Res Opin* 2013;29:205-16.
- [167] Sutton EE, Riche DM. Denosumab, a RANK ligand inhibitor, for postmenopausal women with osteoporosis. *The Annals of pharmacotherapy* 2012;46:1000-9.
- [168] Lewiecki EM, Bilezikian JP. Denosumab for the treatment of osteoporosis and cancer-related conditions. *Clinical pharmacology and therapeutics* 2012;91:123-33.
- [169] Johnson GL. Denosumab (prolia) for treatment of postmenopausal osteoporosis. *American family physician* 2012;85:334-6.
- [170] Dempster DW, Laming CL, Kostenuik PJ, Grauer A. Role of RANK ligand and denosumab, a targeted RANK ligand inhibitor, in bone health and osteoporosis: a review of preclinical and clinical data. *Clinical therapeutics* 2012;34:521-36.
- [171] Crane JL, Cao X. Bone marrow mesenchymal stem cells and TGF-beta signaling in bone remodeling. *J Clin Invest* 2014;124:466-72.
- [172] Crane JL, Cao X. Function of matrix IGF-1 in coupling bone resorption and formation. *Journal of molecular medicine* 2014;92:107-15.
- [173] Silver IA, Murrills RJ, Etherington DJ. Microelectrode studies on the acid microenvironment beneath adherent macrophages and osteoclasts. *Exp Cell Res* 1988;175:266-76.



- [174] Riccardi D, Kemp PJ. The calcium-sensing receptor beyond extracellular calcium homeostasis: conception, development, adult physiology, and disease. *Annu Rev Physiol* 2012;74:271-97.
- [175] Dvorak-Ewell MM, Chen TH, Liang N, Garvey C, Liu B, Tu C, et al. Osteoblast extracellular Ca<sup>2+</sup>-sensing receptor regulates bone development, mineralization, and turnover. *J Bone Miner Res* 2011;26:2935-47.
- [176] Chang W, Dvorak M, Shoback D. Assessing constitutive activity of extracellular calcium-sensing receptors in vitro and in bone. *Methods Enzymol* 2010;484:253-66.
- [177] Dvorak MM, Chen TH, Orwoll B, Garvey C, Chang W, Bikle DD, et al. Constitutive activity of the osteoblast Ca<sup>2+</sup>-sensing receptor promotes loss of cancellous bone. *Endocrinology* 2007;148:3156-63.
- [178] Dvorak MM, Siddiqua A, Ward DT, Carter DH, Dallas SL, Nemeth EF, et al. Physiological changes in extracellular calcium concentration directly control osteoblast function in the absence of calciotropic hormones. *Proc Natl Acad Sci U S A* 2004;101:5140-5.
- [179] Marie PJ. The calcium-sensing receptor in bone cells: a potential therapeutic target in osteoporosis. *Bone* 2010;46:571-6.
- [180] Chattopadhyay N, Yano S, Tfelt-Hansen J, Rooney P, Kanuparthi D, Bandyopadhyay S, et al. Mitogenic action of calcium-sensing receptor on rat calvarial osteoblasts. *Endocrinology* 2004;145:3451-62.
- [181] Marie PJ. The calcium-sensing receptor in bone cells: A potential therapeutic target in osteoporosis. *Bone* 2009.

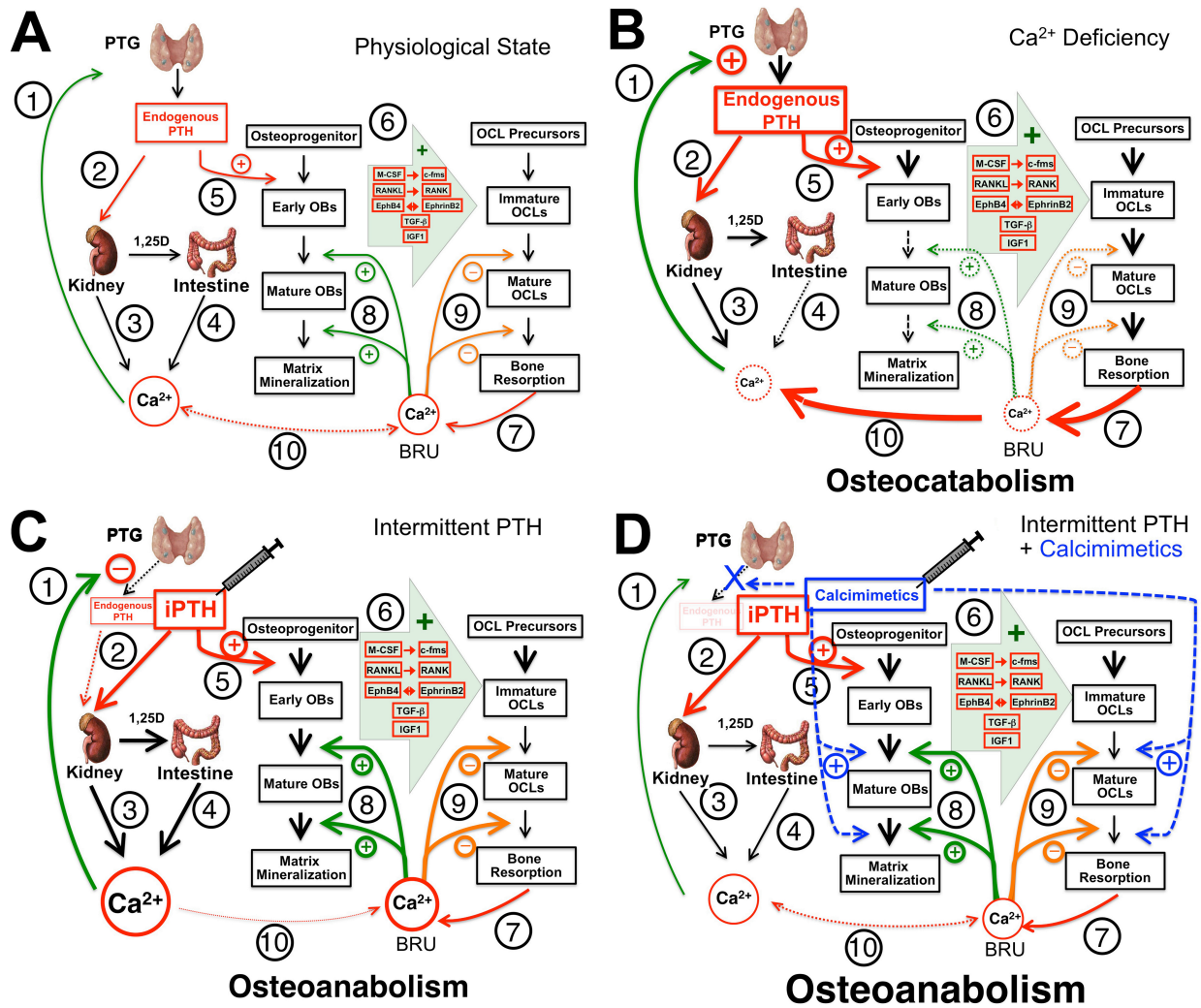
- [182] Ye CP, Yamaguchi T, Chattopadhyay N, Sanders JL, Vassilev PM, Brown EM. Extracellular calcium-sensing-receptor (CaR)-mediated opening of an outward K(+) channel in murine MC3T3-E1 osteoblastic cells: evidence for expression of a functional CaR. *Bone* 2000;27:21-7.
- [183] Hu F, Pan L, Zhang K, Xing F, Wang X, Lee I, et al. Elevation of extracellular Ca<sup>2+</sup> induces store-operated calcium entry via calcium-sensing receptors: a pathway contributes to the proliferation of osteoblasts. *PLoS One* 2014;9:e107217.
- [184] Ho C, Conner DA, Pollak MR, Ladd DJ, Kifor O, Warren HB, et al. A mouse model of human familial hypocalciuric hypercalcemia and neonatal severe hyperparathyroidism [see comments]. *Nat Genet* 1995;11:389-94.
- [185] Liu F, Woitge HW, Braut A, Kronenberg MS, Lichtler AC, Mina M, et al. Expression and activity of osteoblast-targeted Cre recombinase transgenes in murine skeletal tissues. *Int J Dev Biol* 2004;48:645-53.
- [186] Datta HK, MacIntyre I, Zaidi M. The effect of extracellular calcium elevation on morphology and function of isolated rat osteoclasts. *Biosci Rep* 1989;9:747-51.
- [187] Malgaroli A, Meldolesi J, Zallone AZ, Teti A. Control of cytosolic free calcium in rat and chicken osteoclasts. The role of extracellular calcium and calcitonin. *J Biol Chem* 1989;264:14342-7.
- [188] Zaidi M, Kerby J, Huang CL, Alam T, Rathod H, Chambers TJ, et al. Divalent cations mimic the inhibitory effect of extracellular ionised calcium on bone resorption by isolated rat osteoclasts: further evidence for a "calcium receptor". *J Cell Physiol* 1991;149:422-7.

- [189] Mentaverri R, Yano S, Chattopadhyay N, Petit L, Kifor O, Kamel S, et al. The calcium sensing receptor is directly involved in both osteoclast differentiation and apoptosis. *FASEB J* 2006;20:2562-4.
- [190] House MG, Kohlmeier L, Chattopadhyay N, Kifor O, Yamaguchi T, Leboff MS, et al. Expression of an extracellular calcium-sensing receptor in human and mouse bone marrow cells. *J Bone Miner Res* 1997;12:1959-70.
- [191] Bennett BD, Alvarez U, Hruska KA. Receptor-operated osteoclast calcium sensing. *Endocrinology* 2001;142:1968-74.
- [192] Shalhoub V, Grisanti M, Padagas J, Scully S, Rattan A, Qi M, et al. In vitro studies with the calcimimetic, cinacalcet HCl, on normal human adult osteoblastic and osteoclastic cells. *Crit Rev Eukaryot Gene Expr* 2003;13:89-106.
- [193] Gowen M, Stroup GB, Dodds RA, James IE, Votta BJ, Smith BR, et al. Antagonizing the parathyroid calcium receptor stimulates parathyroid hormone secretion and bone formation in osteopenic rats. *J Clin Invest* 2000;105:1595-604.
- [194] Quinn SJ, Bai M, Brown EM. pH Sensing by the calcium-sensing receptor. *J Biol Chem* 2004;279:37241-9.
- [195] Zhu J, Siclari VA, Liu F, Spatz JM, Chandra A, Divieti Pajevic P, et al. Amphiregulin-EGFR signaling mediates the migration of bone marrow mesenchymal progenitors toward PTH-stimulated osteoblasts and osteocytes. *PLoS One* 2012;7:e50099.
- [196] Li JY, Adams J, Calvi LM, Lane TF, DiPaolo R, Weitzmann MN, et al. PTH expands short-term murine hemopoietic stem cells through T cells. *Blood* 2012;120:4352-62.

- [197] Alvarez MB, Childress P, Philip BK, Gerard-O'Riley R, Hanlon M, Herbert BS, et al. Immortalization and characterization of osteoblast cell lines generated from wild-type and Nmp4-null mouse bone marrow stromal cells using murine telomerase reverse transcriptase (mTERT). *J Cell Physiol* 2012;227:1873-82.
- [198] Datta NS, Kolailat R, Fite A, Pettway G, Abou-Samra AB. Distinct roles for mitogen-activated protein kinase phosphatase-1 (MKP-1) and ERK-MAPK in PTH1R signaling during osteoblast proliferation and differentiation. *Cell Signal* 2010;22:457-66.
- [199] Rickard DJ, Wang FL, Rodriguez-Rojas AM, Wu Z, Trice WJ, Hoffman SJ, et al. Intermittent treatment with parathyroid hormone (PTH) as well as a non-peptide small molecule agonist of the PTH1 receptor inhibits adipocyte differentiation in human bone marrow stromal cells. *Bone* 2006;39:1361-72.
- [200] Kim SH, Jun S, Jang HS, Lim SK. Identification of parathyroid hormone-regulated proteins in mouse bone marrow cells by proteomics. *Biochem Biophys Res Commun* 2005;330:423-9.
- [201] National Osteoporosis Foundation. What is Osteoporosis? <http://noforg/articles/7> 2014.
- [202] Al-Dujaili SA, Koh AJ, Dang M, Mi X, Chang W, Ma P, et al. Calcium sensing receptor function supports osteoblast survival and acts as a co-factor in PTH anabolic actions in bone. *J Cell Biochem* 2015;(in press).
- [203] Wesseling-Perry K, Salusky IB. Phosphate binders, vitamin D and calcimimetics in the management of chronic kidney disease-mineral bone disorders (CKD-MBD) in children. *Pediatr Nephrol* 2013;28:617-25.

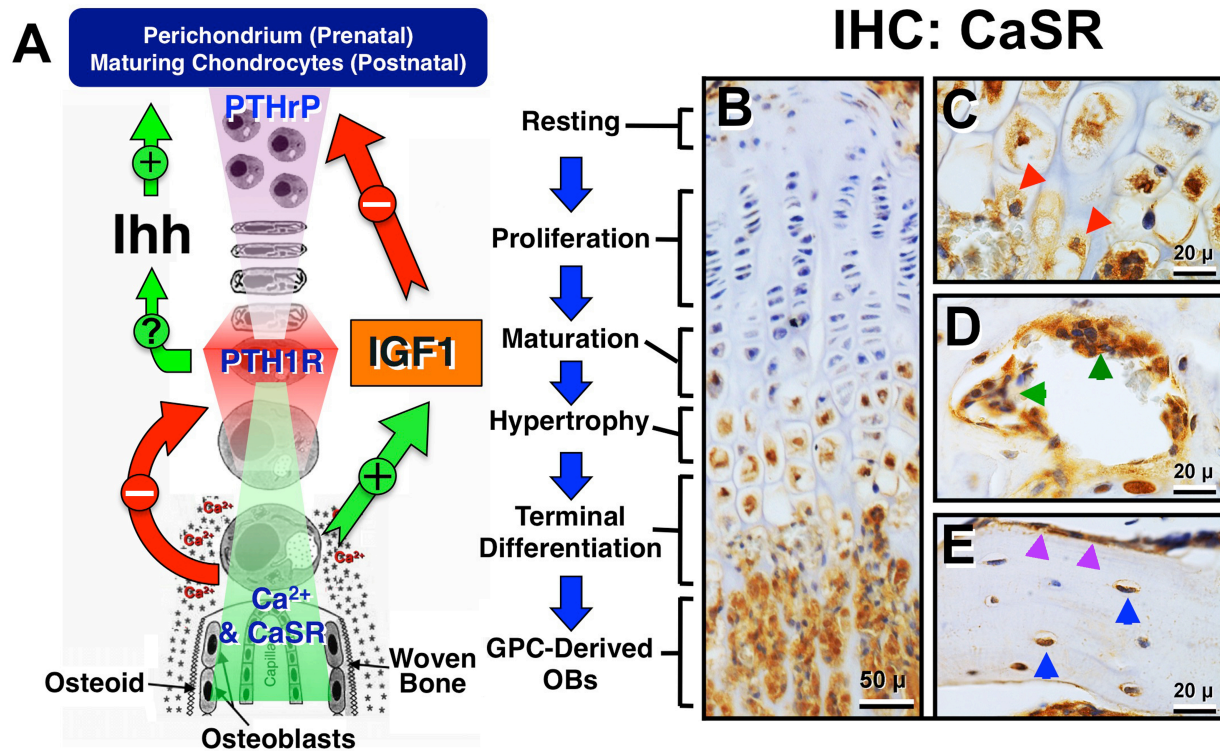
- [204] Verheyen N, Pilz S, Eller K, Kienreich K, Fahrleitner-Pammer A, Pieske B, et al. Cinacalcet hydrochloride for the treatment of hyperparathyroidism. Expert opinion on pharmacotherapy 2013;14:793-806.
- [205] Palmer SC, Nistor I, Craig JC, Pellegrini F, Messa P, Tonelli M, et al. Cinacalcet in patients with chronic kidney disease: a cumulative meta-analysis of randomized controlled trials. PLoS medicine 2013;10:e1001436.
- [206] Nemeth EF, Shoback D. Calcimimetic and calcilytic drugs for treating bone and mineral-related disorders. Best Pract Res Clin Endocrinol Metab 2013;27:373-84.
- [207] Santa Maria C, Li A, Cheng Z, Song F, Shoback D, Tu C-L, et al. Skeletal Anabolism By Concurrently Targeting the PTH1R and CaSR. ASBMR Annual Meeting, Seattle, USA 2015.

**Figure 1.1**



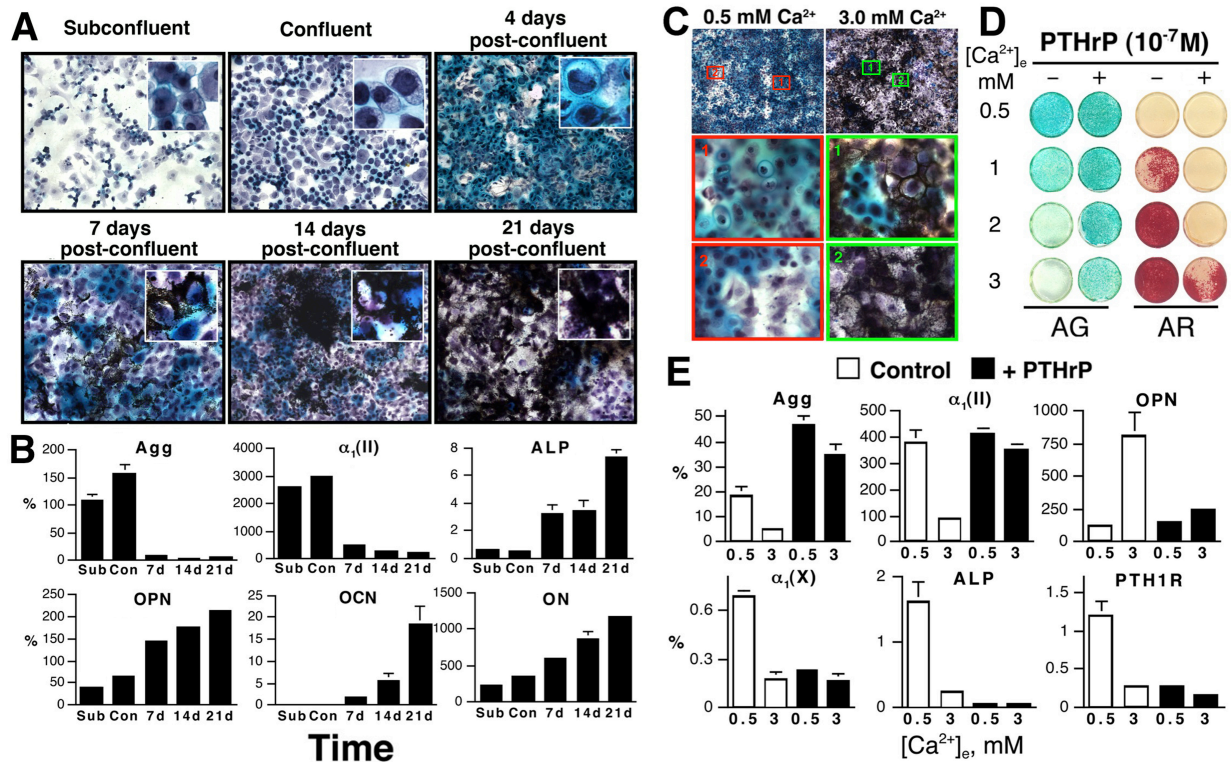
**Figure 1.1.** Schemas for the actions of PTH/PTH1R and Ca<sup>2+</sup>/CaSR signaling in the regulation of mineral and skeletal metabolism under (A) a physiological state and (B) Ca<sup>2+</sup> deficiency and its responses to (C) iPTH or (D) combined iPTH and calcimimetics treatment. See the text for detailed descriptions.

Figure 1.2



**Figure 1.2.** (A) A schema for growth plate chondrocyte differentiation and its regulation by PTHrP/PTH1R/Ihh, IGF1/IGF1R, and Ca<sup>2+</sup>/CaSR signaling pathways. See the text for detailed descriptions. (B-E) Immunohistochemical (IHC) detection of CaSR protein in (B) mouse growth plate and primary spongiosa; (C) chondro-osseous junction; (D) resorbing pits in the secondary spongiosa, and (E) cortical bone of the tibia. Red, green, purple, blue arrowheads depict terminally differentiated chondrocyte being released from cartilage matrix in (C), osteoclasts in (D), and bone-lining OBs and osteocytes in (E), respectively.

**Figure 1.3**



**Figure 1.3.** Direct actions of  $\text{Ca}^{2+}$  and CaSR on chondrocyte differentiation (A) PG accumulation and mineral deposition by Alcian green and von Kossa staining, respectively, in mouse GPCs cultured for different times. Cultures were counterstained with hematoxylin. Insets: high-power (100x) views. (B) RNA levels, assessed by q-PCR, for Agg, and  $\alpha_1(\text{II})$ , ALP, OPN, OCN, and ON, in mouse GPCs cultured for various times [subconfluent (Sub), confluent (Con), 7, 14, and 21 days post-confluence]. The level of gene is expressed as “%” of L19 expression. (C) Effects of different  $[\text{Ca}^{2+}]_e$  on proteoglycans (PG) accumulation, mineralization in mouse GPCs cultured at 0.5 or 3.0 mM  $\text{Ca}^{2+}$  for 14 days after confluence and viewed at 20x and 100x in upper and 2 lower panels, respectively. (D) PG accumulation and mineral accumulation assessed by Alcian green and Alizarin red staining, respectively, and (E) RNA expression assessed by qPCR in mouse GPCs cultured at different  $[\text{Ca}^{2+}]_e$  (0.5 to 3.0 mM) in the absence (-) or presence (+) of  $10^{-7}$  M PTHrP for 14 days. RNA levels are presented as the percentage of ribosomal L19 gene expression.



## **Chapter 2:**

# **Enhanced Skeletal Anabolism by Targeting the Parathyroid Hormone-1 Receptor (PTH1R) and Extracellular Calcium-Sensing Receptor (CaSR)**

## 2.1 Introduction

The incidence of osteoporosis is rising dramatically in aging societies across the globe. At present,  $\approx 10$  million Americans have osteoporosis [1]. This number is expected to reach 12 million by 2025 [2]. Osteoporosis is predicted to cause 3 million fractures and incur \$25 billion in costs each year [2]. Hip fractures cause the most dramatic morbidity and mortality. Within the first year of a hip fracture, overall mortality is 18% (but mortality rates reach as high as 30% in men) [3-5]. Disability rates of post-hip fractures are also startlingly high. 30% of patients are permanently disabled; 40% are unable to walk independently again; and 80% lose the ability to perform at least one key activity of daily living [1]. Thus, such fractures greatly impact the survival and quality of life of elderly people and impose steep financial and emotional burdens on society.

Bisphosphonates are the current first-choice drugs for various diseases associated with enhanced bone resorption, including osteoporosis [6,7]. These drugs promote apoptosis of osteoclasts (OCLs), thereby suppressing bone resorption [8]. This mechanism of action interferes with bone remodeling, which requires a precise coupling of osteoblast (OB) and OCL activities. Thus, skeletal adaptation and repair in response to changes in mechanical signals and/or the accumulation of microdamage is impaired. This may ultimately weaken the structural integrity of bone and cause possible long-term complications of chronic anti-resorptive therapy, including osteonecrosis of the jaw and atypical femoral fractures [9-12]. Such pitfalls of therapy, although rare, fuel the search for regimens to promote formation of bone with strong mechanical properties.

To date, once-daily injections of PTH(1-34) or Teriparatide, comprising the first 34 amino acids of full-length PTH [PTH(1-84)], is a mainstay treatment available in the US that has skeletal anabolic effects to treat osteoporosis by stimulating bone remodeling. This regimen administered under  $\text{Ca}^{2+}$ -sufficient conditions (i.e. with  $\text{Ca}^{2+}$  and Vitamin D supplementation) increases trabecular bone mass in normal and osteoporotic animal models and in patients [13-17]. The osteoanabolism of PTH occurs in an “anabolic window” when bone-forming activities of OBs exceed the bone resorbing activities of OCLs at the beginning of treatment. While PTH increases bone turnover, it also improves the microarchitecture by remodeling damaged bone. The anabolic actions of PTH are site-dependent. Anabolism of PTH(1-34) in trabecular-rich vertebral bodies and appendicular bone has been well-documented, although the same regimen has less or even catabolic effects (e.g. increasing porosity) on cortical bone. Recent interest has also been developed regarding its potential for tissue regeneration such as fracture healing of long bones and repair of osseous defects in the oral cavity [18-21]. Studies of animal models with or without induced osteoporosis support the impact of PTH on bone formation and remodeling in the craniofacial region [22-24]. Rodent studies with PTH(1-34) treatments show increased mandibular bone density, reversed periodontitis-induced bone loss, accelerated implant osseointegration and improved mandibular fracture healing [25]. Also, pre-clinical studies have shown promising results with PTH(1-34) for periodontal regeneration and the treatment of osteonecrosis of the jaw related to the use of anti-resorptive drugs [26-28]. These studies together provide sound rationale for the use of PTH in facilitating craniofacial bone regeneration.

The exact mechanisms underlying the osteoanabolic actions of PTH remain unclear. Given its role as a  $\text{Ca}^{2+}$  depot in a greater scheme of mineral homeostasis, the outcomes of skeletal metabolism likely depend on systemic  $\text{Ca}^{2+}$  demands, which is subject to tight regulation by a dynamic feedback loop that begins with the ability of parathyroid cells (PTCs) to sense minute changes in circulating  $[\text{Ca}^{2+}]$ . When serum  $[\text{Ca}^{2+}]$  is lowering, inactivation of CaSR in PTCs permits tonic PTH secretion to promote renal  $\text{Ca}^{2+}$  reabsorption, enhance intestinal  $\text{Ca}^{2+}$  absorption [via the production of 1,25-dihydroxy-vitamin  $\text{D}_3$  (1,25D)], and mobilize  $\text{Ca}^{2+}$  from bone, thus raising serum  $[\text{Ca}^{2+}]$  toward normal<sup>29</sup>. In contrast, increasing serum  $[\text{Ca}^{2+}]$  beyond its physiological set-point activates CaSRs in PTCs to suppress PTH secretion and its ensemble of calcemic activities. In addition, via activation of the same CaSR, high serum  $[\text{Ca}^{2+}]$  also increases  $\text{Ca}^{2+}$  excretion in renal tubule cells to further reduce circulating  $[\text{Ca}^{2+}]$  [30]. Growing evidence further demonstrates CaSR expression in chondrocytes, osteoblasts, and osteocytes and abilities of  $[\text{Ca}^{2+}]$  to promote terminal differentiation and mineralizing functions of the cells. In vitro studies have shown that raising extracellular  $[\text{Ca}^{2+}]$  could suppress differentiation and resorbing functions of osteoclast and promote their apoptosis [31-32]. These effects of raising local  $[\text{Ca}^{2+}]$  on osteoblasts and osteoclasts together provide a potential mechanism to redeposit surplus  $\text{Ca}^{2+}$  back into bone and create an anabolic window for skeletal anabolism in response to PTH when demands of systemic  $\text{Ca}^{2+}$  are low in conditions of  $\text{Ca}^{2+}$  sufficiency.

Based on the above regulatory scheme, hypercalcemic effects of intermittent PTH treatment could be a prerequisite for its anabolic action. However, hypercalcemia is

afflicting and was a major limiting factor in the approval of the current PTH therapy by the FDA, as aberrant increases in serum  $[Ca^{2+}]$  can cause nausea, vomiting, headaches, altered mental status, dehydration and even kidney stones. Another side-effect considered by the FDA was oncogenic effects of the peptide. In rats subjected to daily doses of PTH(1-34) for 24 months in toxicological studies developed osteosarcomas at substantial rates [13, 15] that increased with the doses of PTH(1-34) tested [10, 33]. Given these potential side-effects, the FDA approved a daily dose of 20  $\mu$ g PTH(1-34) for a maximum of 2 years for the treatment of severe osteoporosis, despite the fact that doses above 20  $\mu$ g/day produced greater BMD responses in the pivotal phase 3 trial<sup>7</sup> and in other trials [34, 35]. Clearly future optimization of intermittent PTH therapy requires strategies to increase the potency of the peptide by increasing its efficacy and/or duration of action, and minimize its hypercalcemic side-effects while producing more robust anabolic effects at different skeletal sites. With regards to enhancement of potency in targeting PTH1R, PTH analogs have been designed to prolong cAMP responses to sustain PTH1R-dependent effects on systemic  $Ca^{2+}$  and active 1,25-D levels [36-39], which in turn produces an anabolic effect on bones [40,41]. A remarkable PTH analog, which emerged from efforts initially aimed at optimizing the N-terminal region of PTH(1-34) [42, 43] and culminated in the joining of the optimized N-terminal PTH(1-14) sequence to a C-terminal segment derived from the (15-36) region of PTHrP [38]. This long-acting PTH analog, or LA-PTH, induces prolonged cAMP production from endosomes much more than PTH(1-34) and was shown to also induce calcemic responses in blood that far exceeded those observed for PTH(1-34) in both magnitude and duration [44], thus limiting in clinical

potential.

Motivated by the counteracting calcemic actions of PTH1R and CaSR and their potential synergistic actions in producing skeletal anabolism as outlined in the above sections and Chapter 1, this dissertation tested the mineral and skeletal effects of a novel combined PTH and calcimimetic (a non-ionic allosteric CaSR agonist) therapy in physiological and pathological contexts. Specifically, we performed once daily co-injections of combined PTH(1-34) or LA-PTH with NPS-R568, an injectable calcimimetic, in C57/B6 mice of different ages and sexes and in mice subjected to non-fixed tibial fracture. We compared the abilities of the combined treatment versus PTH or LA-PTH alone to promote bone anabolism or enhance fracture healing using micro-computed tomography ( $\mu$ CT) imaging and analysis, automated biochemical assays, histomorphometry, biomechanics testing, and novel Nanostring nCounter gene expression profiling. Similar experiments were also performed in mice with Tamoxifen (Tam)-inducible ablation of *Casr* in osteoblasts to demonstrate a non-redundant role of CaSR in mediating the anabolic effects of the combined treatment.

## 2.2 Results

### Calcimimetics abrogated PTH-induced hypercalcemia

We first optimized a combination of PTH(1-34) with calcimimetic (NPS-R568) that would yield normalization of serum  $[Ca^{2+}]$  and  $[PO_4^{3-}]$ , be most physiologically tolerable, and enhance the osteoanabolic effect of PTH. Previous studies have shown that 20  $\mu\text{mol/kg}$  NPS-R568 results in acute hypocalcemia in mouse/rat model [45-51] and thus was chosen to be co-injected with 10, 20, 40, and 80  $\mu\text{g/kg}$  of PTH(1-34) for 4 weeks. Mice injected with 40  $\mu\text{g/kg}$  PTH(1-34), a common dose known to produce significant anabolic effects on bone, was used as “PTH alone” control. As anticipated, daily injections of 40  $\mu\text{g/kg}$  PTH(1-34), or PTH-40, produced transient hypercalcemia in 3-month old male C57/B6 mice (**Figure 2.1 A**, ○ vs ○), while daily injections of 20  $\mu\text{mol/kg}$  NPS-R568 calcimimetic expectedly produced hypocalcemia and hypophosphatemia 3 hours after injections (**Figure 2.1 A**, ○ vs ○). In support of our hypothesis, co-injections of NPS-R568 counteracted the acute  $Ca^{2+}$ -elevating effects of PTH in a dose-dependent manner, and produced normocalcemia with PTH-40. However, the hypercalcemic effect of 80  $\mu\text{g/kg}$  PTH(1-34) was not completely normalized by NPS-R568 (**Figure 2.1 A**, ○ vs ○). Interestingly, the mice treated with NPS-R568 alone developed chronic hypercalcemia, likely due to long-term exposure to hypocalcemic action of the compound (**Figure 2.1 B**, ○ vs ○). No such effect was seen in mice treated with PTH with or without NPS-R568 (**Figure 2.1 B**, ○ or ○ vs ○). Expectedly, treatment with either PTH(1-34) alone, in which elevating serum Ca activates CaSR directly, or in any combination of PTH with NPS-R568 that allosterically activates CaSR in parathyroid glands, suppressed endogenous intact PTH(1-84)

secretion (**Figure 2.1 A**), highlighting the functional potency of both drugs on the glandular function and indirectly on other target organs. We also measured both acute and sustained blood urea nitrogen (BUN), creatinine (CREAT), albumin (ALB), and alkaline phosphatase (ALP) levels to assess acute or chronic renal and liver status (as summarized in **Figure 2.1**). Acute changes in BUN:CREAT and ALB were mostly restored to normal levels by the end of 4-week treatment, indicating no permanent alterations in renal and liver functions. In contrast, significant changes in acute and chronic increases in non-specific serum ALP could be indicative of more permanent changes in bone function. Lastly, only mice treated with NPS-R568 alone had a significant decrease in body weight, which indicates the deleterious physiological effects of chronic hypocalcemia and hypophosphatemia (**Figure 2.1 B, B.Wt**).

We also tested a similar combination regimen with 10, 40, and 80  $\mu\text{g}/\text{kg}$  PTH(1-34) on 12-month-old female mice (**Figure 2.2**). NPS-R568 prevented acute hypercalcemia in the mice 3 hours after the last injection of combined NPS-R568 with either 40 or 80  $\mu\text{g}/\text{kg}$  PTH(1-34) during a 6-week course of treatment (**Figure 2.2 A**), supporting our hypothesis that calcimimetic co-injection will prevent PTH-induced hypercalcemia regardless of age and sex and even with very high doses (80  $\mu\text{g}$ ) of PTH. The ability of NPS-R568 to normalize hypercalcemic effects of 80  $\mu\text{g}/\text{kg}$  PTH(1-34) in these aged females (**Figure 2.2 A**), but not in young males (**Figure 2.1 A**), indicating sex and/or age differences in the response to the drug. Acute and chronic phosphate metabolism is unaffected in these 12-month-old female mice (**Figure 2.2 A, B**). Similar to the 3-month-



male cohort, the acute and chronic increases to nonspecific serum ALP are likely indicative of prolonged skeletal changes.

*Calcimimetics enhanced the osteoanabolic effect of PTH(1-34) in adult male and aged female mice*

Skeletal analyses by  $\mu$ CT (micro-computed tomography) showed that PTH alone modestly increased Tb bone mass (Tb. BV/TV) and thickness (Tb. Th) by  $\approx$ 10% in distal femurs of 3-month-old male mice when compared to vehicle-injected controls (**Figure 2.3 A and B**, ○ vs ○). Although NPS-R568 alone had no effect on these Tb bone parameters (**Figure 2.3 A and B**, ○ vs ○), when it was co-injected with PTH(1-34), there were robust increases in Tb. BV/TV (of  $\approx$ 25%) and in Tb.Th (of  $\approx$ 22%) (**Figure 2.3 B**, 40  $\mu$ g/kg PTH, ○ vs ○). Treatment with PTH alone resulted in a reduced Tb BMD. However, co-injecting with NPS-R568 rescued this effect, supporting the ability of CaSR activation to restore mineralizing function in bone in accordance with our hypothesis (**Figure 2.3 B**, 40  $\mu$ g/kg PTH, ○ vs ○). Furthermore, the reduced Tb. SMI values in mice treated with combined PTH/R568 indicate an increase in plate-like trabeculae in the distal femurs, which are indicative of increased mechanical strength. Increases in Tb. BV/TV and Tb. Th with reduced Tb. SMI was also found in the L5 vertebrae of the same animals treated with combined PTH and NPS-R568 (**Figure 2.3 C**). At the tibiofibular junction (TFJ), PTH alone had no significant effects on Ct.TV, Ct.BV, and Ct.Th (**Figure 2.3 D**, ○ vs ○). However, injections of NPS-R568 alone significantly reduced these Ct parameters (**Figure 2.3 C**, ○ vs ○), perhaps because the drug caused chronic hypocalcemia due to reduced secretion of endogenous PTH

without supplementation of exogenous PTH, as shown in **Figure 1.1**. Despite the potential of negative effects of NPS-R568 on Ct bone, co-injections of NPS-R568 with PTH instead significantly increased Ct.TV, Ct.BV, and Ct.Th by 24-28% in these 3-month-old male mice (**Figure 2.3 D**, 40 µg/kg PTH + 20 µmol/kg, **○** vs **○**). Furthermore, mechanical testing showed increased bone strength in the femurs of 3-month-old male mice injected with both PTH(1-34) and NPS-R568 vs those injected with PTH alone or vehicle as indicated by a significant increase in the ultimate force to failure (Fu) in the co-treated bones (**Figure 2.4**). These data suggest that the osteoanabolism induced by the combined PTH/calcimimetic produces stronger bone that may resist fracture.

Using sequential labeling protocol for bone described in (**Figure 2.5 A**) dynamic histomorphometric analyses of TFJ showed robust periosteal bone formation in the first 3 weeks of PTH(1-34) with NPS-R568 treatment, as indicated by the outward concentric fluorescent labels (#1-4). (**Figure 2.5 B**, left panel). However, the progressively reduced width and intensity of the labels and the shortened distances between the labels (white double-head arrows), suggest that this periosteal expansion waned and stalled 3 weeks after the treatment as indicated by the lack of fluorescent labels #5 and #6, which were injected at beginning of week 5 and 6 of the treatment, respectively (left panel). The latter finding indicates the closure of the anabolic window for these Ct effects, which began ≈3 weeks after the treatment. Interestingly, we found intense bone-forming activities in the first week of treatment with PTH alone, as indicated by a long interval between labels #1 and #2 (**Figure 2.5 B**, right panel), but only small amount of demeclocycline (label #3; in orange) was detected in the areas, which showed

characteristics of actively remodeling pits (right panel, arrowheads), which could be due to increases in perilacunar remodeling (PLR) of osteocyte and/or osteoclastic activities. The latter structures are less prominent in PTH/calcimimetic-treated bones (left panel). If those remodeling structures are confirmed by assessment of OCL activities with TRAP staining and/or assessment of PLR by silver staining, it will suggest that, in Ct bone treated with PTH alone, PLR and/or OCL-mediated bone loss quickly catches up with formation to close the anabolic window. This may explain the ineffectiveness of intermittent PTH alone at sites rich in Ct bone. The absence or reduced frequency of those remodeling structures in the periosteum of PTH/calcimimetic-treated Ct bones will support our hypothesis that the calcimimetic inhibits PTH-induced OCL and PLR activities to extend its anabolic window. Future experiments will quantify dynamic bone formation, OCL, and PLR parameters in these labeled skeletons to clearly define the anabolic windows of PTH vs combined PTH/calcimimetic treatment on Ct bone.

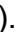





These data therefore demonstrate synergy between PTH and calcimimetic in promoting osteoanabolism at both Tb and Ct sites in adult male mice. Given that bone mass is lost during ageing, especially for post-menopausal women, we also applied this regimen to 12-month-old female mice (**Figure 2.6**). Although there is an increase in Tb bone mass (Tb. BV/TV) at the distal femur with combined therapy at 80  $\mu\text{g}/\text{kg}$ , we deemed this to be an unreliable site due to the overall lack of Tb bone, which results in variation of data points (**Figure 2.6 A**, BV/TV,%). As an alternative site to assess trabecular bone, we scanned L5 vertebrae of the same animals. Synergistic effects of PTH and calcimimetic similar to those in 3-month-old mice were observed in Tb bone in the L5 vertebrae and









Ct bone at TFJ with maximal responses at 80 µg/kg (**Figure 2.6 B, C, ○ vs ○**) These data support the idea that the ability of NPS-R568 to control hypercalcemia permits the use of higher doses of PTH that is required to enhance osteoanabolism in older mice. Notably, mice with doses lower than 80 µg/kg did not produce significant osteoanabolism, highlighting the insufficiency of PTH(1-34) and/or decreased PTH1R signaling response in aged animals.

*NPS-R568 calcimimetic normalizes the hypercalcemic effects of LA-PTH and produces even more robust osteoanabolism than PTH(1-34)*

Previous studies into the structural determinants that optimize PTH1R signaling for patients with hypoparathyroidism yielded the generation of PTH analogs [52-57]. Notably, LA-PTH, in which the of N-terminal PTH(1-14) amino acid substitutions is fused to C-terminal PTHrP(15-36), was shown to induce prolonged downstream signaling responses by lengthening its occupancy time on the PTH1R in bone and kidney target cells, and consequently resulted in increased calcemic responses in blood that surpass those detected for PTH(1-34). Accordingly, we tested whether NPS-R568 can normalize the strong hypercalcemic effect of LA-PTH in order to take advantage of its potential for enhanced osteoanabolism (**Figure 2.7**). As expected, animals treated with PTH(1-34) and LA-PTH (both at 40 µg/kg) displayed increases in serum [Ca<sup>2+</sup>] (**Figure 2.7 A, ○ and ○ vs ○**) while those treated with NPS-R568 (20 µmol/kg) showed transient decrease in serum [Ca<sup>2+</sup>] (**○ vs ○**). However, the combined regimen completely normalized these individual calcemic effects (**○ and ○ vs ○**), similarly to that seen with 3-month-old male mice. Treatment with PTH(1-34), LA-PTH, and NPS-R568 resulted in

transient hypophosphatemia. While NPS-R568 with PTH(1-34) rescues this effect, the calcimimetic cannot overcome it with LA-PTH, suggesting LA-PTH's pharmacodynamics is more potent in mediating phosphate metabolism. Endogenous PTH secretion was decreased by all treatments (**Figure 2.7 A**) as expected, indicating once again that our drugs are functionally suppressive at the parathyroid gland. We also measured blood urea nitrogen (BUN), creatinine (CREAT), albumin (ALB), and alkaline phosphatase (ALP) to assess renal and liver status (**Figure 2.7 B**). Mice treated with LA-PTH with and without NPS-R568, have decreased serum ALB and increased ALP, which could suggest permanent, and possibly deleterious, changes due to chronically robust PTH1R signaling. Further studies into the toxicological extent of daily treatment with this compound are needed.

In a cohort of 3-month-old male mice, treatments with LA-PTH produced a much more profound effect on osteoanabolism compared to PTH(1-34). Skeletal analysis with  $\mu$ CT of LA-PTH treated mice revealed markedly increased Tb. bone mass (BV/TV,%) of over 200% along with increased trabecular number, thickness, and bone surface (**Figure 2.8 B**, ,  vs ). The significant decrease of Tb. SMI (**Figure 2.8 B**, ,  vs ) is a reflection of the transition to mostly plate-like trabecular structures, with little to no rod-like trabeculae. The enhanced osteoanabolic effect of LA-PTH is further corroborated by the significant increase of serum ALP (**Figure 2.7 B**), which although nonspecific, likely indicates a substantial skeletal transformation. While NPS-R568 rescued PTH(1-34)-mediated decrease in BMD (**Figure 2.8 B**) as seen in previous experiments, this calcimimetic did not restore mineralizing ability of trabecular bone in mice treated with

LA-PTH (**Figure 2.8 B**, Tb BMD ,  vs ). This along with the significant increases in serum bone turnover markers, P1NP and TRAcP5b shown in **Figure 2.7 B**, suggests that new bone is being synthesized at a faster rate than it can be mineralized. Histomorphometry analysis will further reveal the amount of immature bone/ osteoid in these mice treated with LA-PTH. At the tibiofibular junction, PTH(1-34) alone had no significant effects on Ct.TV or Ct.BV (**Figure 2.8 D**,  vs ). However, LA-PTH with and without NPS-R568 exhibited increased Ct. BV and BV/TV (**Figure 2.8 D**, ,  vs ). 2D and 3D  $\mu$ CT imaging also revealed bony extensions from the cortical endosteum and periosteum (**Figure 2.8 C**, LA-PTH, LA-PTH + R568), which highlights the more robust cortical expansion effect of LA-PTH compared to PTH(1-34). Furthermore,  $\mu$ CT images of show increased cortical porosity, which suggests a surge in perilacunar/ canalicular remodeling by osteocytes (**Figure 2.8 C**, LA-PTH, LA-PTH + R568). Unfortunately, the enhanced anabolic effect proved toxic to some mice (N = 3 out of 10) that were treated with LA-PTH alone for 4 weeks. We suspect that the lethality of LA-PTH could be attributed to 1) chronic hypercalcemia and/or 2) anemia due to shrinking bone marrow space due to continued endosteum expansion, (**Figure 2.8 A**). Co-treating with NPS-R568 increased survivability of the animals, as none died before the time course was completed.

These data demonstrates cooperation between LA-PTH and calcimimetic in promoting osteoanabolism at both Tb and Ct sites, which far exceed those observed with PTH(1-34) with no hypercalcemic side effects. To determine if the efficacy of LA-PTH in osteoanabolism is maintained in aged mice, we tested a similar regimen on 12 -month-

old male and female mice (**Figure 2.9**). In this pilot study, instead of once-daily injections for 4 weeks, we performed 3 injections per week for 4 weeks due to suspicion of physiologically intolerable and deleterious effects of LA-PTH in the older mice. In both aged male and female mice, serum  $[Ca^{2+}]$  was normalized after 4 weeks of treatment with LA-PTH and NPS-R568 (**Figure 2.9 A, B**). As was not the case with female mice, aged male mice treated with LA-PTH maintained significantly higher serum  $[Ca^{2+}]$ , indicating sex-dependent difference in drug responses at this age. In both male and female mice, nonspecific ALP was normalized to vehicle control levels when co-injected with NPS-R568, while those treated with LA-PTH alone maintained a significantly higher level (**Figure 2.9 A, B**). Chronically robust PTH1R signaling through LA-PTH likely resulted in sustained changes to liver and bone, which can be attenuated with calcimimetics. Future experiments will include more N and collection of retro-orbital serum to analyze acute changes in mineral homeostasis and bone turnover markers in LA-PTH-treated mice with and without calcimimetics.

Skeletal analyses by  $\mu$ CT showed site-specific effects of LA-PTH with or without calcimimetics. For example, while LA-PTH treatment alone resulted in robust bone anabolism in both male and female distal femur trabeculae (**Figure 2.10 A, 2.11 A**), co-injection with NPS-R568 shows no significant difference when compared to Vehicle controls. With regards to cortical bone at the TFJ, LA-PTH alone causes a thinning of cortical thickness with male and females, which is rescued with co-injection with NPS-R568 (**Figure 2.10 B, 2.11 B**). In L5-vertebrae of mice treated with LA-PTH and calcimimetics, females have greater Tb bone mass while males exhibit no difference

from Vehicle controls (**Figure 2.10 C, 2.11 C**). These data support the use of NPS-R568 to control hypercalcemia permitting the use of LA-PTH in aged mice regardless of sex, however, whether calcimimetics will enhance osteoanabolism remains to be confirmed with studies using various combinations of drug doses and duration and frequency of drug injection.

*The anabolic effects of the combined iPTH and NPS-R568 treatment were abrogated in osteoblast-specific CaSR knockout mice*

To determine whether expression and activation of CaSRs in OBs are required for the osteoanabolism of intermittent PTH and the combined PTH with NPS-R568 treatment, we compared the effects of these regimens on skeletal parameters in mice with their CaSR genes knocked-out specifically in early OBs. The specific deletion is in exon 7 of the gene, which encodes the seven transmembrane domains and four intracellular loops of the CaSR.  $^{2.3Col(l)}CaSR^{\Delta flox/\Delta flox}$  mice showed that ablation of CaSRs early in the OB lineage abrogated osteoanabolism induced by the combined PTH with calcimimetic treatment (**Figure 2.12**), supporting our hypothesis that OB CaSRs play an essential role in mediating skeletal responses to treatment. In fact, we observed significant bone loss (45% of Tb) in those mice vs the  $^{2.3Col(l)}CaSR^{\Delta flox/\Delta flox}$  mice injected with vehicle (**Figure 2.12**). Surprisingly, we also found that  $^{2.3Col(l)}CaSR^{\Delta flox/\Delta flox}$  resulted in higher bone mass compared to controls injected with vehicle.

Based on what we have learned from the skeletal phenotypes of the constitutive  $^{Col(l)}CaSR^{\Delta flox/\Delta flox}$  KO mice (citation 18) we speculate that the bone loss is caused by (i)



increased OB apoptosis, (ii) reduced OB proliferation, and/or (iii) inability of OBs to deposit  $\text{Ca}^{2+}$  into their surrounding matrix in an orderly manner. This may lead to a mismatch between resorption and formation caused by the PTH excess. Thus, we anticipate seeing hypercalcemia (due to  $\text{Ca}^{2+}$  release from bone and poor  $\text{Ca}^{2+}$  deposition into matrix), increased TUNEL staining, reduced numbers of PCNA-(+) OBs, and the accumulation of unmineralized osteoid reflected in the analysis of Goldner staining of the PTH/R568-treated vs. vehicle-treated  $^{2.3\text{Col}(I)}\text{CaSR}^{\Delta\text{flox}/\Delta\text{flox}}$  mice. The above serum and skeletal abnormalities are anticipated to be even more severe in  $^{2.3\text{Col}(I)}\text{CaSR}^{\Delta\text{flox}/\Delta\text{flox}}$  mice treated with PTH alone, due to additional catabolic actions of endogenous PTH, which are absent in PTH/R568-treated mice. We anticipate the ablation of CaSRs in mature OBs to block some, but not all, skeletal effects of the combined PTH/calcimimetic treatment in  $^{\text{OCN}}\text{CaSR}^{\Delta\text{flox}/\Delta\text{flox}}$  mice. This is based on our hypothesis that CaSRs mediate mineralizing functions, but not cell proliferation and survival, after OBs reach maturity. Therefore, we anticipate the combined drug regimen to retain the ability to promote proliferation (by PCNA staining), reduce apoptosis (by TUNEL-staining), increase quantity of bone as osteoid form (by histomorphometry) in the  $^{\text{OCN}}\text{CaSR}^{\Delta\text{flox}/\Delta\text{flox}}$  mice, but loss of the ability to promote mineralization, which will be reflected by reduced tissue mineral density (by  $\mu\text{CT}$ ) and immature apatite lattice in their bone matrices. Further studies into delineating the underlying mechanism by examining the effects of the compounds on the proliferation, survival, differentiation, and mineralizing functions of OBs with their CaSR genes acutely deleted in vitro are also warranted.

### *Nanostring confirms gene expression shift towards bone anabolism*

To further characterize gene expression changes during the osteoanabolic action of our PTH analog versus PTH analog with calcimimetic, we used a customized Nanostring code set containing 625 genes involved in chondrogenic, osteogenic, osteocytic, osteoclastic, adipogenic, inflammatory and metabolic pathways. Intact femurs and tibias dissected free of surrounding muscle, tendon, and fibrous tissues were used for RNA extraction without flushing of the marrow space in order to gain an integral view of changes in gene expression patterns. Duplicate samples of isolated total mRNA were processed by Nanostring technology as stated in the Methods section.

We first compared intact femurs and tibias from mice treated with PTH(1-34) vs vehicle (**Figure 2.13 A**) or PTH(1-34) with calcimimetic (**Figure 2.13 B**) 3 hours after treatment. 74/650 genes changed with PTH(1-34) alone while 119/650 genes changed in the combination therapy cohort. Acute changes with PTH(1-34) alone result in a resorptive profile, as *Ctsk* and *Mmp13* are upregulated while transcripts for OB differentiation and bone anabolism, such as BMPs, *Bglap*, *Col10a1*, and Wnt/  $\beta$ -catenin signaling, are downregulated. In contrast, treatment with PTH(1-34) with NPS-R568, exhibit a strong shift towards bone formation, as BMPs, *Rank*, and Wnt/  $\beta$ -catenin signaling transcripts are more abundant, while *Ctsk* and *Mmp13* are no longer significantly altered. This Nanostring data is consistent with known physiological function of PTH to mobilize serum  $\text{Ca}^{2+}$  and also our data above showing enhanced osteoanabolic potential of co-treating with calcimimetics.

Bone from mice treated with PTH(1-34) for 4 weeks exhibit an expected change towards osteoprogenitor maintenance and function (Efnb1) and bone remodeling; formation (Alpl, Dmp1, Mepe) and resorption (Ctsk) (**Figure 2.13 C**). In support of our hypothetical model (**Figure 1.1**), co-treatment with PTH(1-34) with NPS-R568 shifts gene expression towards bone anabolism (**Figure 2.13 D**), as evidenced by an increase in transcripts from genes involved in OB differentiation (Satb2) and OB matrix mineralization (Alpl, Bglap, Col1a1, Dmp1, and Enpp1).

As our data has shown, LA-PTH's bone remodeling and osteoanabolic potential far exceeds that of PTH(1-34). Over 70% of the 625 bone-related transcripts we tested were demonstrated to have significant changes in LA-PTH treatment, whereas co-treatment with calcimimetics decreased it to approximately 30% (**Figure 2.13 E,F**). This combined with our  $\mu$ CT data, suggest the potential for NPS-R568 to tune the robust anabolic effect of LA-PTH.

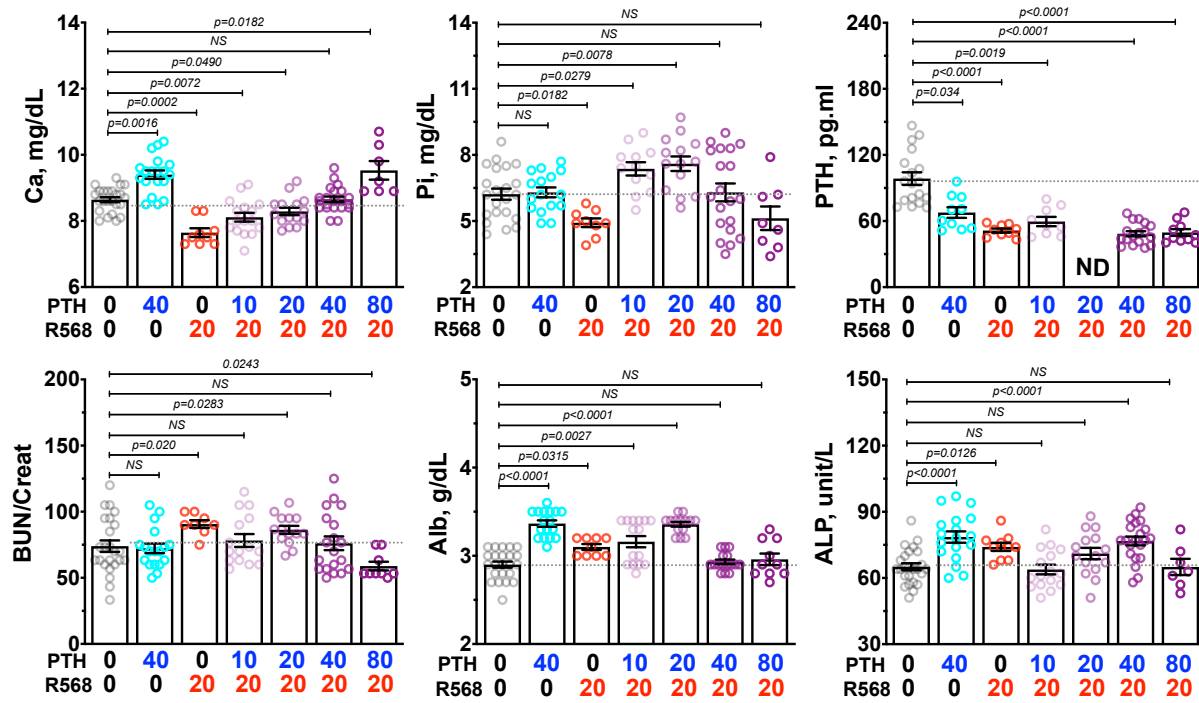
#### *Co-injections of calcimimetic NPS-R568 produce synergistic osteoanabolism in bony calluses*

Given the anabolic actions of CaSRs in callus chondrocytes and OBs [58, 59] we examined the potential for targeting the CaSR to enhance fracture repair. Closed-unfixed tibia midshaft fractures were generated as described in Materials and Methods and illustrated in **Figure 2.14**. We compared the osteogenic activity in fracture calluses from mice subjected to daily injections of vehicle, PTH(1-34) (40  $\mu$ g/kg) alone, or the PTH(1-34)/R568 (20  $\mu$ mol/kg) combination for 4 weeks. Analyses of hard calluses

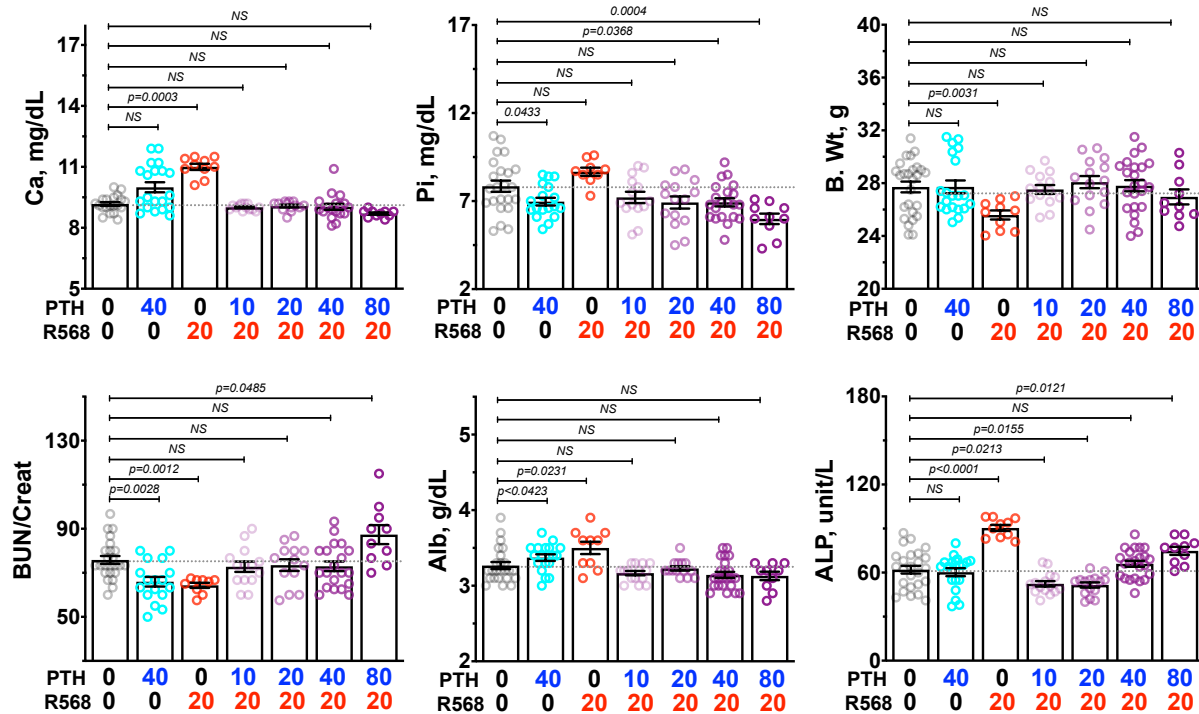
treated with PTH(1-34) alone by  $\mu$ CT with a 400 mg HA/cm<sup>3</sup> threshold showed a significant increase in Cal.BV/TV (by  $\approx$ 12% vs vehicle controls,  $p < 0.05$ ), but had no significant effects on Cal.Th or mineral density (Cal.BMD) (**Figure 2.15**). In contrast, co-treatments with combined PTH(1-34) (40  $\mu$ g/kg) and R568 increased Cal.BV/TV by 20% ( $p < 0.01$ ), Cal.Th by 10% ( $p < 0.05$ ), and Cal.BMD by 2.5% ( $p < 0.05$ ), when compared to vehicle controls (**Figure 2.15**), indicating more robust osteoanabolism than the treatments with PTH1-34 alone. We reasoned that the increased levels of apparent Cal.Th and Cal.BMD might be due to increasing amount of higher-density bone, considering the ability of CaSR activation (by R568) to promote mineralizing functions in chondrocytes and OBs. In supporting this hypothesis,  $\mu$ CT analyses using a higher threshold to segment out bone with a higher mineral density (1000-2100 mg HA/ cm<sup>3</sup>) showed a larger increase in Tb.BV/TV (by 27% or 13%) and Tb.Th (by 17% or 13%) vs calluses treated with vehicle or PTH(1-34) alone, respectively (**Figure 2.15**). These data together indicate that the combined PTH(1-34)/R568 treatment produces stronger anabolic effects than PTH(1-34) alone without the unwanted calcemic side-effects. Given our results with LA-PTH treatments, experiments are underway involving its use in combination with NPS-R568 calcimimetic in the same fracture model.

Figure 2.1

A. 3 hours post-injection, retro-orbital serum



B. 24 hours post-injection, terminal serum

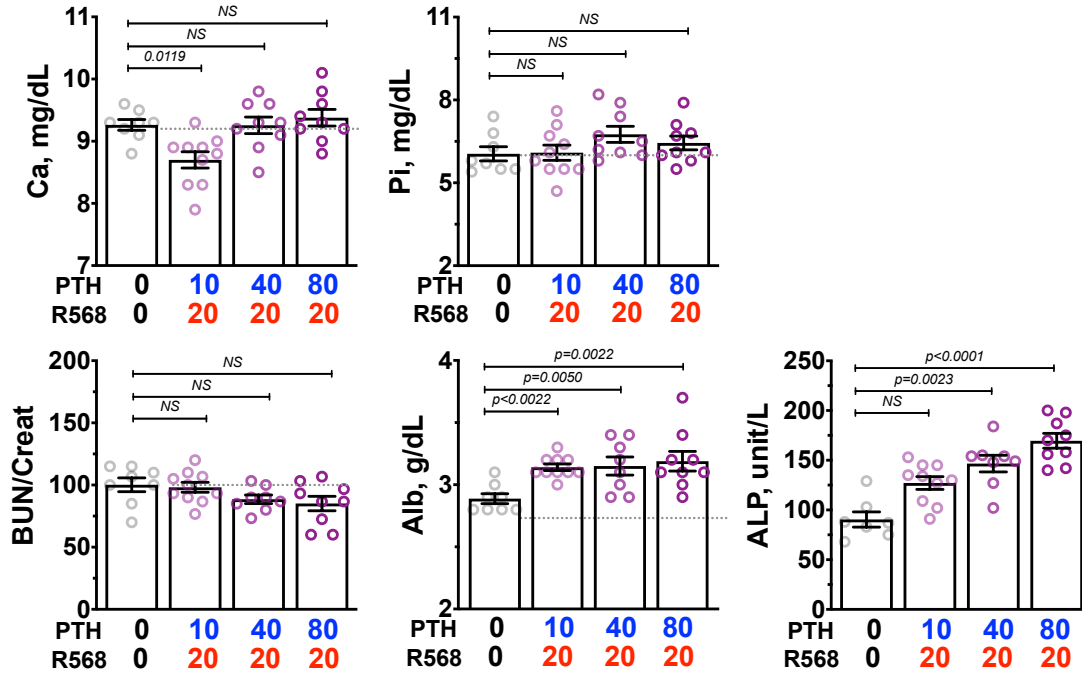


**Figure 2.1. Co-injections of the calcimimetic NPS-R568 offset the hypercalcemic side-effects of PTH(1-34) in 3-month-old male mice.**

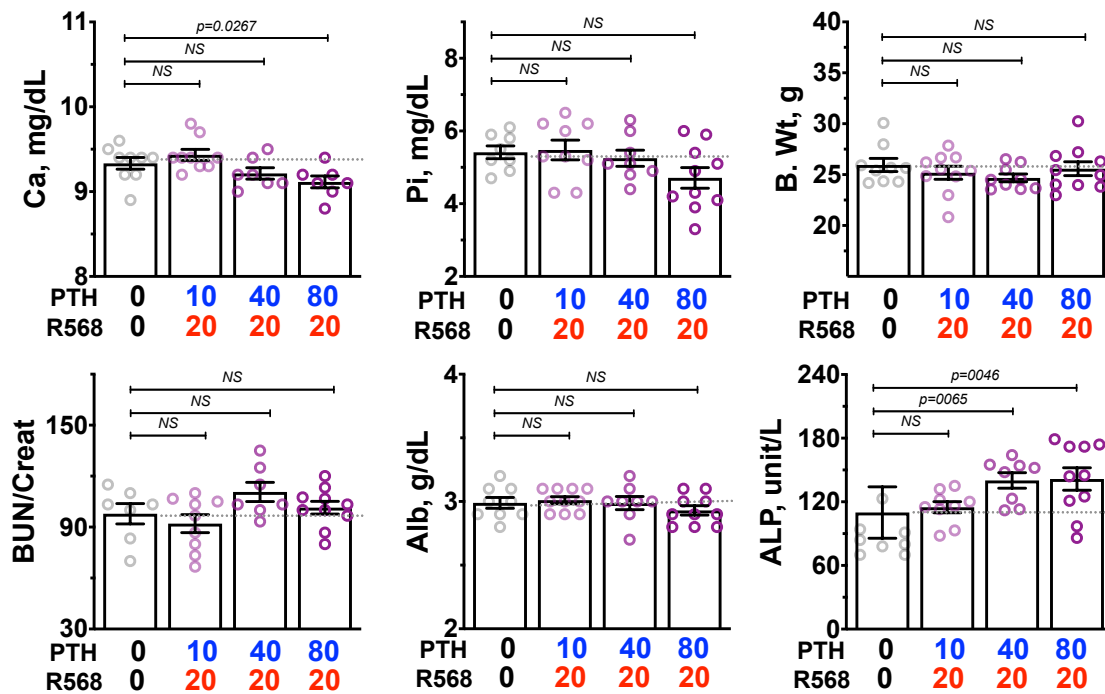
Serum  $\text{Ca}^{2+}$ , phosphate (Pi), albumin (Alb), non-specific alkaline phosphatase (ALP), blood urea nitrogen/ creatinine ratio (BUN/Creat), endogenous parathyroid hormone (PTH), body weight (B. Wt) from mice treated daily with Vehicle, 40ug/kg PTH(1-34), NPS-R568 (20 umol/kg), or increasing PTH(1-34) 10, 20, 40, 80 ug /kg B. wt. in combination with NPS-R568 for 28 days. Serum  $\text{Ca}^{2+}$  show the ability of injectable calcimimetics to offset hypercalcemic effects by PTH(1-34) **(A)** 3 hours post-injection with 40 ug/kg and **(B)** 24 hours post-injection in a dose-dependent manner. Both PTH(1-34) and NPS-R568 achieve dampening of endogenous PTH secretion 3 hours post-injection **(A)**. Kidney and liver functions were most normal with 40 ug/kg (PTH 1-34) treatment. N=10-27 mice per group with each individual mouse represented by a colored circle; p-values labeled per comparison as determined by one-way ANOVA. NS = not significant.

Figure 2.2

A. 3 hours post-injection, retro-orbital serum



B. 24 hours post-injection, terminal serum



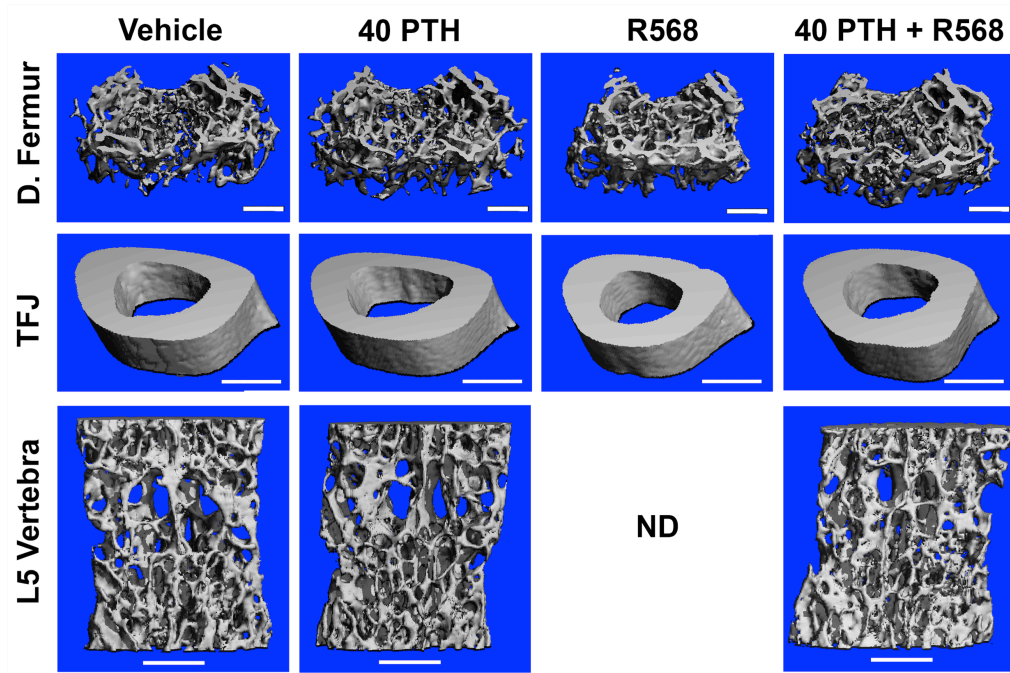
**Figure 2.2. Co-injections of the calcimimetic NPS-R568 offset the hypercalcemic side-effects of PTH(1-34) 12-month-old female mice.**

Serum  $\text{Ca}^{2+}$ , phosphate (Pi), albumin (Alb), non-specific alkaline phosphatase (ALP), blood urea nitrogen/ creatinine ratio (BUN/Creat), body weight (B. Wt) from mice treated daily with Vehicle, increasing PTH(1-34) of 10, 40, 80 ug /kg B. wt. in combination with NPS-R568 for 42 days. Serum  $\text{Ca}^{2+}$  show the ability of injectable calcimimetics to offset hypercalcemic effects by PTH(1-34) **(A)** 3 hours post-injection with 40 and 80 ug/kg and **(B)** 24 hours post-injection with 10 and 40 ug/kg. Non-specific ALP is shown to increase in both acute **(A)** and chronic conditions **(B)** of PTH(1-34) with calcimimetic. N=9-10 mice per group with each individual mouse represented by a colored circle; p-values labeled per comparison as determined by one-way ANOVA. NS = not significant.

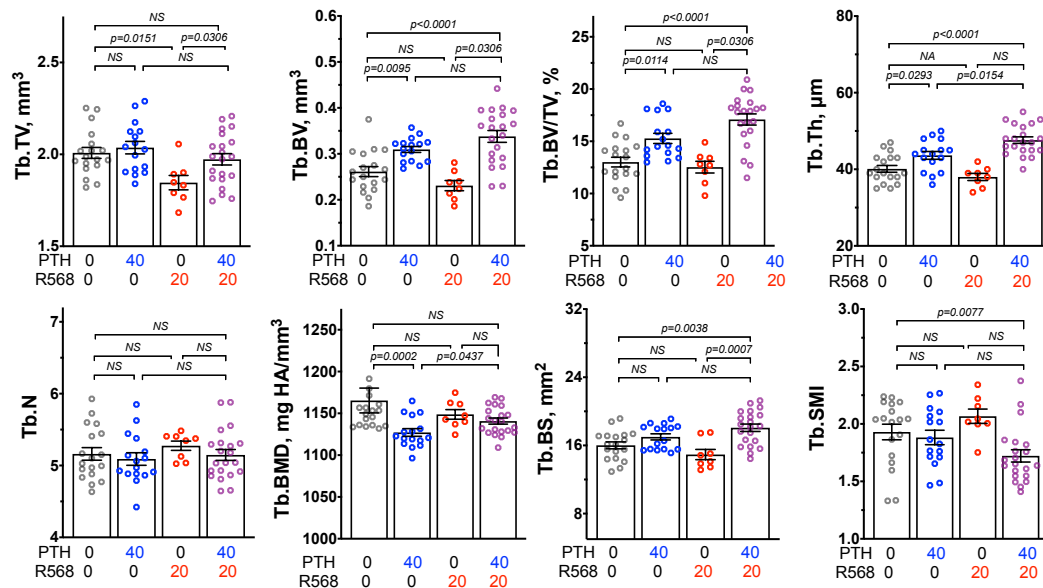


Figure 2.3

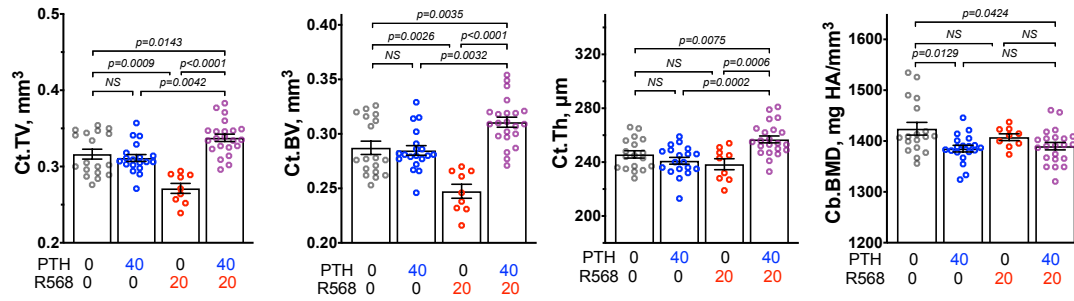
A.  $\mu$ CT 3D and 2D images summary



B.  $\mu$ CT skeletal parameters of distal femur trabecular bone



### C. $\mu$ CT skeletal parameters of TFJ cortical bone



### D. $\mu$ CT skeletal parameters of L5-vertebrae trabecular bone

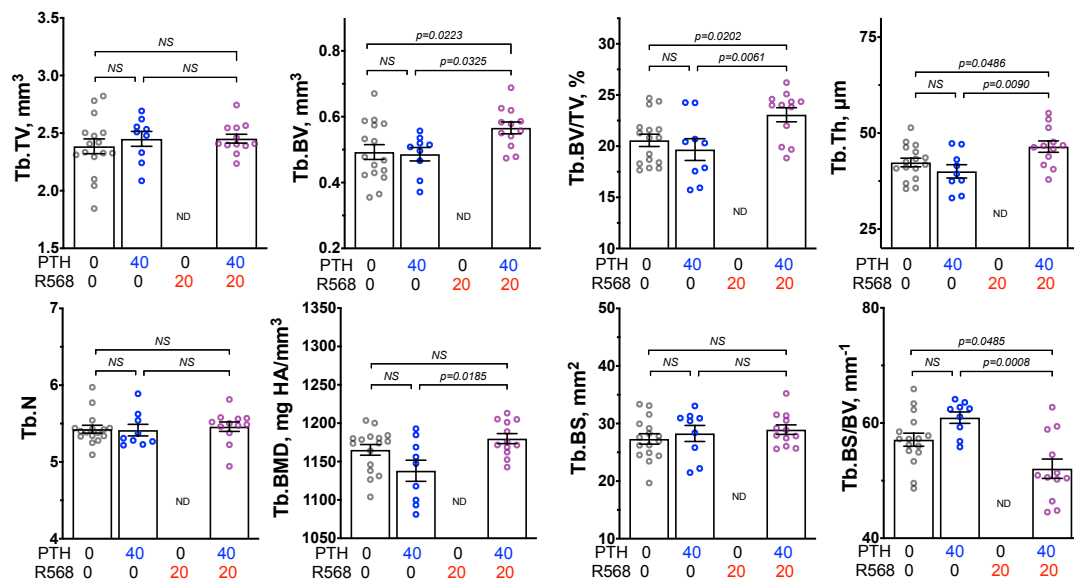


**Figure 2.3. Co-injections of the calcimimetic NPS-R568 produce additive osteoanabolic effects in trabecular and cortical bone of 3-month-old male mice.**

3D and 2D  $\mu$ CT images (A) and their corresponding structural parameters: total volume (TV), bone volume (BV), bone mass (BV/TV,%), bone surface (BS), thickness (Th), number (N), bone mineral density (BMD), structural model index (SMI) for (B) distal femur trabecular bone (C) tibiofibular junction cortical bone and (D) L5-vertebrae trabecular bone. Skeletal parameters show synergistic effects of NPS-R568 to enhance osteoanabolism of PTH(1-34). N=9-22 mice per group, with each individual mouse represented by a colored circle; p-values labeled per comparison as determined by one-way ANOVA. NS = not significant.

**Figure 2.4**

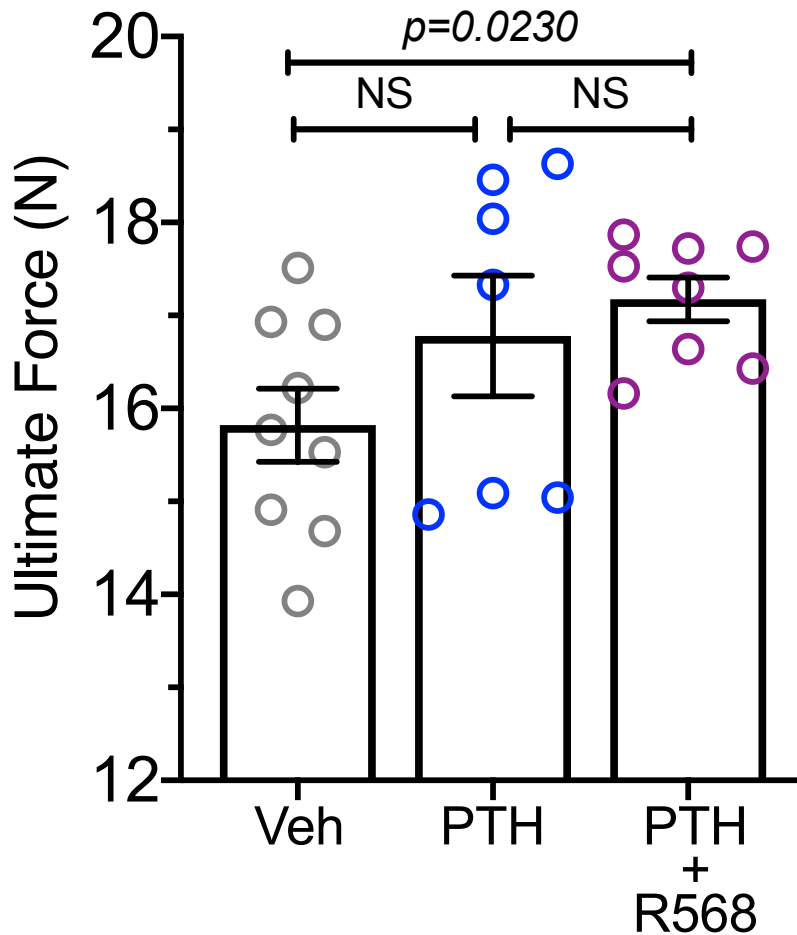
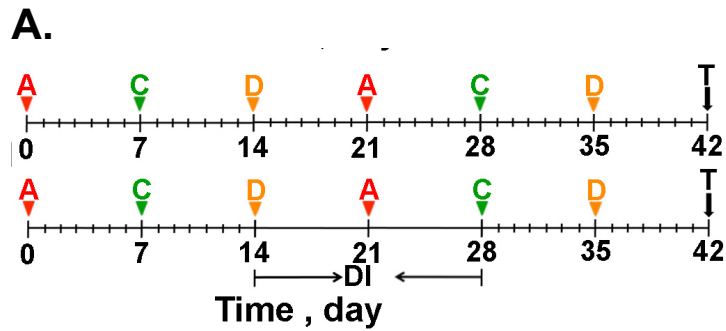


**Figure 2.4. Mice treated with combined PTH(1-34) and NPS-R568 exhibit increased compressive strength at the mid-femur.**

Ultimate compressive strength assessed in femurs from 3-month-old male mice treated with Vehicle (Veh), PTH(1-34) (PTH), or PTH(1-34) with calcimimetic (PTH+R568). Bones were loaded to failure by three-point bending on the Bose Electroforce 3200 instrument as described in Methods section. Force is in Newtons needed to fracture femur at the midshaft with each individual mouse represented by a colored circle; p-values labeled per comparison as determined by one-way ANOVA. NS = not significant.

**Figure 2.5**



**A:** alizarin red  
**C:** calcein  
**D:** demecloxydin  
**DI:** drug interruption  
**T:** tissue harvest

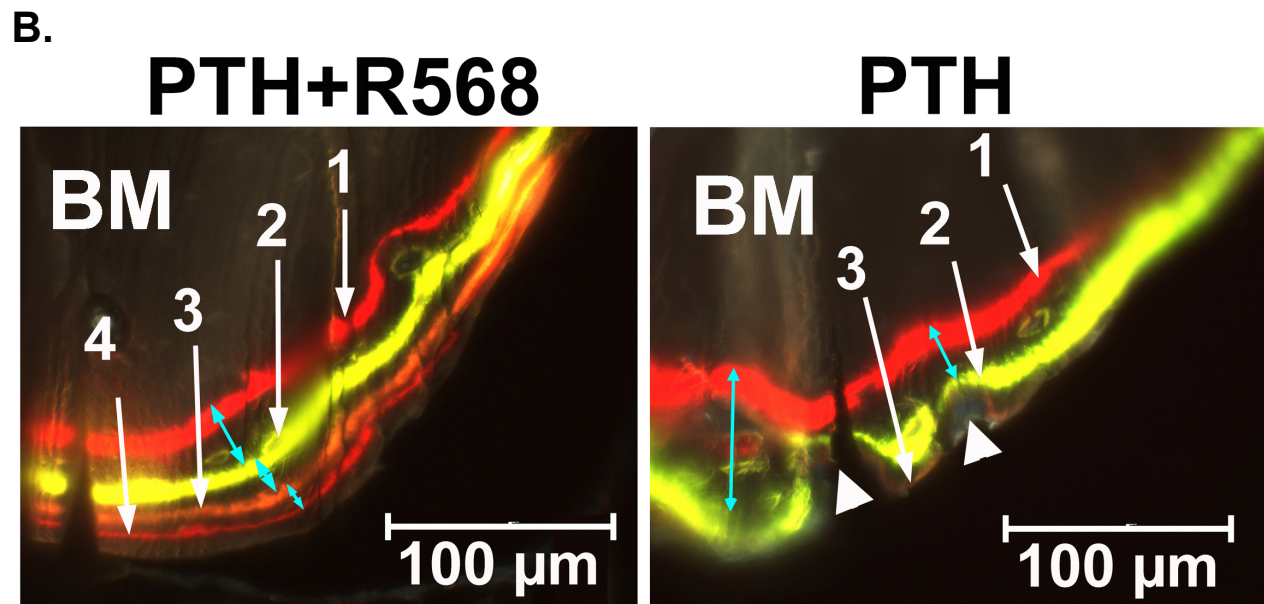
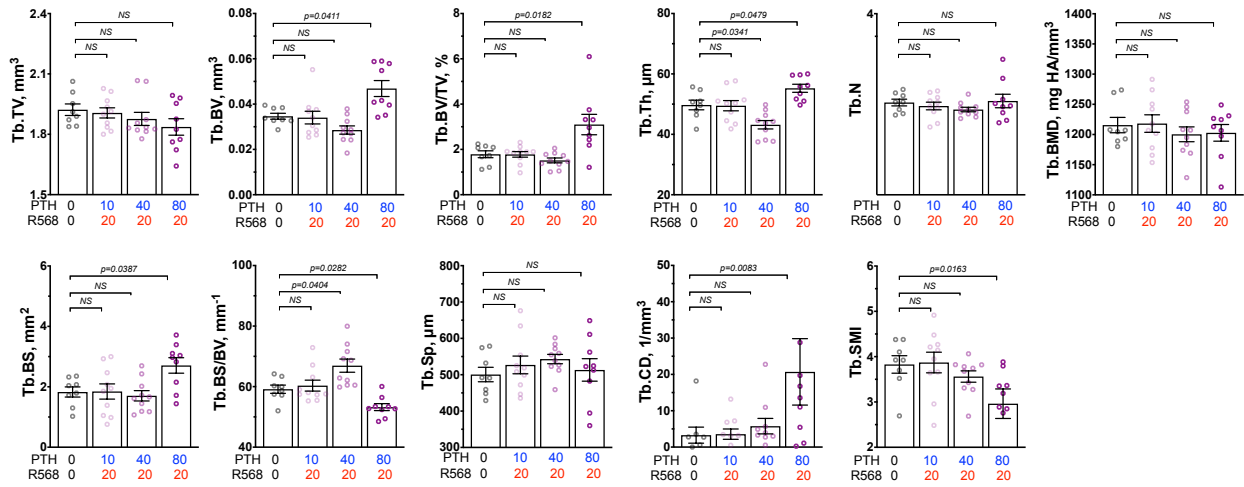


**Figure 2.5. Mice treated with combined PTH(1-34) and NPS-R568 exhibit increased fluorescent labeling**

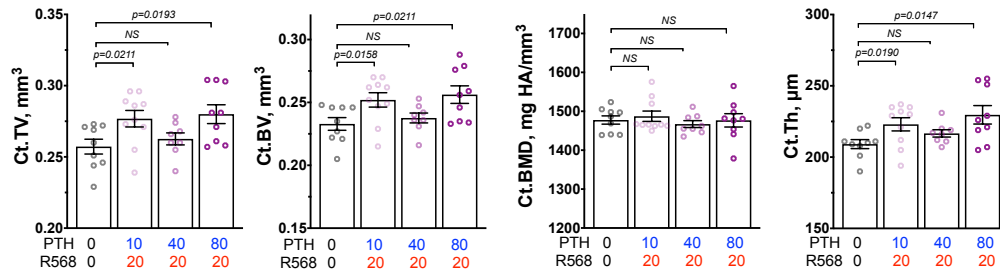
**(A)** Schedules for drug injection, bone labeling, and blood/tissue harvests. Drugs are injected daily. **(B)** Fluorescent labels of tibial periosteum at TFJs in 3-month-old male mice injected with PTH (40  $\mu\text{g}/\text{kg}/\text{day}$ )+R568 (20  $\mu\text{mole}/\text{kg}/\text{day}$ ) or PTH alone for 6 weeks using the schedule described in Figure 8A indicate distinct temporal changes in bone formation rates following the treatments. White numbers and arrows indicate sequences of the labels. White double-head arrows indicate distances between 2 consecutive labels. Arrowheads depict potential resorbing pits. BM: Bone matrix.

Figure 2.6

A. Distal femur trabecular bone skeletal parameters



B. Tibiofibular junction (TFJ) cortical bone skeletal parameters



## C. L5 – Vertebrae trabecular bone skeletal parameters

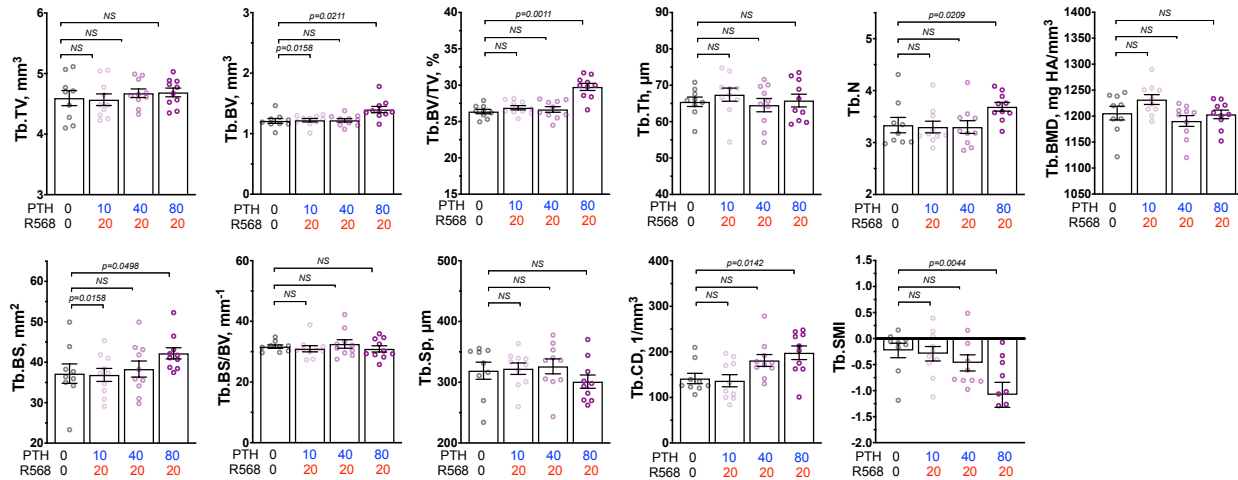
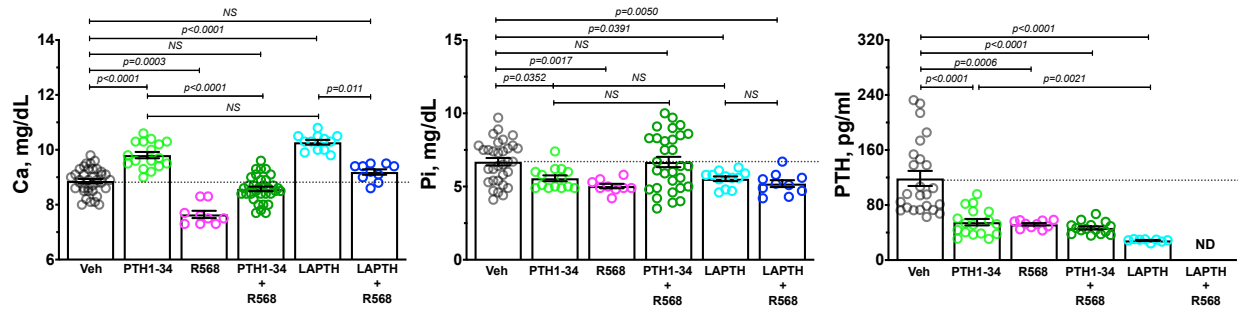


**Figure 2.6. Co-injections of the calcimimetic NPS-R568 produce additive osteoanabolic effects in trabecular and cortical bone of 12-month-old female mice.**

3D and 2D  $\mu$ CT images (**A**) and their corresponding structural parameters: total volume (TV), bone volume (BV), bone mass (BV/TV,%), bone surface (BS), spacing (Sp), thickness (Th), connectivity density (CD), number (N), bone mineral density (BMD), structural model index (SMI) for (**B**) distal femur trabecular bone (**C**) tibiofibular junction cortical bone and (**D**) L5-vertebrae trabecular bone. Skeletal parameters show synergistic effects of NPS-R568 to enhance osteoanabolism of PTH(1-34) most effectively at 80 ug/kg. Mice were treated with either Vehicle, or 10/40/80 ug/kg of PTH(1-34) with NPS-R568. N=9-10 mice per group, with each individual mouse represented by a colored circle; p-values labeled per comparison as determined by one-way ANOVA. NS: not significant.

**Figure 2.7**

**A. 3 hours post-injection, retro-orbital serum**



**B. 24 hours post-injection, terminal serum**

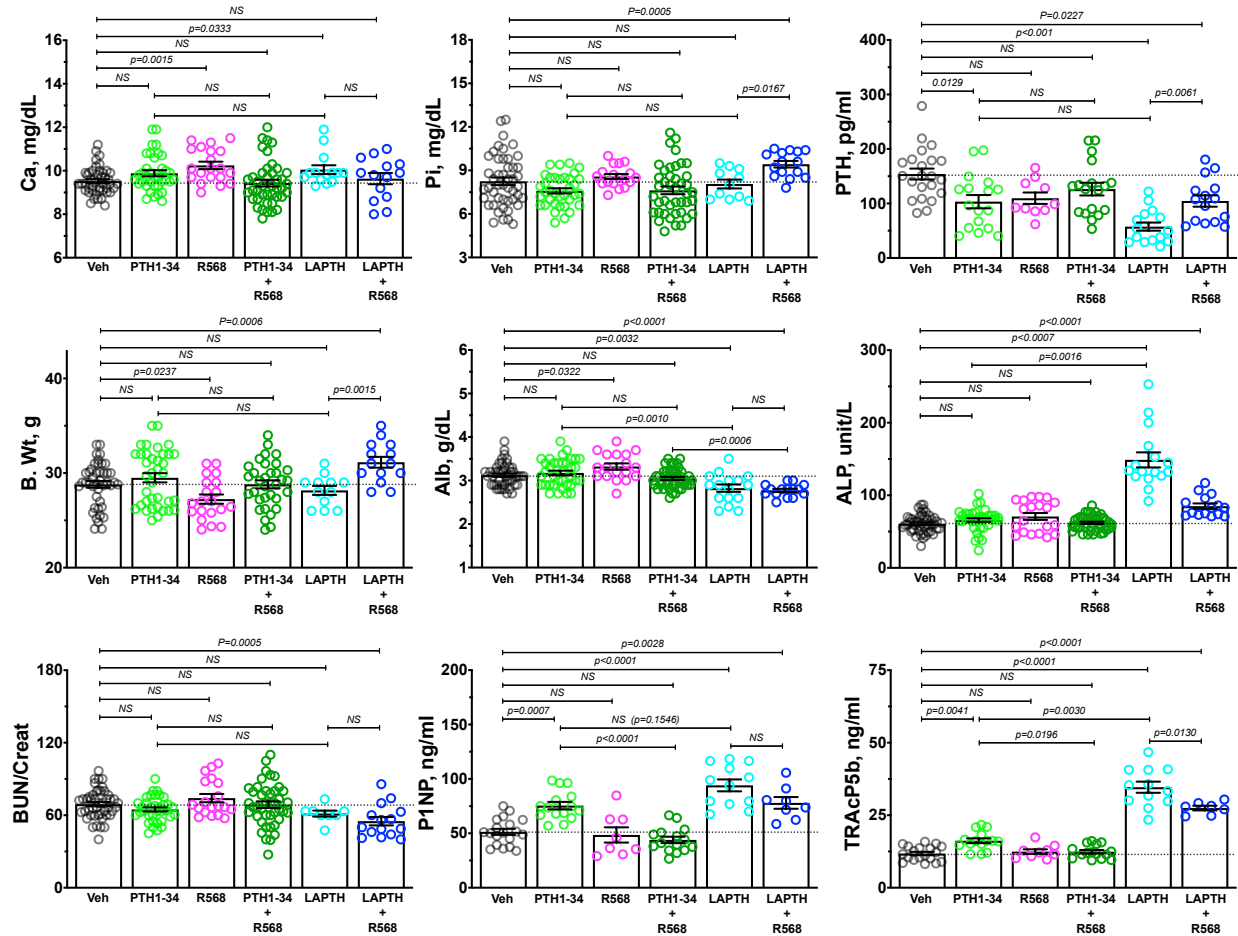


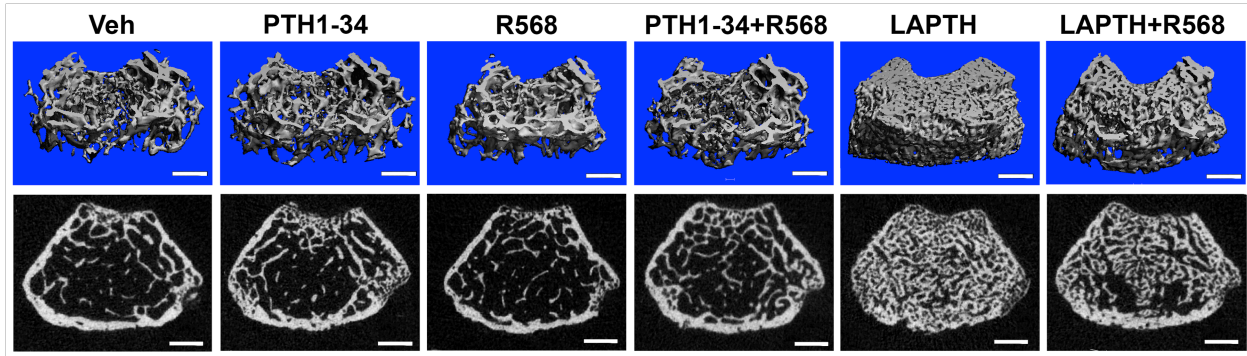
**Figure 2.7. Co-injections of the calcimimetic NPS-R568 offset the hypercalcemic side-effects of analogs PTH(1-34) and Long-Acting PTH (LA-PTH) in 3-month-old male mice.**

Serum  $\text{Ca}^{2+}$ , phosphate (Pi), albumin (Alb), non-specific alkaline phosphatase (ALP), blood urea nitrogen/ creatinine ratio (BUN/Creat), procollagen 1 intact N-terminal propeptide (P1NP), tartrate-resistant acid phosphatase 5b (TRACP 5b), body weight (B. Wt) from mice treated daily for 28 days with Vehicle, 40ug/kg PTH(1-34), 20umol/kg NPS-R568, PTH, 40 ug/kg PTH(1-34) with 20 umol/kg, 40 ug/kg LA-PTH, or 40 ug/kg LA-PTH with 20 mol/kg NPS-R568. **(A)** 3 hours post-injection, endogenous PTH was inhibited by PTH analogs and NPS-R568 while serum  $\text{Ca}^{2+}$  show the ability of injectable calcimimetics to offset hypercalcemic effects by PTH(1-34) and with more potent LA-PTH. **(B)** 24 hours post-injection, increases in serum bone turnover markers, P1NP and TRAcP 5b, were comparatively higher in LA-PTH, and LA-PTH + R568 than in PTH(1-34) treated mice, suggesting enhanced remodeling of skeletal sites and was further corroborated by dramatic increases in ALP. N=15-45 mice per group with each individual mouse represented by a colored circle; p-values labeled per comparison as determined by one-way ANOVA. NS = not significant.

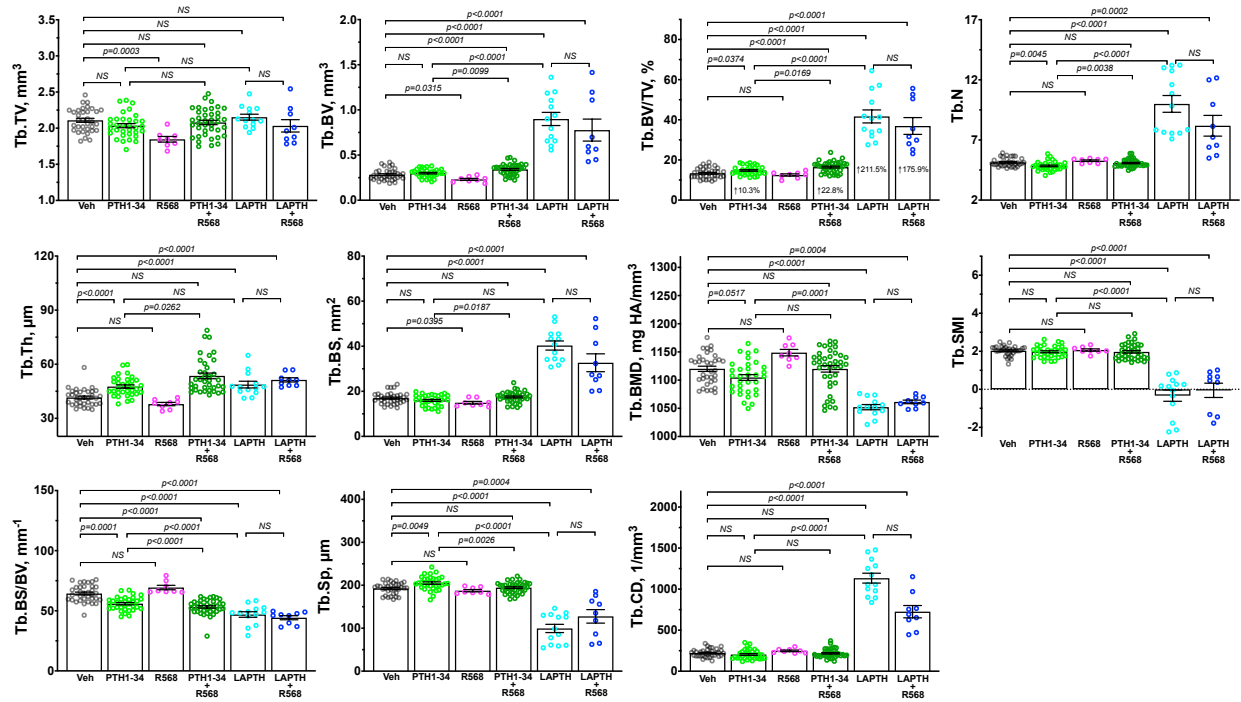


Figure 2.8.

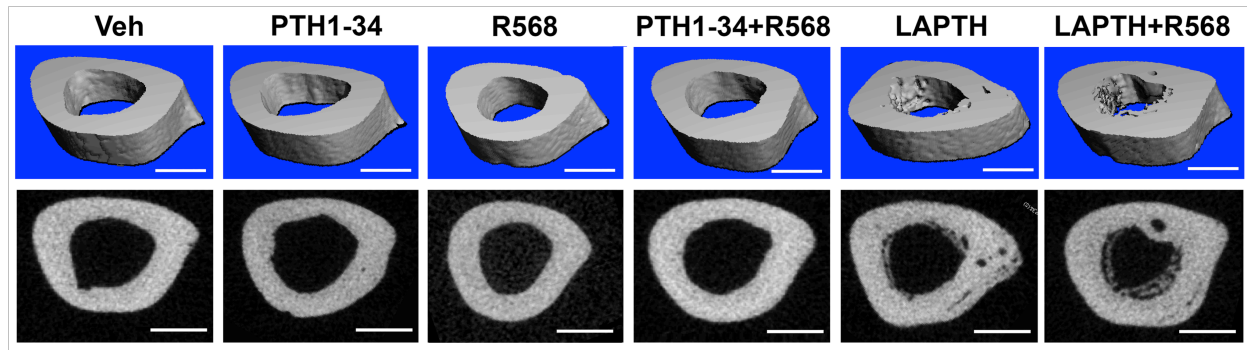
A. Distal femur trabecular bone, 3D and 2D images



B. Distal femur trabecular bone skeletal parameters



## C. Tibiofibular junction cortical bone, 3D and 2D images



## D. TFJ cortical bone skeletal parameters

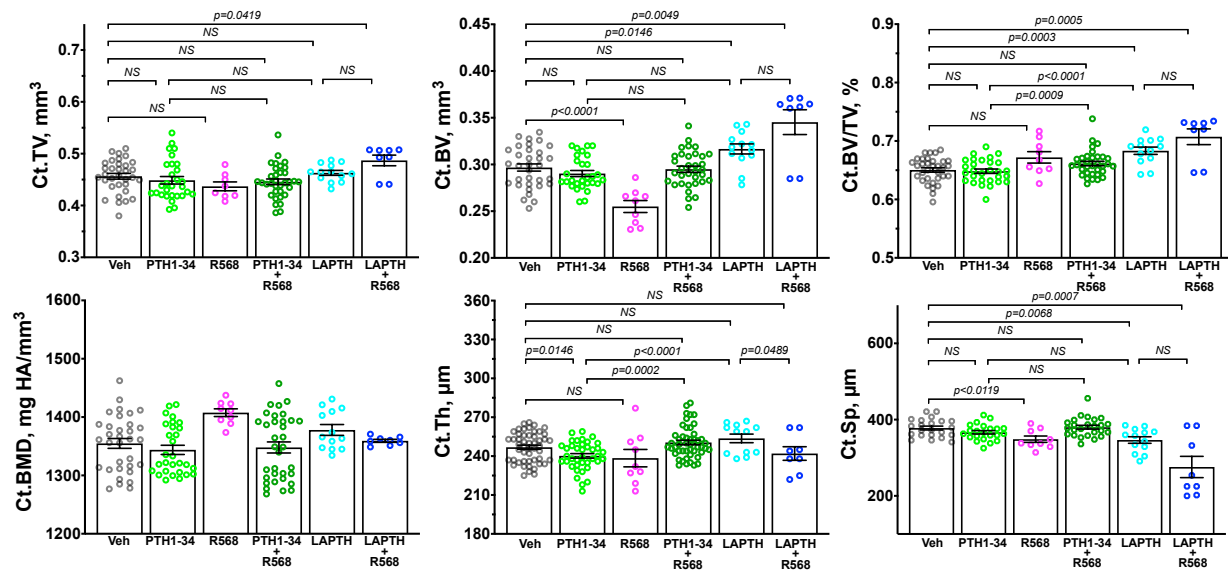
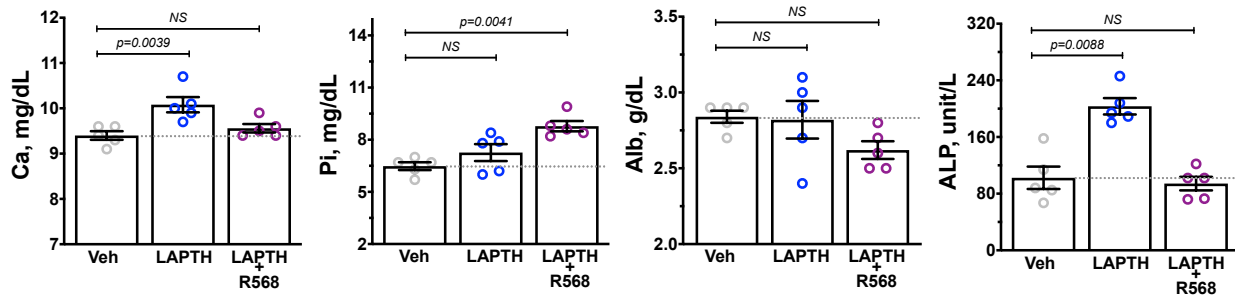


**Figure 2.8. LA-PTH produces more robust osteoanabolic effects in trabecular and cortical bone than PTH(1-34) with and without co-injection with calcimimetic NPS-R568.**

3D and 2D  $\mu$ CT images (A) and their corresponding structural parameters: total volume (TV), bone volume (BV), bone mass (BV/TV,%), bone surface (BS), thickness (Th), spacing (Sp), number (N), bone mineral density (BMD), structural model index (SMI) for (B) distal femur trabecular bone (C) tibiofibular junction cortical bone and (D) L5-vertebrae trabecular bone. Skeletal parameters show synergistic effects of NPS-R568 to enhance osteoanabolism of PTH(1-34) and LA-PTH. LA-PTH shows more robust anabolic effect compared to PTH(1-34) in both trabecular and cortical bone. Increased bone remodeling is further evident in the endo/periosteum of the cortical bone. N=9-37 mice per group, with each individual mouse represented by a colored circle; p-values labeled per comparison as determined by one-way ANOVA. NS = not significant.

## Figure 2.9

### A. 12-month-old female: 3-injections/ week, terminal serum



### B. 12-month-old-male: 3-injections/ week terminal serum

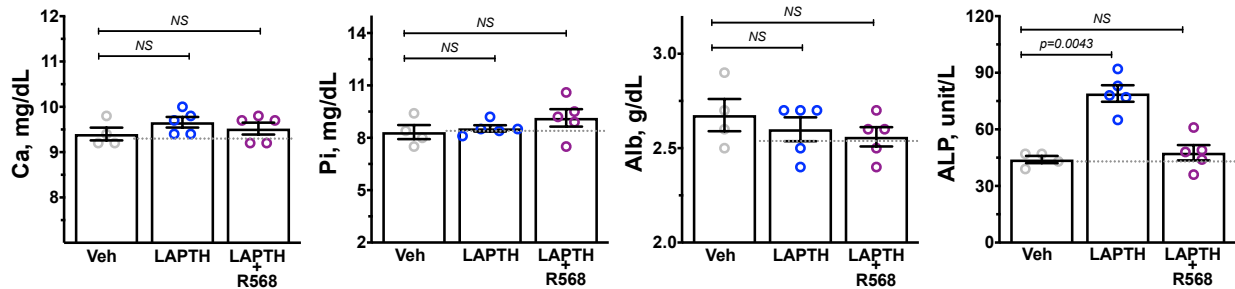
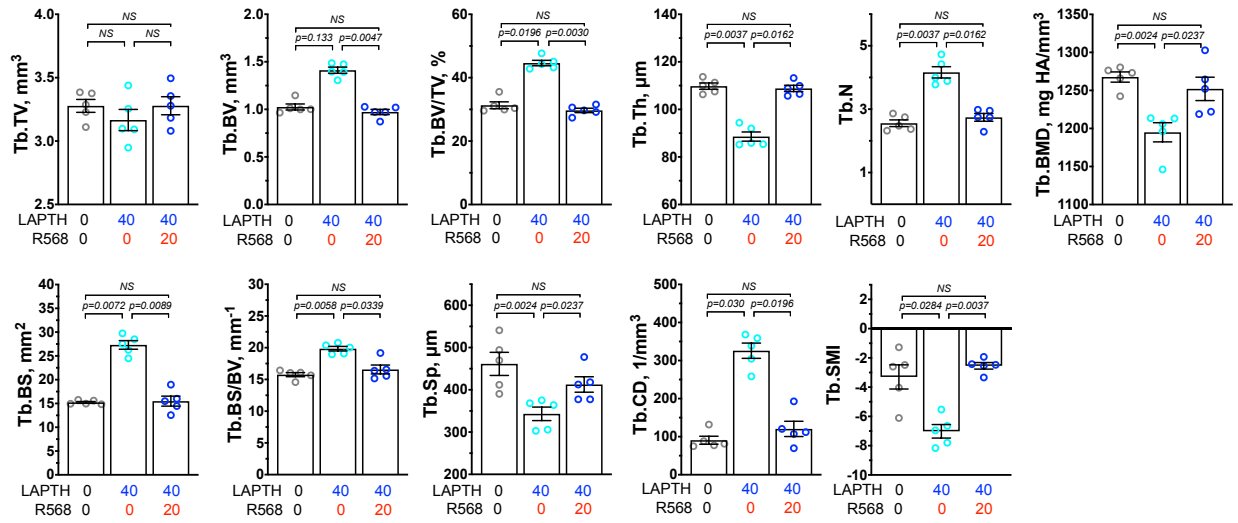


**Figure 2.9. Co-injections of the calcimimetic NPS-R568 offset the hypercalcemic side-effects of Long-Acting PTH (LA-PTH) in 12-month-old female and male mice.**

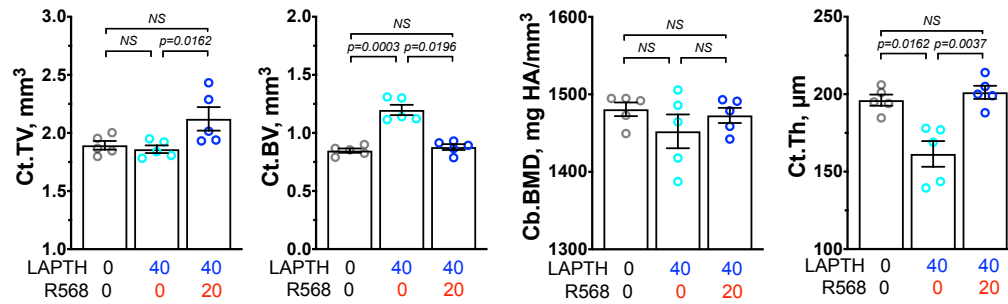
Serum  $\text{Ca}^{2+}$ , phosphate (Pi), albumin (Alb), and non-specific alkaline phosphatase (ALP) from mice treated 3 times per week, every other day, for 4 weeks with Vehicle, LA-PTH, 40 ug/kg, or LA-PTH 40 ug/kg with 20 mol/kg NPS-R568. 12 hours post-final injection, the calcimimetic offset the hypercalcemic effects of LA-PTH in both **(A)** female and **(B)** male mice and also dampened the increased ALP. N=4-5 mice per group with each individual mouse represented by a colored circle; p-values labeled per comparison as determined by one-way ANOVA. NS = not significant.

**Figure 2.10**

**A. Distal femur trabecular bone skeletal parameters**



**B. TFJ cortical bone skeletal parameters**



## C. L5 – Vertebrae trabecular bone skeletal parameters

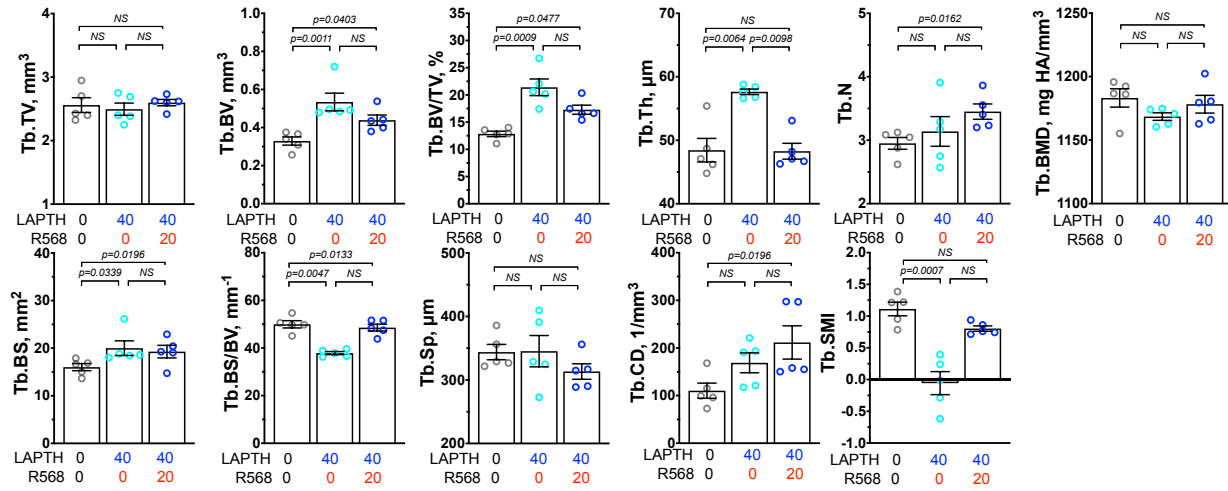
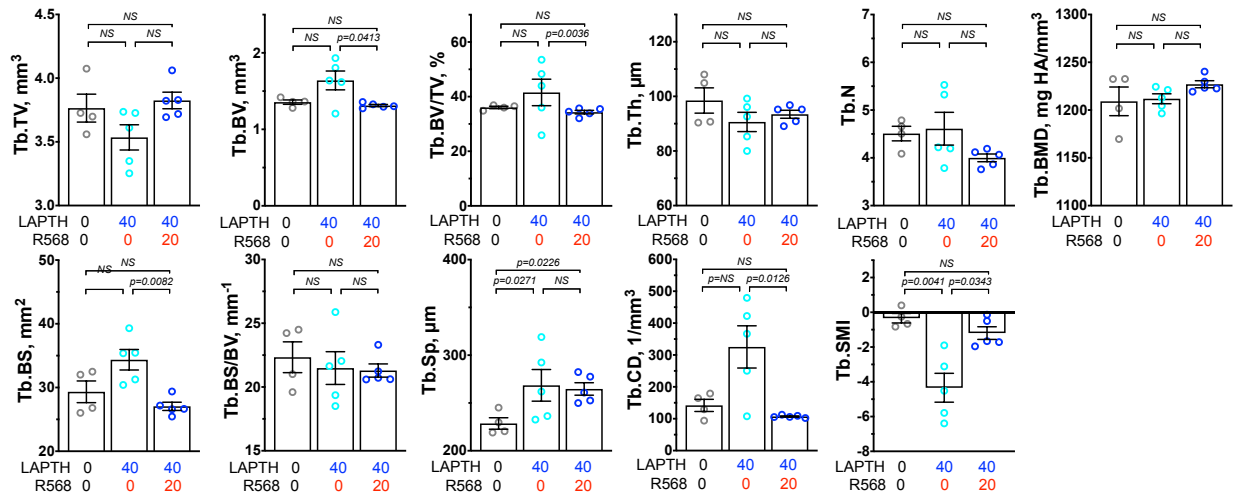


**Figure 2.10. LA-PTH produces more robust osteoanabolic effects in trabecular and cortical bone, which is generally annulled with calcimimetics in aged female mice.**

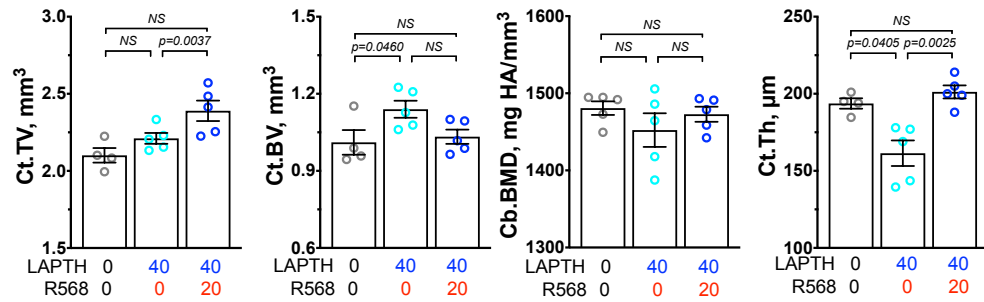
Skeletal structural parameters: total volume (TV), bone volume (BV), bone mass (BV/TV,%), thickness (Th), number (N), bone mineral density (BMD), bone surface (BS), spacing (Sp), structural model index (SMI) for **(B)** distal femur trabecular bone **(C)** tibiofibular junction cortical bone and **(D)** L5-vertebrae trabecular bone. Female mice were injected 3 times per week during a 4-week course. Skeletal parameters exhibit the LA-PTH anabolic effect, which is generally lost except in case of L5 vertebrae trabecular bone. In cortical bone, LA-PTH has a catabolic effect which is rescued with co-injection with calcimimetics. N=4-5 mice per group with each individual mouse represented by a colored circle; p-values labeled per comparison as determined by one-way ANOVA. NS = not significant.

Figure 2.11

A. Distal femur trabecular bone skeletal parameters



B. TFJ cortical bone skeletal parameters



## C. L5 – Vertebrae trabecular bone skeletal parameters

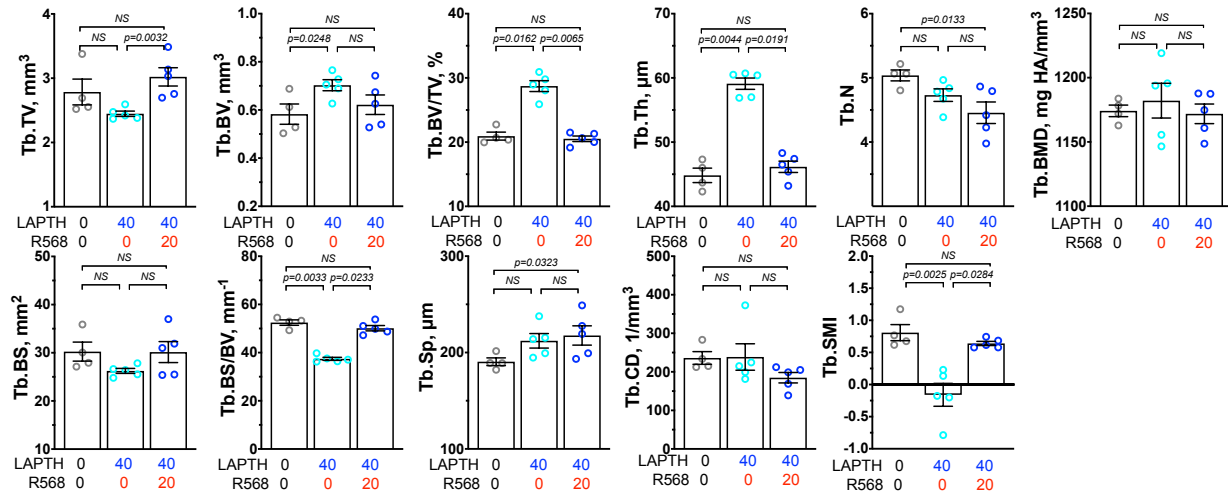


**Figure 2.11. LA-PTH produces more robust osteoanabolic effects in trabecular and cortical bone, which is generally annulled with calcimimetics in aged female mice.**

Skeletal structural parameters: total volume (TV), bone volume (BV), bone mass (BV/TV,%), thickness (Th), number (N), bone mineral density (BMD), bone surface (BS), spacing (Sp), structural model index (SMI) for **(B)** distal femur trabecular bone **(C)** tibiofibular junction cortical bone and **(D)** L5-vertebrae trabecular bone. Male mice were injected 3 times per week during a 4-week course. Skeletal parameters exhibit the LA-PTH anabolic effect, which is generally lost except in case of L5 vertebrae trabecular bone. In cortical bone, LA-PTH has a catabolic effect, which is rescued with co-injection with calcimimetics. N=4-5 mice per group with each individual mouse represented by a colored circle; p-values labeled per comparison as determined by one-way ANOVA. NS = not significant.

**Figure 2.12**

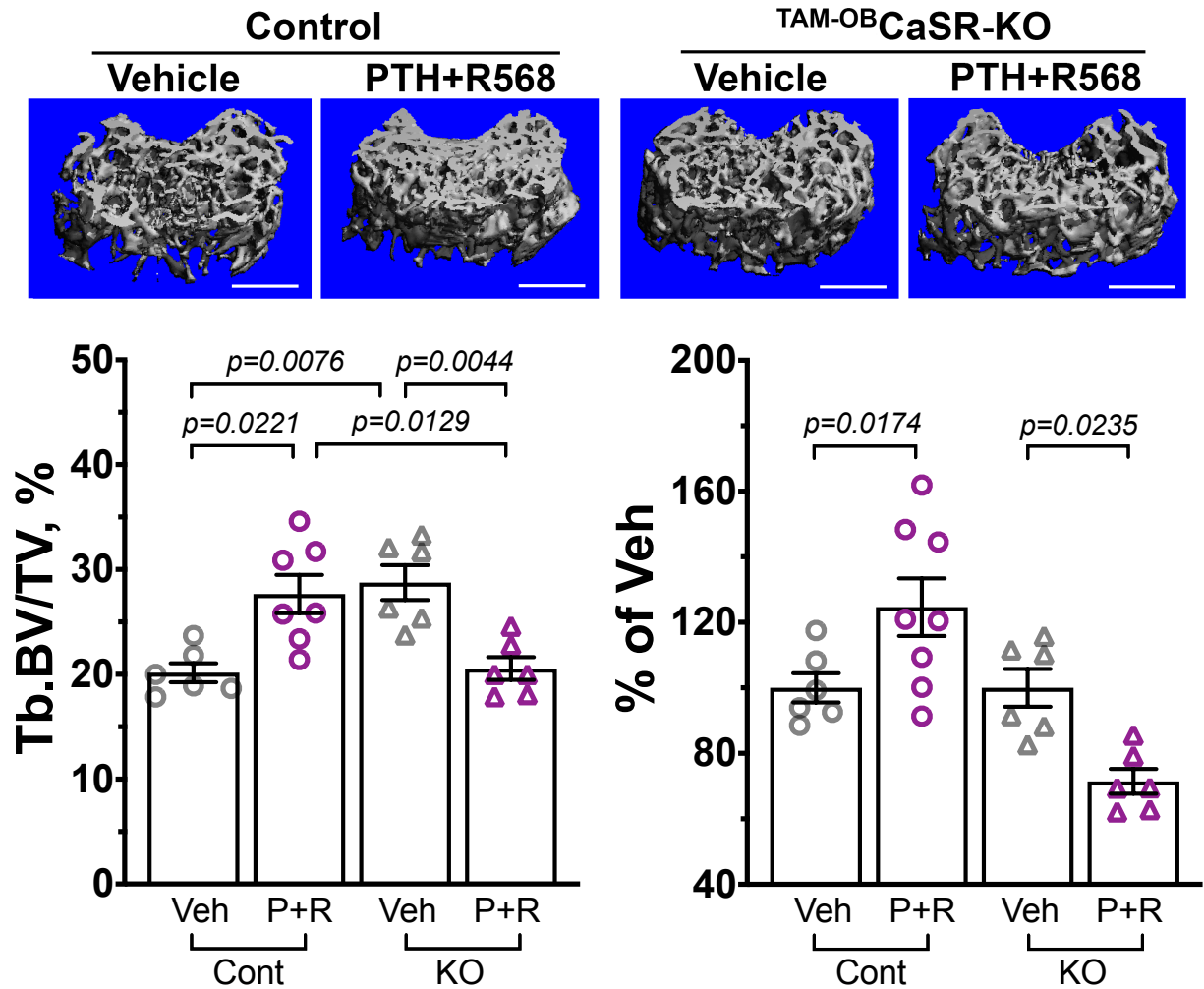


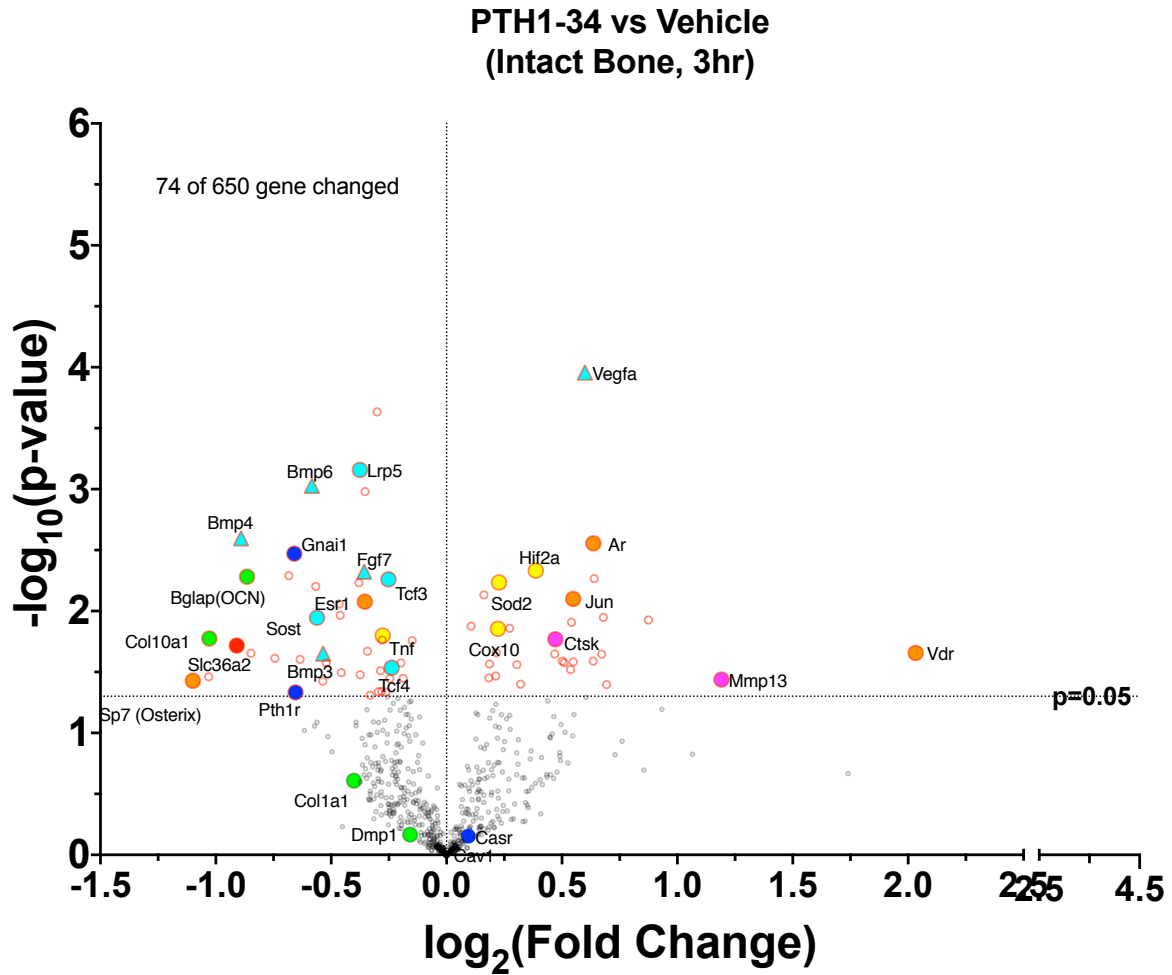
**Figure 2.12. The osteoanabolic effects of intermittent PTH and NPS-R568 treatment were abrogated in osteoblast-specific CaSR knockout mice.**

3D  $\mu$ CT images and their corresponding Tb bone mass (BV/TV%) on the left and % normalized to Vehicle controls.  $^{2.3\text{Col}(1)}\text{CaSR}^{\Delta\text{flox}/\Delta\text{flox}}$  mice showed that ablation of CaSRs early in the OB lineage abrogated osteoanabolism induced by the combined PTH with calcimimetic treatment. N=5-8 mice per group, with each individual mouse represented by a colored circle; p-values labeled per comparison as determined by one-way ANOVA. NS = not significant.



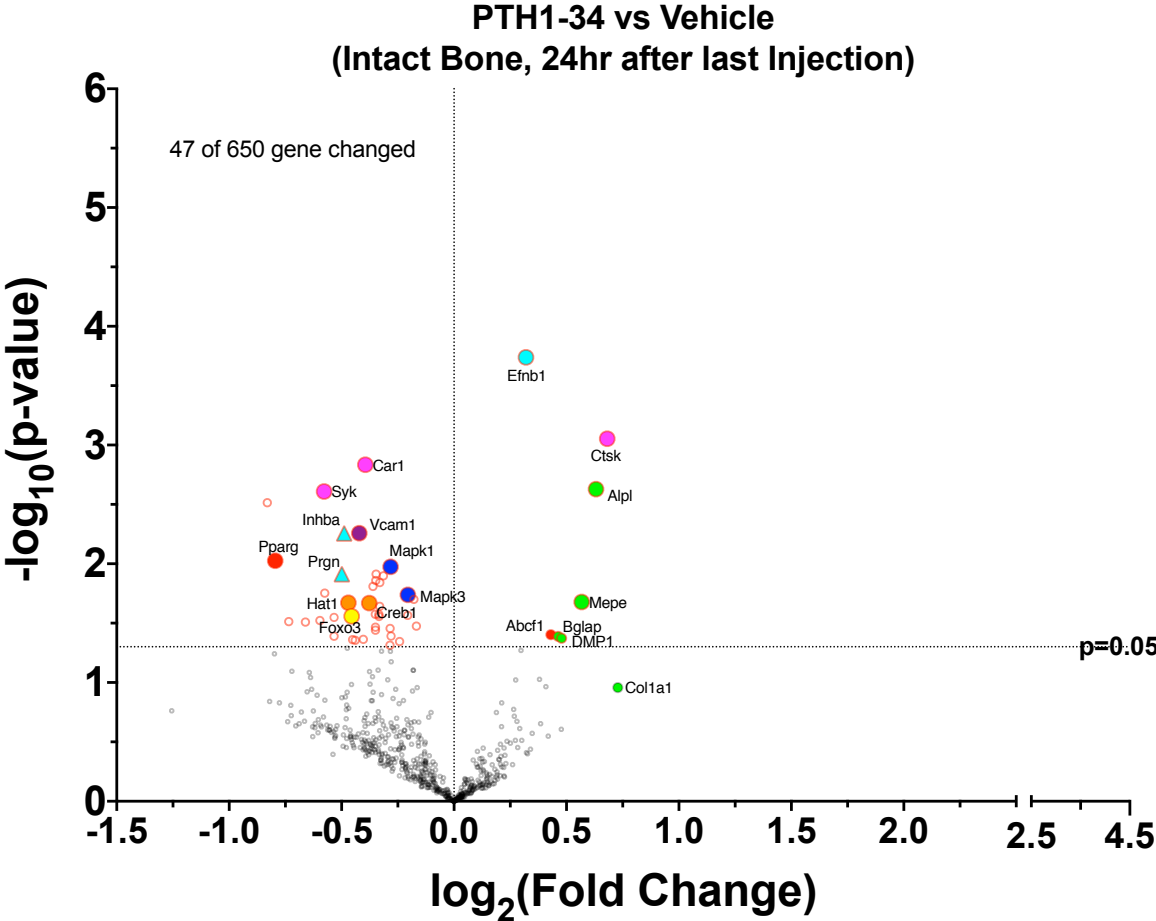
Figure 2.13

A. Changes in gene expression of PTH(1-34) vs Vehicle, 3 hours post-injection

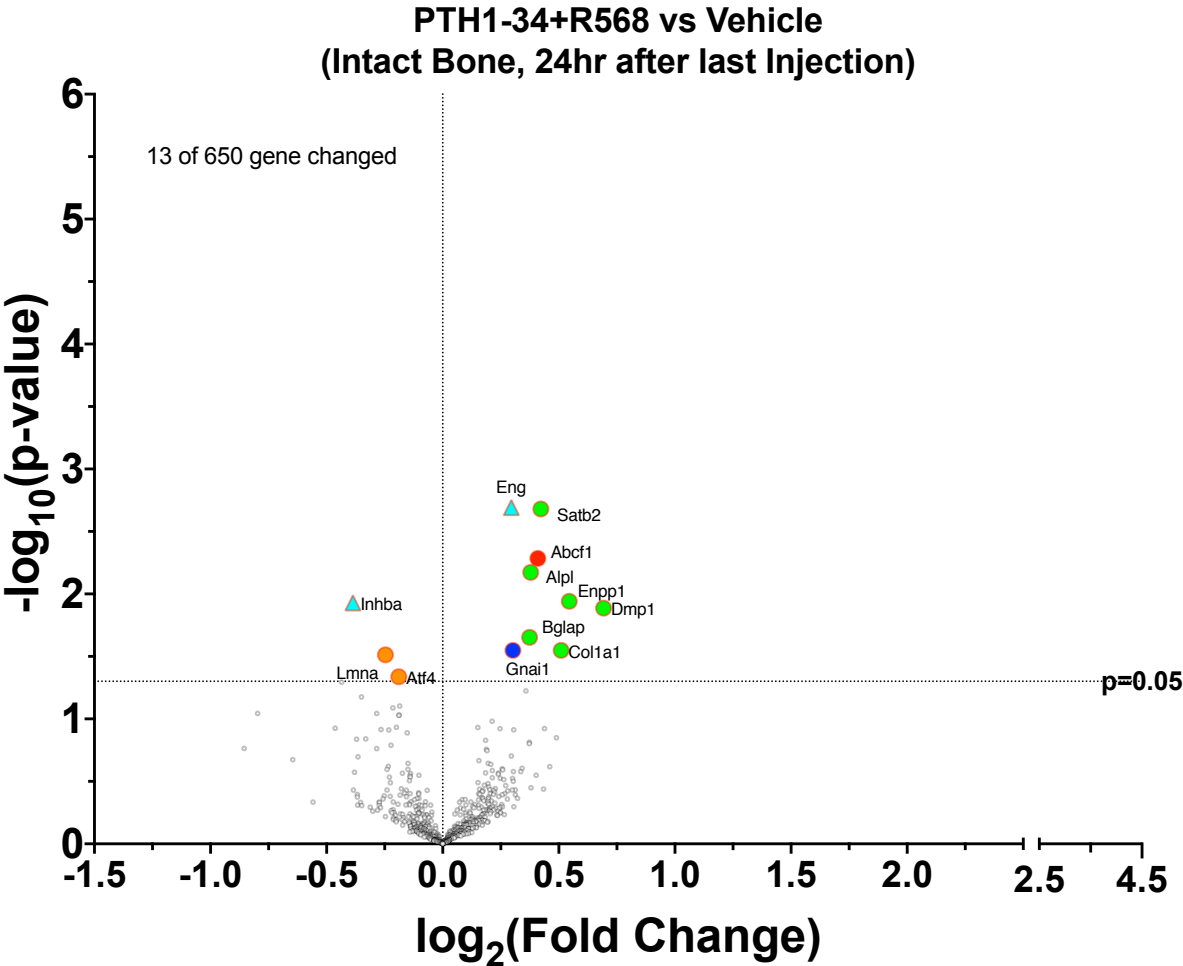




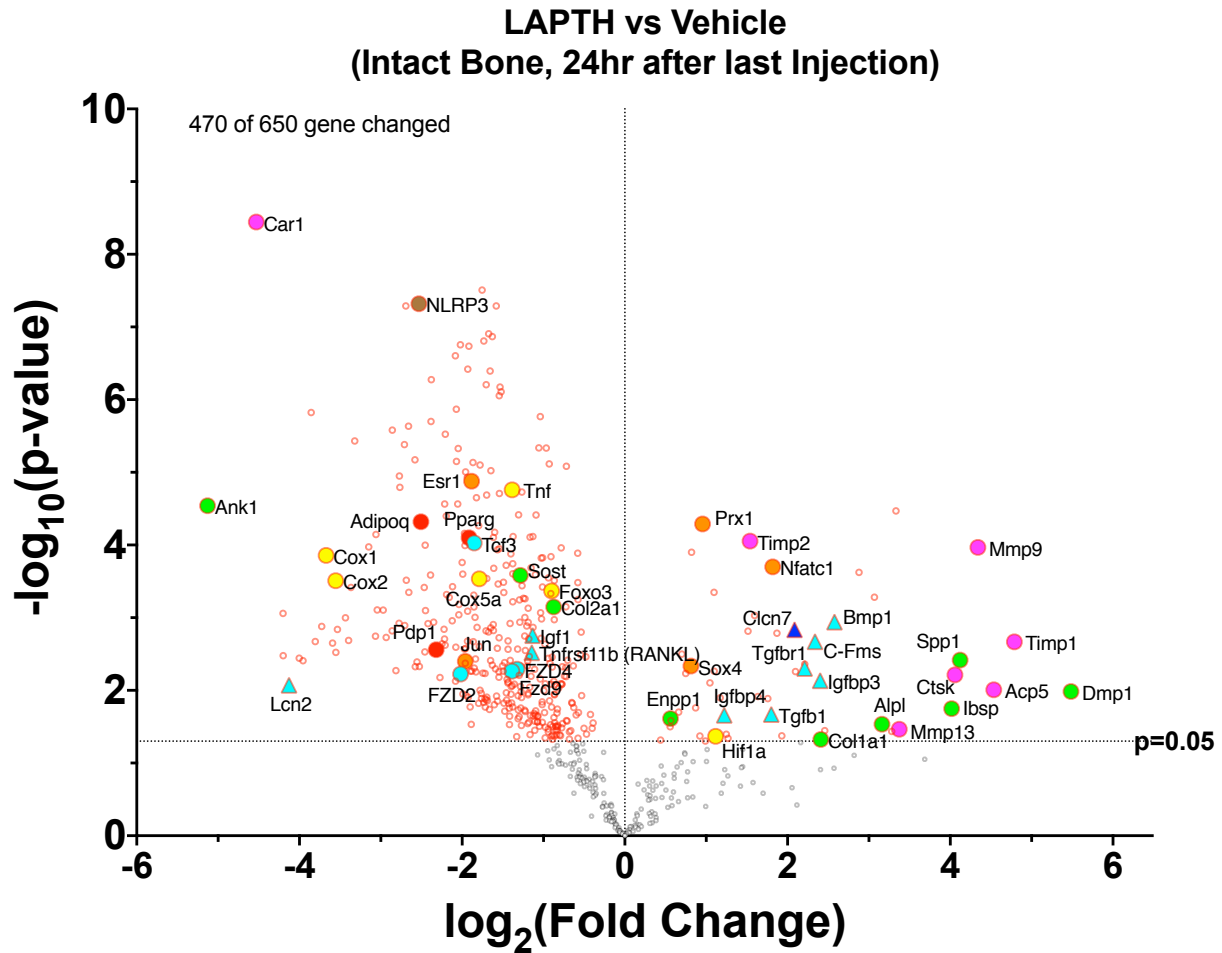
### C. Changes in gene expression of PTH(1-34) vs Vehicle, 24 hours post-injection



### D. Changes in gene expression of PTH(1-34) + NPS-R568 vs Vehicle, 24 hours post-injection



### E. Changes in gene expression of LA-PTH vs Vehicle, 24 hours post-injection



## F. Changes in gene expression of LA-PTH + NPS-R568 vs Vehicle, 24 hours post-injection

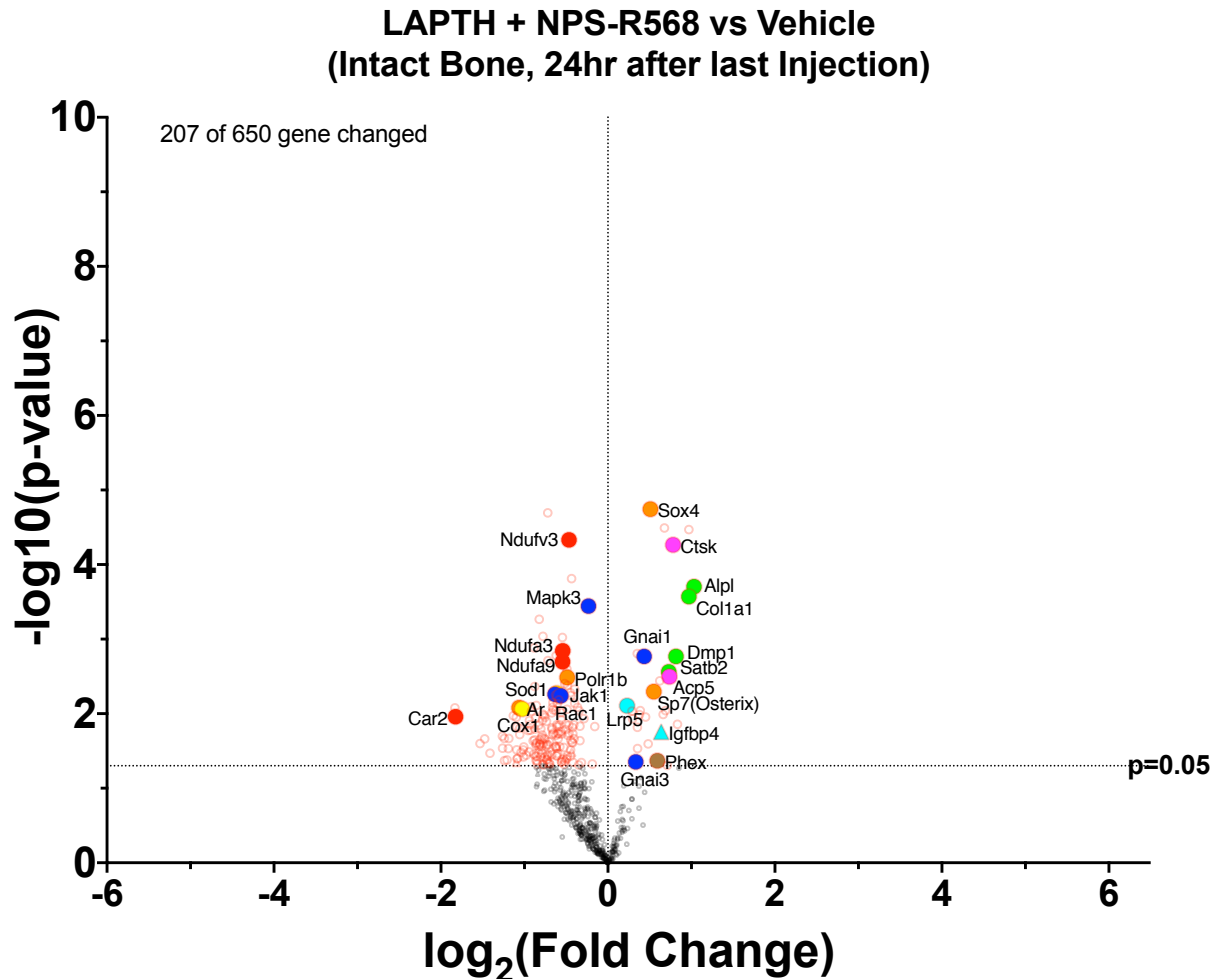


**Figure 2.13. Nanostring confirms gene expression shift towards bone anabolism**

Total RNA was isolated from intact femur and tibia of mice treated with Vehicle, PTH(1-34), LA-PTH, or LA-PTH with NPS-R568. mRNA abundance was quantified by NanoString nCounter using a bone specific Code of 625 genes involved in chondrogenic, osteogenic, osteocytic, osteoclastic, adipogenic, inflammatory and metabolic pathways. X-axes indicated fold change while Y-axes measure  $-\log$  of p-value (dotted horizontal line corresponds to  $p = 0.05$ ). Vertical dotted line represents no change in mRNA transcripts. Genes labeled on the left indicate decreased expression while genes on the right indicate increased expression.

Figure 2.14

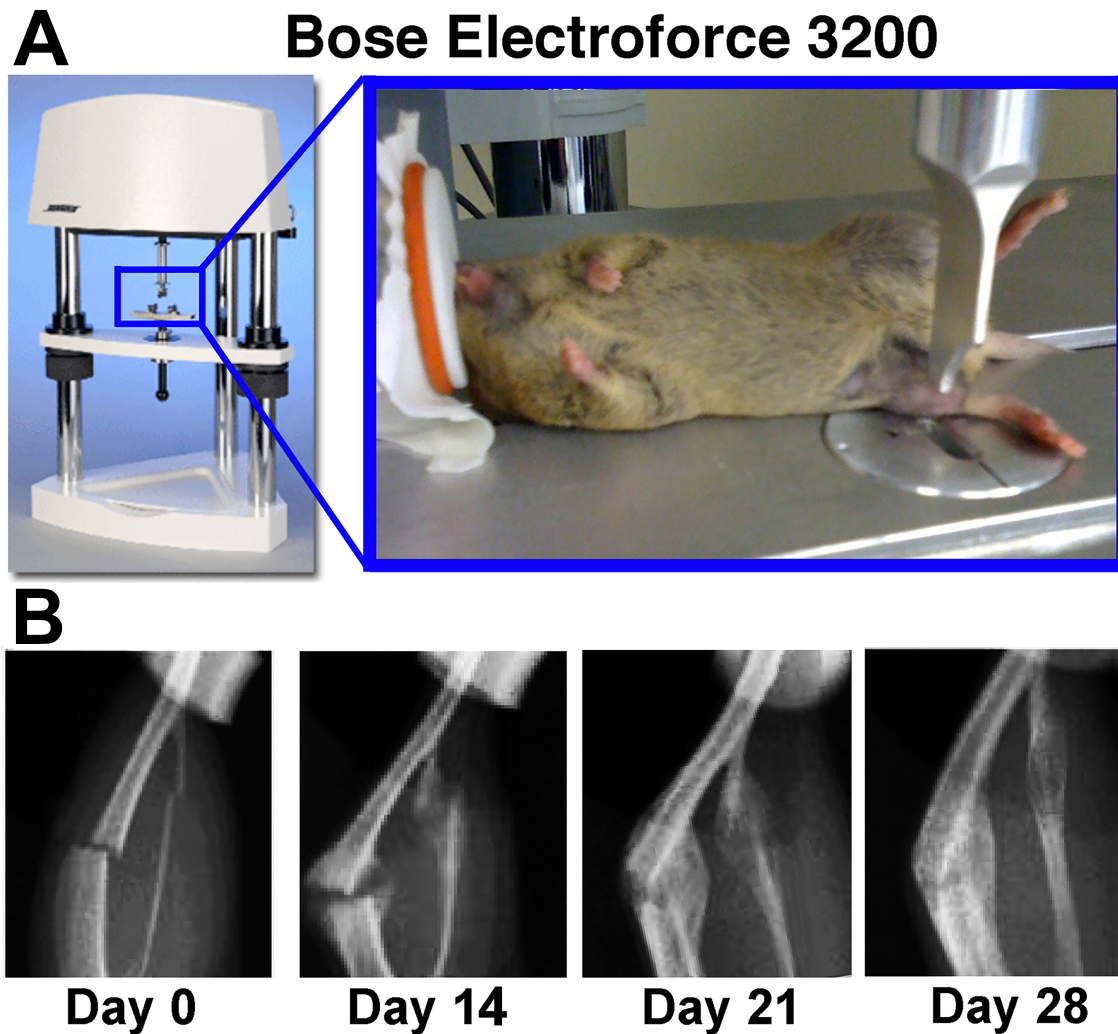
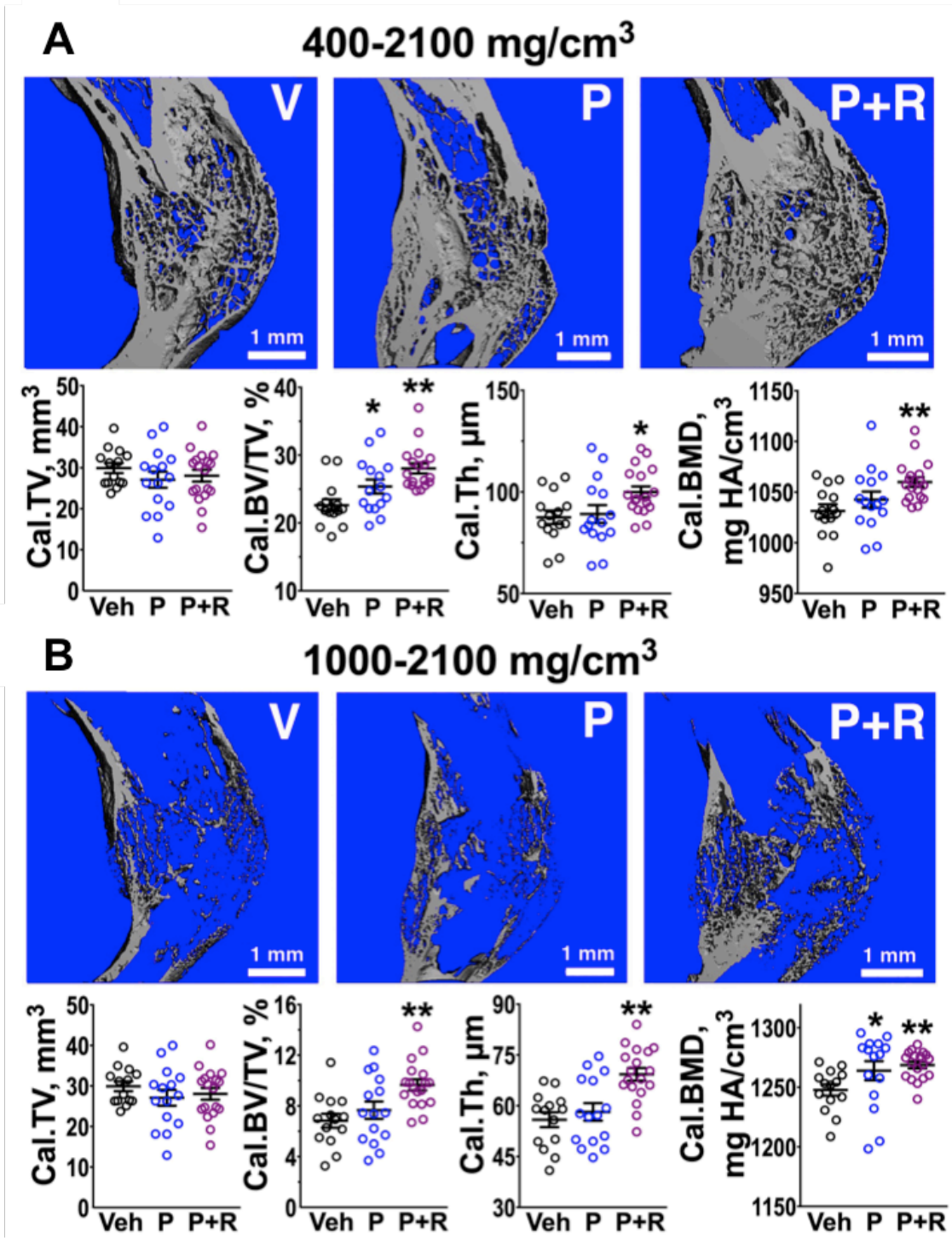


Figure 2.14. Using 3-point-bending to create closed-unfixed tibial midshaft fractures in mice.

(A) Picture of Bone Electroforce 3200 material tester that was adapted to produce tibial mid-shaft fracture by 3-point bending on anesthetized mice. (B) The time course of fracture healing in normal mouse tibia by X-ray scans at different time points after fracture.

Figure 2.15





**Figure 2.15. Co-injections of the calcimimetic NPS-R568 produce additive osteoanabolism in bony calluses.**

Co-injections of calcimimetic NPS-R568 produce synergistic osteoanabolism in bony calluses.  $\mu$ CT analyses of bony calluses in 3-month-old male C57/B6 male mice subjected to tibial fracture and daily injections of vehicle (V), PTH(1-34) (P, 40  $\mu$ g/kg B.Wt.), or PTH(1-34)+R568 (P + R, 20  $\mu$ mol/kg B.Wt) for 28 days. (A,B) 3D  $\mu$ CT images and their structural parameters (histograms) assessed with (A) 400–2100 mg HA/cm<sup>3</sup> or (B) 1000–2100 mg HA/cm<sup>3</sup> thresholds, which measure total and high-density bone, respectively, show the synergistic effects of R568 to increase osteoanabolism of PTH(1-34). Mean  $\pm$  SEM,  $n = 15$ – $17$  mice/group; \* $p < 0.05$ ; \*\* $p < 0.01$  versus vehicle, two-way ANOVA with Tukey's test for multiple comparisons.

**Table 2.1 Primer sets used for Genotyping Assays**

	Primer sequences
Tam-Card <sup>T</sup> CreER <sup>T</sup>	Upper: 5'-GCA AAA CAG GCT CTA GCG TTC G-3' Lower: 5'-CTG TTT CAC TAT CCA GGT TAC GG-3'
Floxed-CaSR	Upper: 5'-CTT CCC AGC TTG CTA CTC TAG G-3' Lower: 5'-CAG GCT TGC AAT GAG ACA TGG G-3'
CaSR excision	Upper: 5'-TGA GAC GTA GCG AGA TTG CTG TA-3' Lower: 5'-CAG GCT TGC AAT GAG ACA TGG G-3'

## 2.2 Discussion

Simultaneous pharmacological activation of the PTH1R and CaSR is a novel strategy to enhance the potential of PTH analogs, PTH(1-34) and LA-PTH, for skeletal anabolism. In this dissertation, we demonstrate that a combined PTH and NPS-R568 regimen overcomes the complications of hyper- or hypocalcemia that can be found, respectively, with each compound alone, while producing a more superior osteoanabolic effect than targeting the PTH1R alone. The exact mechanisms normalizing serum  $\text{Ca}^{2+}$  by the combined drug treatment remains to be defined but likely involve cooperative calcitropic actions in multiple organs, like the parathyroid glands, kidney, intestine, and bone. First, blockade of endogenous PTH by synergistic activation of CaSR in parathyroid glands through  $\text{Ca}^{2+}$ -elevating actions of exogenous PTH(1-34) or LA-PTH and positive allosteric modulation by calcimimetics could already tone down the associated calcitropic activities. Second, increased renal  $\text{Ca}^{2+}$ -excretion by NPS-R568-induced CaSR activation is expected to provide additional  $\text{Ca}^{2+}$ -lowering action. Third, NPS-R568 is assumed to block osteoclastic activities, according to previous report on the ability of calcimimetics to suppress osteoclastic differentiation and resorbing functions [60]. Fourth, our nCounter gene expression profiling (**Figure 16**) show the ability of NPS-R568 to acutely repress genes involved in osteocytic perilacunar remodeling (PLR), i.e., *Ctsk* [61] and *Mmp13* [62], constituting another mechanism to prevent PTH-induced hypercalcemia. The latter osteocytic actions require future confirmation by direct histomorphometric assessment of PLR activities as well as studies of mice with osteocyte-targeted *Ctsk* and/or *Mmp13* KO. Finally, the NPS-R568 is assumed to promote mineralizing functions of osteoblasts to re-deposit  $\text{Ca}^{2+}$  into

bone matrix, presenting additional  $\text{Ca}^{2+}$ -lowering action, according to our working models (**Figure 1**). The above mechanisms also provide the molecular bases for synergism of PTH and calcimimetics in producing skeletal anabolism. Future comprehensive studies of mice with tissue-specific ablation of PTH1R and/or CaSR mouse models are needed to further define the actions of these receptors in mediating both systemic calcemic actions as well as their skeletal effects. Indeed, failure of combined PTH(1-34)/NPS-R568 treatment to produce anabolic effects on bone in our mice with Tam-induced *Casr* gene KO in osteoblasts provisionally supports an essential role of osteoblastic CaSR in mediating such skeletal synergism.

In addition to its more superior bone-building actions, our combined PTH/NPS-R568 regimens produce osteoanabolism beyond Tb elements and cause cortical expansion that is not impacted by treatment of PTH(1-34) alone. This cortical action is consistent with the increased mechanical strength assessed by 3-point bending test (**Figure 7**) in femurs from mice subjected to combined PTH/NPS-R568 regimens. However, detailed actions of the latter regimens on cortical bone require future histomorphological assessment of both statics and dynamic bone parameters.

As a first-in-mouse pharmacological attempt of our regimen, this study explored various doses of PTH(1-34) in the context of a fixed NPS-R568 concentration. As we screened for the most effective combination dose that would, at minimum, normalize the hypercalcemic effect of PTH(1-34), we did not change the concentration of NPS-R568. Although we achieved normalized serum  $\text{Ca}^{2+}$  at 20 ug/kg, future studies are needed to

elucidate the dose of NPS-R568 that achieves maximum efficacy of bone formation. For example, in LA-PTH treated mice, increased mineralization of newly synthesized bone matrices may be achieved with a higher concentration dose of calcimimetic. Similarly, we did not test a range of concentrations of LA-PTH, which has far more hypercalcemic and osteoanabolic potential than PTH(1-34). We did however decrease the amount of injections from 5 to 3 during a 4-week course in the pilot study with older male and female mice due to consideration of toxic effects that we found in healthy adult male mice. Future studies will involve manipulating the 1) number of doses, 2) time course, and 3) dosage concentration of drugs to achieve the most physiologically tolerable and robust osteoanabolism. The discoveries from modifications in treatment dose and schedule to fine-tune hormonal and mineral metabolism will provide insights in achieving optimal safety and efficacy. The flexible adjustments of doses in this manner are fundamental as we move into an age of more personalized medicine for patients.

This study has several strengths in experimental design and execution. First, a robust number of animals ensures statistical power for the *ex vivo* assessments of bone microarchitecture and highly variable hormonal factors, like PTH. Second, mice with different ages and sexes were used. Third, all experiments are performed at least twice with different batches of drug compounds for reproducibility. Fourth, skeletal assessments include multiple skeletal sites that correspond to increased fracture risk in aged populations and postmenopausal women for clinical relevance. This study also has several limitations, including the sole use of healthy animals that lack of disease contexts, the incomplete histomorphometry data which were prevented by laboratory

lock down amid COVID-19 pandemic, and lack of additional biomechanical testing at the vertebrae.

In summary, this work is highly significant as it uncovers a novel mechanism underlying the skeletal actions of PTH and develops a translatable regimen that is ready for testing in clinical setting. Given that the PTH(1-34) (Forteo<sup>®</sup>) and oral form of calcimimetics (Sensipar<sup>®</sup>) are already in clinical use with abundant safety data, our proof-of-concept preclinical studies readily provide a blueprint for designs of clinical trials to assess safety and efficacies of our combined therapy in humans.

## 2.4 Materials and Methods

### Mice

All mouse protocols were approved and performed according to guidelines by the Institutional Animal Care and Use Committee (IACUC), of the University of California, San Francisco, and the San Francisco Department of Veterans Affairs Medical Center. C57BL/6 mice were obtained from The Jackson Laboratory.

Floxed-CaSR ( $\text{CaSR}^{\text{flox/flox}}$ ) mice were bred with  $\text{Cart-CreER}^{\text{T}}$  mice, which carry a tamoxifen (Tam)-inducible  $\text{CreER}^{\text{T}}$  transgene under the control of *Col1a1* gene promoter for chondrocyte-specific expression, to produce  $\text{Tam.Cart.CaSR}^{\text{flox/flox}}$  mice that developed normally in the absence of Tam.  $\text{Tam.Cart.CaSR}^{\text{flox/flox}}$  mice were injected daily with Tam (2 mg/25 g body weight, in corn oil [Millipore Sigma, Burlington, MA, USA; #C8267]) through the intraperitoneal (IP) route according to specified schedules to induce *Casr* gene KO in the resulting  $^{2.3\text{Col}(1)}\text{CaSR}^{\Delta\text{flox}/\Delta\text{flox}}$  mice.  $\text{CaSR}^{\text{flox/flox}}$  mice without expression of  $\text{Cart-CreER}^{\text{T}}$  transgene were injected with Tam to serve as controls. All mutant mice were in C57/B6 background. Mouse genotypes were determined by PCR analyses of genomic DNAs from tail snips with primer sets for the *Cre* transgene and the loxP sequence flanking the exon 7 of *Casr* gene.

Mice were ear-tagged for identification, randomly assigned to groups, and subcutaneously injected daily, or as specified in results, with the drugs individually or in combination with specified doses for 4-6 weeks. All mice were kept in a climate-controlled room (22°C; 45% to 54% relative humidity) with a 12-hour light/12-hour dark

cycle. Water and standard chow (1.3% calcium and 1.03% phosphate) were given *ad libitum*. All experiments are performed on 3-month-old adult male mice to avoid 1) pre- and perinatal developmental defects due to early ablation of *Casr* gene and 2) female-specific side-effects of Tam on hormonal and reproductive systems, which could complicate data interpretation and prevent a definitive conclusion from our study. All animal experiments (Protocol #18–013) were approved and performed according to guidelines of the Institutional Animal Care and Use Committee at the San Francisco Department of Veterans Affairs Medical Center.

## **Drugs**

- Parathyroid Hormone PTH(1-34) (rat) (Bachem, Torrance, CA, USA; Cat# H-5460), was dissolved in 1mM hydrochloric acid solution containing 2% BSA, and stored at -80°C.

- NPS-R568 hydrochloride (Tocris, Minneapolis, MN, USA; Cat# 3815), a positive allosteric modulator of human extracellular Ca<sup>2+</sup>-sensing receptor (CaSR), was dissolved in DMSO and stored at -80°C.

- Long-Acting PTH, or LA-PTH, a hybrid of ([Ala<sup>1,3,12</sup>,Gln<sup>10</sup>, Arg<sup>11</sup>,Trp<sup>14</sup>]PTH(1-14))/[Ala<sup>18,22</sup>,Lys<sup>26</sup>]PTHrP(15-36)COOH), was gifted from Dr. Jean-Pierre Vilardaga from the University of Pittsburgh.

## ***Ex-vivo* Micro-computed Tomography (μCT)**

To assess mineral content and structure, we performed μCT scans at two sites: distal femur and L5-vertebrae for trabecular (Tb) bone and tibio-fibular junction (TFJ) for



cortical (Ct). Briefly, femurs and tibiae were fixed in 10% phosphate-buffered formaldehyde (PBF) for 24 hrs, stored in 70% ethanol, and scanned by a SCANCO  $\mu$ CT 50 (SCANCO Medical AG, Basserdorf, Switzerland) with 10.5  $\mu$ m voxel size and 55 kVp X-ray energy. For Tb bone in the distal femoral metaphysis, 100 serial cross-sectional scans (1.05 mm) of the secondary spongiosa were obtained from the end of the growth plate extending proximally. For Tb bone in L5 vertebrae, trabecular bone was obtained end-to-end within the vertebral body. For Ct bone, 100 serial cross-sections (1.05 mm) of the tibia were obtained from the TFJ extending proximally. Linear attenuation was calibrated using a  $\mu$ CT hydroxyapatite phantom.  $\mu$ CT image analysis and 3D reconstructions were done using the manufacturer's software to obtain the following structural parameters: Tb tissue volume (Tb.TV), Tb bone volume (Tb.BV), Tb.BV/TV ratio, Tb number (Tb.N), Tb connectivity density (Tb.CD), Tb thickness (Tb.Th), Tb spacing (Tb.Sp), Ct tissue volume (Ct.TV), and Ct thickness (Ct.Th).

**Von Kossa (VK), Goldner, and tartrate-resistant acid phosphatase (TRAP) staining and dynamic fluorescent bone labeling.**

For bone histomorphometry, femurs and cortical bone at TFJ were isolated from 3-month-old mice, fixed overnight in 10% PBF, dehydrated with ethanol, defatted with xylene, and embedded in methyl methacrylate (MMA) (Sigma, St. Louis, MO). Adjacent sections (5 or 10  $\mu$ m in thickness) were cut and mounted on gelatin-coated slides for different staining procedures. Bone images were acquired by Zeiss AXIO Imager M1 Microscope with an automated stage and analyzed using BioQuant computer stations with BioQuant OSTEO 2009 software (Version 9.00, BIOQUANT Image Analysis Co.,

Nashville, TN). The region of interest starts  $\approx 150 \mu\text{m}$  below the femoral growth plate, extends 1 mm distally, and flanks the two sides that are  $100 \mu\text{m}$  apart from cortical bone. Three sections ( $\approx 50\text{-}100 \mu\text{m}$  apart) from each bone sample were analyzed per stain, and averages were reported. The terminology and units used are those recommended by the Histomorphometry Nomenclature Committee of the American Society for Bone and Mineral Research. VK staining was performed to detect the phosphate-containing minerals and calculate static bone parameters: Tb.TV, Tb.N, and Tb.Sp. To quantify structural parameters of unmineralized osteoid and osteoclast (OC)-positive resorbing surface, sections were stained with Goldner trichrome and TRAP staining solutions, respectively. The deduced indices include osteoid volume (OV), OV/BV, osteoid surface (OS), OS/BS, osteoid thickness (Mean O.Th), ratios of O.Th/Tb.Th, erosion surface (ES), ES/BS, N.Oc/BS and N.Oc/ES. For dynamic bone formation indices, mice were injected with calcein (15 mg/kg body wt.) and demeclocycline (15 mg/kg body wt.) 7 and 2 days before sample collection, respectively. Unstained MMA-embedded bone sections were obtained as described above and used to quantify mineralizing surface (MS), MS/BS, mineral apposition rate (MAR), and bone formation rate per bone surface (BFR/BS).

### **Serum Measurements**

Blood was drawn from mice at two time-points. Firstly, for acute drug responses, 3 hours after the last injection through the retro-orbital route under anesthesia and isoflurane inhalation. Secondly, at the end of designated drug treatment, usually 24 hours after the last treatment injection, blood was collected by heart puncture after euthanasia by isoflurane inhalation followed by tissue harvests. The blood was allowed

to clot for 30 minutes at room temperature, and sera were collected after centrifugation for 10 minutes at 6000 rpm. Serum samples were separated by a microtainer serum separator tube then aliquoted and frozen at  $-80^{\circ}\text{C}$ . Total serum albumin, alkaline phosphatase, blood urea nitrogen,  $\text{Ca}^{2+}$ , creatinine, inorganic phosphate, and magnesium were measured by an automated ACE Alera/ Axcel Clinical Chemistry bioanalyser (Alfa Wassermann, Inc., West Caldwell, NJ). Serum intact PTH and 1,25-D levels were assessed using commercial ELISA kits made by Immutopics (San Clemente, CA) and Immunodiagnostic Systems Inc. (Scottsdale, AZ), respectively. Tartrate-resistant acid phosphatase (TRAP) 5b and N-terminal propeptide of type I procollagen (P1NP) were assayed using the MouseTRAP enzyme immunoassay (EIA; SB-TR103) and rat/mouse P1NP EIA (AC-33F1) kits from Immunodiagnostic Systems (Fountain Hills, AZ), respectively.

### **Whole bone mechanical strength testing**

Excised bones free of all soft tissue were fresh frozen at  $-80^{\circ}\text{C}$ . Prior to testing, bones are rehydrated overnight in 0.9% NaCl at RT. Whole bones are loaded to failure in three-point-bending performed on a Bose Electroforce 3200 material tester using custom fixtures. The lower support is set at 10 mm apart for femurs and 11.2 mm apart for tibiae. The testing cross-head speed is 0.2 mm/s and force-displacement data are collected every 0.01 s using manufacturer's software (WinTest, Bose). From the collected raw data, a force-displacement curve is created and standard properties are calculated using custom software (Matlab, MathWorks): ultimate force ( $F_U$ , N), yield force ( $F_Y$ , N), stiffness (S, N/mm), and energy to failure ( $U_{PY}$ , mJ). The yield point is

defined using a 0.015 mm offset parallel to the slope of the linear portion of the force-displacement curve.

### **RNA Isolation and Nanostring nCounter Analysis**

Whole femurs and tibias were harvested after drug treatments, placed in pre-chilled sterilized foil, and frozen in liquid nitrogen then stored at -80°C. Whole bones were pulverized, total RNA isolated using RNeasy Mini Kit (Qiagen; Germantown, MD), and quantitated via a Nanodrop ND-1000 spectrophotometer (Thermo Scientific; Waltham, MA). Nanostring nCounter system (Nanostring Technologies; Seattle, WA) was used for gene expression profiling of selected mRNA using a custom nCounter CodeSets composed of 625 probes including 8 housekeeping controls (b-actin, b-2-microglobulin, Giltz, Gusb, Ibsp, GAPDH, Rpl19, and Rplp0). With Nanostring technology fluorescent single strand oligonucleotide probes are hybridized to complimentary target strands of mRNA and quantified based on the fluorescence of each target gene within each sample. Briefly, the Nanostring reporter probe CodeSet was suspended in 70uL of hybridization buffer and 8uL aliquots were combined in sterile microfuge tubes with 5uL of RNA sample (60 ng/uL) and 2uL of the capture probe. Tubes were then centrifuged, and then incubated at 65°C in a thermocycler for 16-18 hours. Hybridized RNA samples were collected and analyzed using the nCounter Max and Digital Analyzer according to manufacturer's instructions.

## **Tibial Midshaft Fracture**

Closed unfixed bone fractures were created unilaterally in the right mid-tibia by three-point bending using a Bose Electroforce 3200 Material Testing System under general anesthesia with locally injected analgesics. The downward middle test probe, positioned exactly at the tibial midshaft by an investigator, was controlled by an automated actuator, which retrieved the test probe immediately after the bone was fractured (as detected by an accelerated downward probe movement) to minimize soft tissue damage. X-ray radiography was performed, immediately after the procedure, to ensure fracture consistency and mice with inadequate fractures were excluded from high resolution microCT scanning and analyses. The mice were monitored daily and allowed to ambulate freely in their cages following successful fracture. Fracture calluses were collected after 28 days and analyzed.

## **Statistics**

Results were organized using PRISM 8 for MacOS software (Graphpad Software, Inc., San Diego, CA) and are shown as grouped graphs that show both individual points and bar with error bar. Statistical significance was identified by one-way ANOVA or unpaired Student's t-test. P-values of less than 0.05 were considered significant.

## 2.5 Conclusion and Future Directions

This dissertation provides novel insights into the osteoanabolic actions of concurrently targeting the PTH1R and CaSR. Here we provide a possible anabolic treatment with less resorptive stimulation to address the unmet needs of a large group of osteoporotic patients who warrant more potent treatment. Consequently, this work pioneered a first-in-human combination therapy for osteoporosis that has recently been approved for clinical trials and currently recruiting patients from the VA population. PTH(1-34), Teriparatide (Forteo<sup>®</sup>), and the calcimimetic, Cincalcat (Sensipar<sup>®</sup>), will be used in the trial. Both have been FDA approved for many years and used to treat hundreds of thousands of patient worldwide: Forteo for the treatment of osteoporosis and Cinacalcet for the treatment of various forms of hyperparathyroidism. Dr. Dolores Shoback, an endocrinologist with affiliations with UCSF and the San Francisco VA Medical Center, will oversee this randomized double-blind, placebo-controlled trial of the combination Teriparatide with the calcimimetic, Sensipar, compared to monotherapy with Teriparatide in 48 men with low bone mineral density. The time frame of treatment is 12-13 months with primary outcomes that measure lumbar spine and femoral neck BMD. The study will also assess acute and chronic serum  $[Ca^{2+}]$  and intact PTH as well as biochemical markers of bone turnover and vitamin D metabolites (i.e. serum P1NP, CTX, bone specific alkaline phosphatase, OPG, RANK-L and 1,25-(OH)<sub>2</sub> Vitamin D). This clinical trial will help to understand whether our effective combination therapy in mice will prove to be effective in men and guide future translational work.

## 2.6 References

- [1] National Osteoporosis Foundation. *1996 and 2015 Osteoporosis Prevalence Figures: State-by-state Report*. (1997).
- [2] National Osteoporosis Foundation. What is Osteoporosis? <http://nof.org/articles/7> (2014).
- [3] Bliuc, D., Nguyen, N. D., Nguyen, T. V., Eisman, J. A. & Center, J. R. Compound risk of high mortality following osteoporotic fracture and refracture in elderly women and men. *J Bone Miner Res* 28, 2317-2324 (2013)
- [4] Gonzalez-Rozas, M., Perez-Castrillon, J. L., Gonzalez-Sagrado, M., Ruiz-Mambrilla, M. & Garcia-Alonso, M. Risk of mortality and predisposing factors after osteoporotic hip fracture: a one-year follow-up study. *Aging clinical and experimental research* 24, 181-187 (2012).
- [5] Vaseenon, T., Luevitoonvechkij, S., Wongtriratanachai, P. & Rojanasthien, S. Long-term mortality after osteoporotic hip fracture in Chiang Mai, Thailand. *J Clin Densitom* 13, 63-67, (2010).
- [6] Cusano, N. E. & Bilezikian, J. P. Combination anabolic and antiresorptive therapy for osteoporosis. *Endocrinol Metab Clin North Am* 41, 643-654, (2012).
- [7] Cooper, C. The crippling consequences of fractures and their impact on quality of life. *Am J Med* 103, 12S-17S; discussion 17S-19S (1997).
- [8] Weinstein, RS., Roberson, PK., Manolagas, SC. Giant osteoclast formation and long-term oral bisphosphonate therapy. *N Engl J Med* 360(1), 53-62, (2009).
- [9] Subramanian, G., Fritton, J. C. & Quek, S. Y. Osteonecrosis and atypical fractures-common origins? *Osteoporos Int* 24, 745-746, (2013).

- [10] Reid, I. R. Osteoporosis treatment: focus on safety. *European journal of internal medicine* 24, 691-697, (2013).
- [11] McClung, M. *et al.* Bisphosphonate therapy for osteoporosis: benefits, risks, and drug holiday. *Am J Med* 126, 13-20, (2013).
- [12] Khosla, S. *et al.* Benefits and risks of bisphosphonate therapy for osteoporosis. *J Clin Endocrinol Metab* 97, 2272-2282, (2012).
- [13] FDA. NDA#21-318: Statistical review and evaluation -- clinical studies.  
[http://www.fda.gov/ohrms/dockets/ac/01/briefing/3761b2\\_04\\_statistics.htm](http://www.fda.gov/ohrms/dockets/ac/01/briefing/3761b2_04_statistics.htm) (2000).
- [14] Jilka, R. L. Molecular and cellular mechanisms of the anabolic effect of intermittent PTH. *Bone* 40, 1434-1446, (2007).
- [15] Neer, R. M. *et al.* Effect of parathyroid hormone (1-34) on fractures and bone mineral density in postmenopausal women with osteoporosis. *N Engl J Med* 344, 1434-1441, (2001).
- [16] Cusano, N. E. & Bilezikian, J. P. Combination anabolic and antiresorptive therapy for osteoporosis. *Endocrinol Metab Clin North Am* 41, 643-654, (2012).
- [17] Aslan, D. *et al.* Mechanisms for the bone anabolic effect of parathyroid hormone treatment in humans. *Scandinavian journal of clinical and laboratory investigation* 72, 14-22, (2012).
- [18] Skripitz, R., Andreassen, TT., Aspenberg, P. Strong effect of PTH(1-34) on regenerating bone: a time sequence study in rats. *Acta Orthop Scand* 71, 619-624 (2000).



- [19] Barnes, GL., Kakar, S., Vora, S., Morgan, EF., Gerstenfeld, LC., Einhorn, TA. Stimulation of fracture-healing with systemic intermittent para- thyroid hormone treatment. *J Bone Joint Surg Am* 90 (Suppl 1), 120-127 (2008).
- [20] Aspenberg, P., Genant, HK., Johansson, T., Nino, AJ., See, K., Krohn, K., *et al.* Teriparatide for acceleration of fracture repair in humans: a prospective, randomized, double-blind study of 102 postmenopausal women with distal radial fractures. *J Bone Miner Res* 25, 404-414 (2010).
- [21] Bashutski JD, Eber RM, Kinney JS, Benavides E, Maitra S, Braun TM, *et al.* The impact of vitamin D status on periodontal surgery outcomes. *J Dent Res* 90, 1007-1012 (2011).
- [22] Kawane, T., Takahashi, S., Saitoh, H., Okamoto, H., Kubodera, N., Horiuchi, N. Anabolic effects of recombinant human parathyroid hormone (1 - 84) and synthetic human parathyroid hormone (1 - 34) on the mandibles of osteopenic ovariectomized rats with maxillary molar extraction. *Horm Metab Res* 34, 293-302 (2002).
- [23] Rowshan, HH., Parham, MA., Baur, DA., McEntee, RD., Cauley, E., Carriere, DT., *et al.* Effect of intermittent systemic administration of recombinant parathyroid hormone (1-34) on mandibular fracture healing in rats. *J Oral Maxillofac Surg* 68, 260-267 (2010).
- [24] Valderrama, P., Jung, RE., Thoma, DS., Jones, AA., Cochran, DL. Evaluation of parathyroid hormone bound to a synthetic matrix for guided bone regeneration around dental implants: a histomorphometric study in dogs. *J Periodontol* 81, 737-747 (2010).

- [25] Chan, HL., McCauley, LK. Parathyroid Hormone Applications in the Craniofacial Skeleton. *Journal of Dental Research* 92, 18-25 (2013).
- [26] Tsai, KY., Huang, CS., Huang, GM., Yu, CT. More on the resolution of bisphosphonate-associated osteonecrosis of the jaw. *J Rheumatol* 37, 675 (2010).
- [27] Lee, JJ., Cheng, SJ., Jeng, JH., Chiang, CP., Lau, HP., Kok, SH. Successful treatment of advanced bisphosphonate-related osteonecrosis of the mandible with adjunctive teriparatide therapy. *Head Neck* 33, 1366-1371 (2011).
- [28] Kwon, YD., Lee, DW., Choi, BJ., Lee, JW., Kim, DY. Short-term teriparatide therapy as an adjunctive modality for bisphosphonate-related osteonecrosis of the jaws. *Osteoporos Int* 23, 2721-2725 (2012).
- [29] Shoback, D. Clinical practice. Hypoparathyroidism. *N Engl J Med* 359, 391-403, (2008).
- [30] Toka, Hakan R et al. "Deficiency of the calcium-sensing receptor in the kidney causes parathyroid hormone-independent hypocalciuria." *Journal of the American Society of Nephrology : JASN* vol. 23,11,1879-90, (2012).
- [31] Kanatani, M et al. "High extracellular calcium inhibits osteoclast-like cell formation by directly acting on the calcium-sensing receptor existing in osteoclast precursor cells." *Biochemical and biophysical research communications* vol. 261,1,144-8, (1999).
- [32] Mentaverri R, Yano S, Chattopadhyay N, et al. The calcium sensing receptor is directly involved in both osteoclast differentiation and apoptosis. *FASEB J.* 2006;20(14):2562-2564.

- [33] Eli Lilly and Company. NDA 21-318 FORTEO® (teriparatide) (rDNA origin):  
Injection risk evaluation and mitigation strategy (REMS).  
<http://www.forteohcp.com/Documents/pdf/forteo-rems.pdf>
- [34] Daddona, P. E., Matriano, J. A., Mandema, J. & Maa, Y. F. Parathyroid hormone (1-34)-coated microneedle patch system: clinical pharmacokinetics and pharmacodynamics for treatment of osteoporosis. *Pharmaceutical research* 28, 159-165, (2011).
- [35] Cosman, F. *et al.* Effect of transdermal teriparatide administration on bone mineral density in postmenopausal women. *J Clin Endocrinol Metab* 95, 151-158, (2010)
- [36] D. White *et al.*, Ca(2+) allosteric in PTH-receptor signaling. *Proc Natl Acad Sci U S A* 116, 3294-3299 (2019).
- [37] S. Lee *et al.*, A Homozygous [Cys25]PTH(1-84) Mutation That Impairs PTH/PTHrP Receptor Activation Defines a Novel Form of Hypoparathyroidism. *J Bone Miner Res* 30, 1803-1813 (2015).
- [38] M. J. Horwitz *et al.*, Continuous PTH and PTHrP infusion causes suppression of bone formation and discordant effects on 1,25(OH)<sub>2</sub> vitamin D. *J Bone Miner Res* 20, 1792-1803 (2005).
- [39] G. Hattersley, T. Dean, B. A. Corbin, H. Bahar, T. J. Gardella, Binding Selectivity of Abaloparatide for PTH-Type-1-Receptor Conformations and Effects on Downstream Signaling. *Endocrinology* 157, 141-149 (2016).
- [40] Okazaki M, Ferrandon S, Vilardaga JP, Boussein ML, Potts JT Jr, Gardella TJ. Prolonged signaling at the parathyroid hormone receptor by peptide ligands

targeted to a specific receptor conformation. *Proc Natl Acad Sci USA*, 105(43):16525–16530 (2008).

- [41] Maeda A, Okazaki M, Baron DM, Dean T, Khatri A, Mahon M, Segawa H, Abou-Samra AB, Juppner H, Bloch KD, Potts JT Jr, Gardella TJ. Critical role of parathyroid hormone (PTH) receptor-1 phosphorylation in regulating acute responses to PTH. *Proc Natl Acad Sci USA*, 110(15):5864–5869, (2013).
- [42] Shimizu M, Potts JT Jr, Gardella TJ. Minimization of parathyroid hormone. Novel amino-terminal parathyroid hormone fragments with enhanced potency in activating the type-1 parathyroid hormone receptor. *J Biol Chem.*, 275(29):21836–21843, (2000).
- [43] Shimizu M, Carter PH, Khatri A, Potts JT Jr, Gardella TJ. Enhanced activity in parathyroid hormone-(1–14) and -(1–11): novel peptides for probing ligand-receptor interactions. *Endocrinology*, 142(7):3068–3074, (2001).
- [44] G. Hattersley, T. Dean, B. A. Corbin, H. Bahar, T. J. Gardella, Binding Selectivity of Abaloparatide for PTH-Type-1-Receptor Conformations and Effects on Downstream Signaling. *Endocrinology* 157, 141-149 (2016).
- [45] Chin, J. *et al.* Activation of the calcium receptor by a calcimimetic compound halts the progression of secondary hyperparathyroidism in uremic rats. *J Am Soc Nephrol* 11, 903-911 (2000).
- [46] Ishii, H. *et al.* Daily intermittent decreases in serum levels of parathyroid hormone have an anabolic-like action on the bones of uremic rats with low-turnover bone and osteomalacia. *Bone* 26, 175-182 (2000).

- [47] Wada, M. *et al.* Calcimimetic NPS R-568 prevents parathyroid hyperplasia in rats with severe secondary hyperparathyroidism. *Kidney Int* 57, 50-58, doi:10.1046/j.1523-1755.2000.00837.x (2000).
- [48] Fox, J., Lowe, S. H., Conklin, R. L. & Nemeth, E. F. The calcimimetic NPS R-568 decreases plasma PTH in rats with mild and severe renal or dietary secondary hyperparathyroidism. *Endocrine* 10, 97-103, doi:10.1385/ENDO:10:2:97 (1999).
- [49] Fox, J., Lowe, S. H., Conklin, R. L., Petty, B. A. & Nemeth, E. F. Calcimimetic compound NPS R-568 stimulates calcitonin secretion but selectively targets parathyroid gland Ca(2+) receptor in rats. *J Pharmacol Exp Ther* 290, 480-486 (1999).
- [50] Fox, J., Lowe, S. H., Petty, B. A. & Nemeth, E. F. NPS R-568: a type II calcimimetic compound that acts on parathyroid cell calcium receptor of rats to reduce plasma levels of parathyroid hormone and calcium. *J Pharmacol Exp Ther* 290, 473-479 (1999).
- [51] Wada, M. *et al.* NPS R-568 halts or reverses osteitis fibrosa in uremic rats. *Kidney Int* 53, 448-453, doi:10.1046/j.1523-1755.1998.00782.x (1998).
- [52] Okazaki M, Ferrandon S, Vilardaga JP, Buxsein ML, Potts JT Jr, Gardella TJ. Prolonged signaling at the parathyroid hormone receptor by peptide ligands targeted to a specific receptor conformation. *Proc Natl Acad Sci U S A.* 105(43):16525-16530 (2008).
- [53] Vilardaga JP, Jean-Alphonse FG, Gardella TJ. Endosomal generation of cAMP in GPCR signaling. *Nat Chem Biol.*10(9):700-706 (2014).

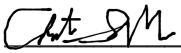
- [54] Shimizu M, Joyashiki E, Noda H, et al. Pharmacodynamic Actions of a Long-Acting PTH Analog (LA-PTH) in Thyroparathyroidectomized (TPTX) Rats and Normal Monkeys. *J Bone Miner Res.* 31(7):1405-1412, (2016).
- [55] Tabacco G, Bilezikian JP. New Directions in Treatment of Hypoparathyroidism. *Endocrinol Metab Clin North Am.* 47(4):901-915, (2018).
- [56] Zhao LH, Ma S, Sutkeviciute I, et al. Structure and dynamics of the active human parathyroid hormone receptor-1. *Science.* 364(6436):148-153, (2019).
- [57] Noda H, Okazaki M, Joyashiki E, et al. Optimization of PTH/PTHrP Hybrid Peptides to Derive a Long-Acting PTH Analog (LA-PTH). *JBMR Plus.* 2020;4(7):e10367, (Published 2020 May 30).
- [58] Chang W, Tu C, Chen TH, Bikle D, Shoback D. The extracellular calcium-sensing receptor (CaSR) is a critical modulator of skeletal development. *Sci Signal.* 2008;1(35):ra1, (published 2008 Sep 2).
- [59] Cheng Z, Li A, Tu CL, et al. Calcium-Sensing Receptors in Chondrocytes and Osteoblasts Are Required for Callus Maturation and Fracture Healing in Mice. *J Bone Miner Res.* 35(1):143-154, (2020).
- [60] Shalhoub V, Grisanti M, Padagas J, et al. In vitro studies with the calcimimetic, cinacalcet HCl, on normal human adult osteoblastic and osteoclastic cells. *Crit Rev Eukaryot Gene Expr.* 13(2-4):89-106, (2003).
- [61] Lotinun S, Ishihara Y, Nagano K, et al. Cathepsin K-deficient osteocytes prevent lactation-induced bone loss and parathyroid hormone suppression. *J Clin Invest.* 2019;129(8):3058-3071. Published 2019 May 21.

[62] Mazur CM, Woo JJ, Yee CS, et al. Osteocyte dysfunction promotes osteoarthritis through MMP13-dependent suppression of subchondral bone homeostasis. *Bone Res.* 2019;7:34. Published 2019 Nov 5.

## Publishing Agreement

It is the policy of the University to encourage open access and broad distribution of all theses, dissertations, and manuscripts. The Graduate Division will facilitate the distribution of UCSF theses, dissertations, and manuscripts to the UCSF Library for open access and distribution. UCSF will make such theses, dissertations, and manuscripts accessible to the public and will take reasonable steps to preserve these works in perpetuity.

I hereby grant the non-exclusive, perpetual right to The Regents of the University of California to reproduce, publicly display, distribute, preserve, and publish copies of my thesis, dissertation, or manuscript in any form or media, now existing or later derived, including access online for teaching, research, and public service purposes.

DocuSigned by:  
  
ABA91CAC6A7A4E6... Author Signature

9/2/2020  
Date